DOKUZ EYLÜL UNIVERSITY
GRADUATE SCHOOL OF NATURAL AND APPLIED SCIENCES

DESIGN PRINCIPLES OF PARABOLIC SOLAR COLLECTORS

by
Sabah N. MAHMOOD

September, 2010
İZMİR

DESIGN PRINCIPLES OF PARABOLIC SOLAR COLLECTORS

A Thesis Submitted to the
Graduate School of Natural and Applied Sciences of Dokuz Eylül University
In Partial Fulfillment of the Requirements for the Degree of Master of Science
in Mechanical Engineering, Thermodynamic Program

by

Sabah N. MAHMOOD

September, 2010
İZMİR

M.Sc THESIS EXAMINATION RESULT FORM

We have read the thesis entitled **"DESIGN PRINCIPLES OF PARABOLIC SOLAR COLLECTORS"** completed by **Sabah N. MAHMOOD** under supervision of **Assoc. Dr. Serhan KÜÇÜKA** and we certify that in our opinion it is fully adequate, in scope and in quality, as a thesis for the degree of Master of Science.

Assoc. Dr. Serhan KÜÇÜKA

(Jury Member)

(Jury Member)

Prof.Dr. Mustafa SABUNCU

Director

Graduate School of Natural and Applied Sciences

ACKNOWLEDGMENTS

I like to express my sincere thanks and appreciation to my supervisor Assoc. Dr. Serhan KÜÇÜKA who I can't forget his favor for his support and organizing this research, and also to my parents and my wife for their love, patience and sense of humor.

Sabah N. MAHMOOD

DESIGN PRINCIPLES OF PARABOLIC TROUGH SOLAR COLLECTORS

ABSTRACT

A performance model has been programmed for solar thermal collector based on a linear, tracking parabolic trough reflector focused on a selective surface absorber tube (receiver) enclosed in an evacuated transparent glass tube: a Parabolic Trough Solar Collector PTSC. This steady state, single dimensional model comprises the fundamental radiative and convective heat transfer and energy balance relations programmed in the Visual Basic 6.0. It considers the effects of ambiance conditions, design conditions, material properties, fluid properties and operating conditions on the performance of the PTSC. The numerical model has been carefully validated with experimental data obtained by Sandia National Laboratories.

Taking into consideration the operation and ambiance condition, the geometric design of the PTSC is done. Depending on the simulation program and the meteorological year data of İzmir city, the hourly, daily, monthly and annually output powers of the PTSC which designed in this study are determined.

Keywords: Parabolic trough solar collector, Numerical analysis models, Solar collectors.

PARABOLİK GÜNEŞ KOLLEKTÖRLERİNİN TASARIM ESASLARI

ÖZ

Bu çalışmada, güneşi izleyen parabolik yansıtıcı bir yüzey ve cam kılıfı içerisine alınarak odak çizgisine yerleştrilmiş bir emici borudan oluşan parabolik güneş kollektörleri için matematiksel performans modeli programlanmıştır. Tek boyutlu kararlı hal durumu için temel olan ışınım-taşınım ısı transfer bağıntıları kullanarak enerji dengesinin kurulduğu matematiksel model, Visual Basic 6.0 programlama dili yardımı ile bilgisayar ortamına aktarılmıştır. Geliştirilen matematiksel model ve simülasyon uygulamaları yardımıyla: çevresel koşullar, tasarımsal koşullar, malzeme özellikleri, akışkan özellikleri ve işletme koşulların etkisinin davranış ve analizleri incelenmiştir. Sistem davranışını tanımlayan matematiksel modelin bilgisayar simülasyon sonuçları, literatürde verilen test ölçüm sonuçları ile karşılaştırılarak doğrulanmıştır.

Oluk tipi parabolic güneş kollektörün geometrik ölçülendirmesi yapılmış uygun yansıtıcı yüzey ve emici boru seçimi ile tasarım tamamlanmıştır. Simülasyon programı yardımıyla, tasarımı yapılan güneş kollektörünün İzmir ili iklim koşullarında üretebileceği saatlik, günlük, aylık ile yıllık ısıl enerji hesaplanmıştır.

Anahtar sözcükler: Parabolik güneş kollektörleri, Sayısal analiz modelleri, Güneş kollektörleri.

CONTENTS

Page

CHAPTER ONE
INTRODUCTION

1.1 Background

The people always looking for new sources of energy to cover their needs in the growing applications of advanced life when the energy plays a great role in it. Everywhere people use electricity, fossil fuels, chemical products etc. In the world, there are lots of energy sources, e.g. petroleum products, hydro-power, coal and in developed countries nuclear energy but nobody should forget that most of the energy sources cause the environmental pollution. On the other hand, cost of the energy is always increased so some alternative sources are developed such as solar energy, wind energy, biomass geothermal energy, tidal energy etc. These energy sources are inexpensive and clean, most of them are regional sources. Therefore, renewable energy sources are of great concern in many countries. It is well known that solar energy seems to hold much promise for the future.

For the industrial purposes, there are various types of solar collectors. If high temperatures are to be achieved in an efficient solar utilization system, concentrators are necessary. A concentrator gathers incoming beam radiation over a relatively large aperture and by means of an optical system focuses the energy on the much smaller surface of the receiver. Concentration allows for localizing heat losses to a relatively small receiver and enables more efficient operation at elevated temperature.

Among the family of solar collectors, parabolic trough solar collector PTSC is currently receiving considerable attention for a wide range of applications from domestic hot water production to steam generation for power and industrial process heat generation. The recommendation of (Bird and Drost 1982) is that the PTSC concept should receive the highest priority for commercial development for low temperature (65–200 ^{o}C) solar process heat applications. The high degree of concentration attainable with parabolic trough collector offsets the disadvantage associated with the requirement of some level of tracking as compared to flat plate

collectors. Also, parabolic trough collectors are structurally simpler than other collectors. The parabolic trough collector considered in this thesis, consists of a cylindrical parabolic reflecting surface, a transparent envelope and a receiver centred along the reflector's focal line which carries the working fluid. Solar heat flux is focused on the receiver tube and, as a result of focusing, receiver's temperatures gets very high and transfers energy to the working fluid. PTSC with evacuated tubular receivers is the main technology currently used in solar thermal electrical power plants (but it is also used in steam generation, absorption cooling, seawater distillation, etc.) because of considerable experience with the systems and the development of small commercial industry to produce and market these system.

It was easy to get high temperatures in parabolic trough collectors, because the controlling factor is a mass flow rate. Parabolic trough collectors have been in use for many years and a renewed attempt to study the aspects of their experimental and theoretical performance have been made recent in years in the wake of the energy problem (Karaduman, 1989).

1.2 Solar Collectors

A collector is a thermal converting unit for solar energy. It is composed of a black absorber plate, where incident solar radiation is converted into heat, and integrated tubes or channels to the absorber plate, through which a heat transfer or heat carrying fluid circulates to remove the heat collected in the absorber plate. Consider accordant literature where gathered information about five mine types of solar collectors described below (Jesco, 2008).

- Tank-type collector
- Pool Collector
- Flat Plate Collectors
- Evacuated tube collector
- Concentrating Collectors

1.2.1 Tank-Type Collector

In an Integral Collector Storage unit, the hot water storage tank is the solar absorber. The tank or tanks are mounted in an insulation box with glazing on one side and are painted black or coated with a selective surface. The sun shines through the glazing and hits the black tank, warming the water inside the tank. The single tanks are typically made of steel, while the tubes are typically made of copper. Achievable temperature with such collectors is a little bit less than in flat-plate collectors.

1.2.2 Pool Collector

The single largest application of active solar heating systems is in heating swimming pools. Special collectors have been developed for heating seasonal swimming pools: they are unglazed and made of a special copolymer plastic. These collectors cannot withstand freezing conditions. Approximate maximum operating temperature of such type of solar collector is 10 – 20 ºC above ambience.

1.2.3 Flat Plate Collectors

Flat plate collectors are the most important and expensive component of any low temperature solar-thermal system. Flat-plate collectors are used typically for temperature requirements up to 75 ºC. A typical flat plate collector is illustrated in figure 1.1. It is composed of a cover glass or glasses, a blackened absorber plate in which all the components are placed.

They may be designed to heat air, water or some other heat transfer fluid. In practice there are two main types of the flat plate collector, which are shown in figure 1.2 and 1.3.

- Water Heaters
- Air Heaters

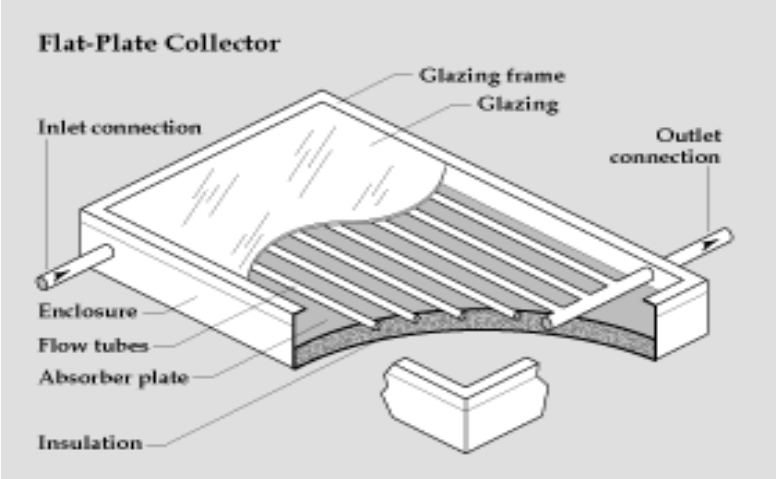

Figure 1.1 A sectional view for a flat plate collectors

Depending on absorbers construction and configuration flat-plate collectors are divided in several types. Flat-plate collectors use both beam and diffuse solar radiation, do not require tracking of the sun, and require little maintenance.

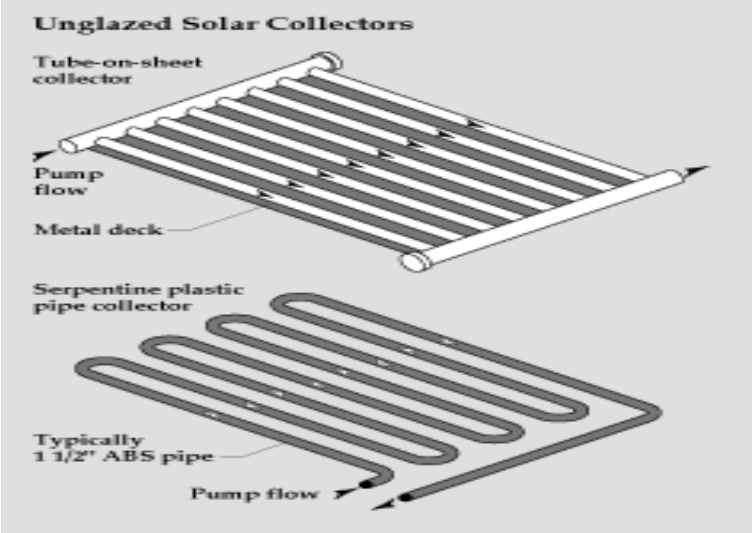

Figure 1.2 A sectional view for flat plate water heater collectors

These collectors have a distinct advantage over other types in that they shed snow very well when installed in climates that experience significant snowfall. The basic physical performance of flat plate collectors for heating water is well understood and much work has also been carried out on air heating collectors (Duffie & Beckman, 1991).

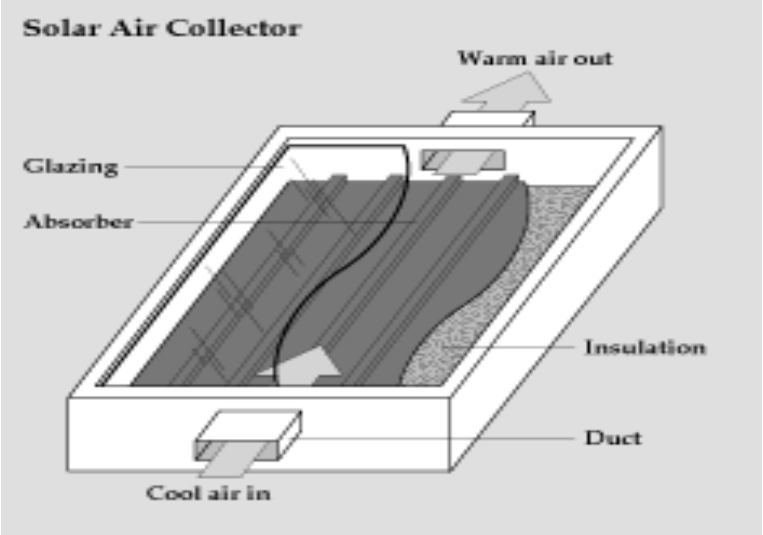

Figure 1.3 A sectional view for Flat plate air heater collectors

The principles of operation are simple; the blackened flat plate exposed to solar radiation will absorb energy and its temperature will rise continuously. If a fluid is circulated through suitable paths formed in the plate, some of the absorbed energy will be transferred to the fluid. The rest of the absorbed energy will be dissipated to the surroundings by radiation, convection and conduction (Duffie & Beckman, 1991). These losses may be reduced by good side and back insulations and by putting translucent covers on the top of casing. Glass, being highly transparent for short-wave radiation and virtually opaque for long-wave radiation, is most commonly used for the top cover. In order to reduce the radiative loss from the plate through the top covers, selective surfaces are used. A selective surface is obtained by a proper treating of the front surface of an absorber plate so that its emittance for long-wave spectrum is reduced without greatly reducing its absorptance in short-wave spectrum [Jesco, 2008]. Because of their high heat loss coefficient, ordinary flat-plate collectors are not practical for elevated temperatures, say above 80 ºC. When higher temperatures are desired, one needs to reduce the heat loss coefficient.

This can be accomplished principally by two methods: evacuation and concentration, either singly or in combination. While several attempts have been made to build evacuated flat plates, they do not seem to hold any promise of commercial success (Jesco, 2008).

1.2.4 Evacuated Tube Collector

While flat-plate collectors are all essentially made the same way and perform the way from one brand to other, evacuated tube collectors vary widely in their construction and operation. Evacuated tube collectors are constructed of a number of glass tubes. Each tube is made of annealed glass and has an absorber plate within the tube, because tube is the natural configuration of an evacuated collector . This type is shown in figure 1.4. During the manufacturing process in order to reduce heat losses through conduction and convection, a vacuum is created inside the glass tube. The only heat loss mechanism remaining is radiation. The absence of air in the tube creates excellent insulation, allowing higher temperatures to be achieved at the absorber plate (Goswami, Kreith & Kreider, 2000).

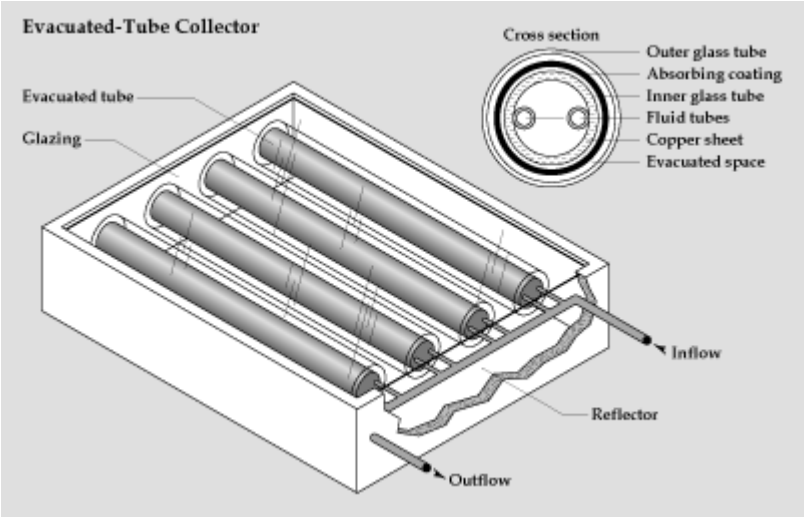

Figure 1.4 A sectional view for evacuated tube solar collector

In order to improve an efficiency of evacuated tube collector there are several types of concentrators depending on its concave radius established. There are many possible designs of evacuated collectors, but in all of them selective coating as an absorber is used because with a nonselective absorber, radiation losses would dominate at high temperatures, and eliminating convection alone would not be very effective. The evacuated collectors are divided into two types (Goswami, Kreith & Kreider, 2000),

- With Heat Pipe
- Without Heat Pipe

A heat pipe provides the most elegant way of extracting heat from an evacuated collector. Heat pipe is hermetically sealed tube that contains a small amount of heat transfer liquid. When one portion of tube is heated the liquid evaporates and condenses at the cold portion, transferring heat with great effectiveness because of the latent heat of condensation. The heat pipe contains a wick or is tilted (or both) to ensure that the liquid follows back to the heated portion to repeat the cycle. It is easy to design a heat pipe (e.g., by giving it the proper tilt) so that it functions only in one direction (Jesco, 2008).

This thermal diode effect is very useful for the design of solar collectors, because it automatically shuts the collector off and prevents heat loss when there is insufficient solar radiation. Also, heat pipes have lower heat capacity than ordinary liquid-filled absorber tubes, thus minimizing warm-up and cool down losses. Heat pipe provides the method of transferring larger amounts of heat from the focal area of a high-concentration solar collector to a fluid with only small temperature difference. It consists of a circular pipe with an annular wick layer situated adjacent to the pipe wall, there is shown in figure 1.5. The circular pipe is perfectly insulated from outside to avoid thermal losses from the circular pipe (Rapp, 1981).

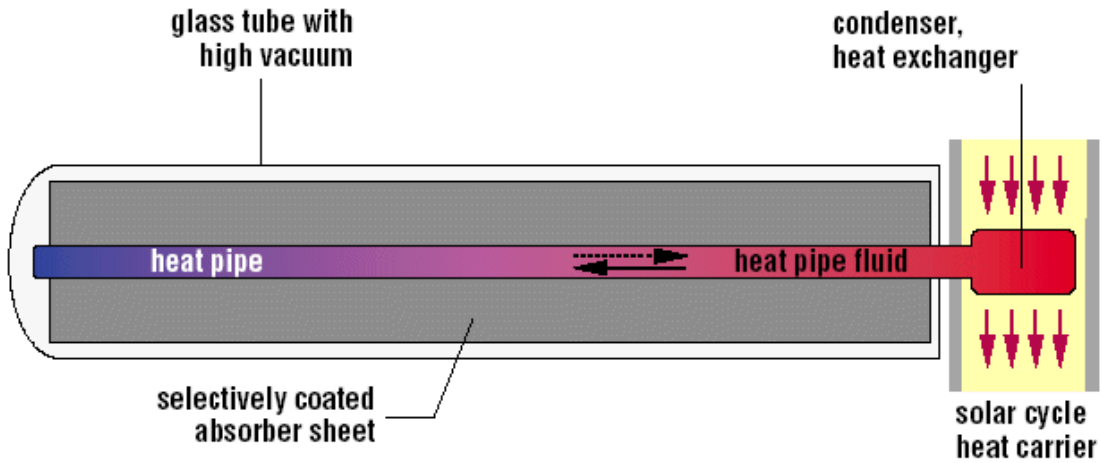

Figure 1.5 A cross sectional for heat pipe

Solar energy falls on evaporator and the fluid inside evaporator boils. The vapor migrates to the condenser where heat of vapor is transferred to a circulation fluid loop. The heat available with circulating fluid is further carried away to the end use point. The circulation fluid after releasing its heat is transferred to the boiler by capillary action in the wick or by gravity and cycle repeats. Gravity return heat pipes can operate without wick but cannot be operated horizontally as a result (Rapp, 1981).

1.2.5 Concentrating Collectors

Concentrating of solar radiation becomes necessary when higher temperatures are desired. Selective surfaces can be used to reduce radiative losses and hence to achieve high temperatures, but for the higher temperatures one must increase the input energy density by concentrating the solar radiation. The concentrating collectors divided into two major types, which are divided into many types as shown in figure 1.7. There are three reasons are commonly cited for using concentrators that is (Kreith & Kreider, 1978):

- To increase energy delivery temperatures in order to achieve a thermodynamic match between temperature level and task. The task may be to operate thermionic, magneto hydrodynamic, thermodynamic, or other higher temperature devices.

- To improve thermal efficiency by reducing the heat loss area relative to the receiver area. There would also be a reduction in transient effects, since the thermal mass is usually much smaller than for a flat plate collector.

- To reduce cost by replacing an expensive receiver by a less expensive reflecting or refracting area. The figure 1.6 is shows the temperature reached by solar absorbers with concentrators optics.

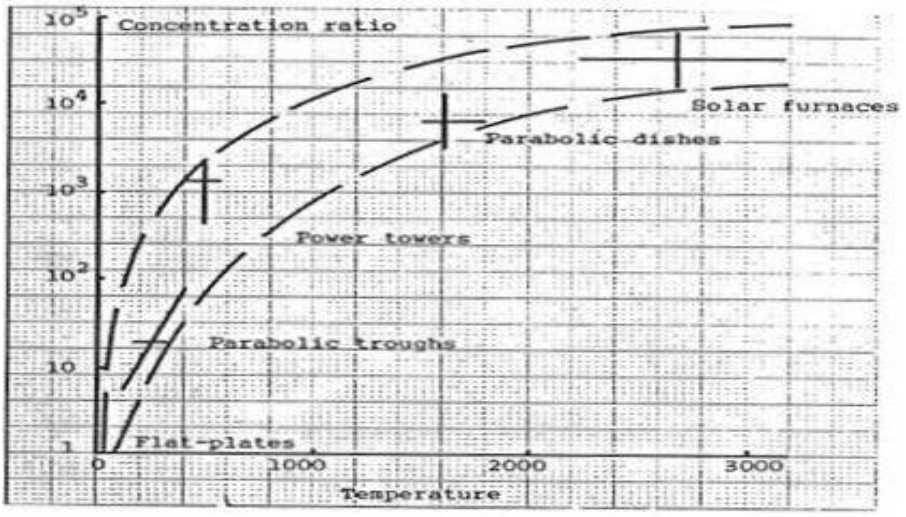

Figure 1.6 Temperature reached by solar absorbers with concentrator optics

In order to the classified of the concentrator solar collectors, there are divided as shown in figure 1.7 into two main groups, that's,

- Fixed or intermittently tracking concentrators
- Continuously tracking concentrators

1.2.5.1 Fixed or Intermittently Tracking Concentrators

The least complex concentrators are those not requiring continuous accurate tracking of the sun. These are necessary of large acceptance angle, moderate concentration ratio, and usually single curvature design. Since the diurnal, angular excursion of the sun is in a north-south plane, the fixed or intermittently turned concentrators must be oriented with their axis of rotation perpendicular to this plane, that is, in an east-west direction, in order to capitalize on the large acceptance angle. The basic fixed or intermittently concentrators consists of this types (Rapp, 1981),

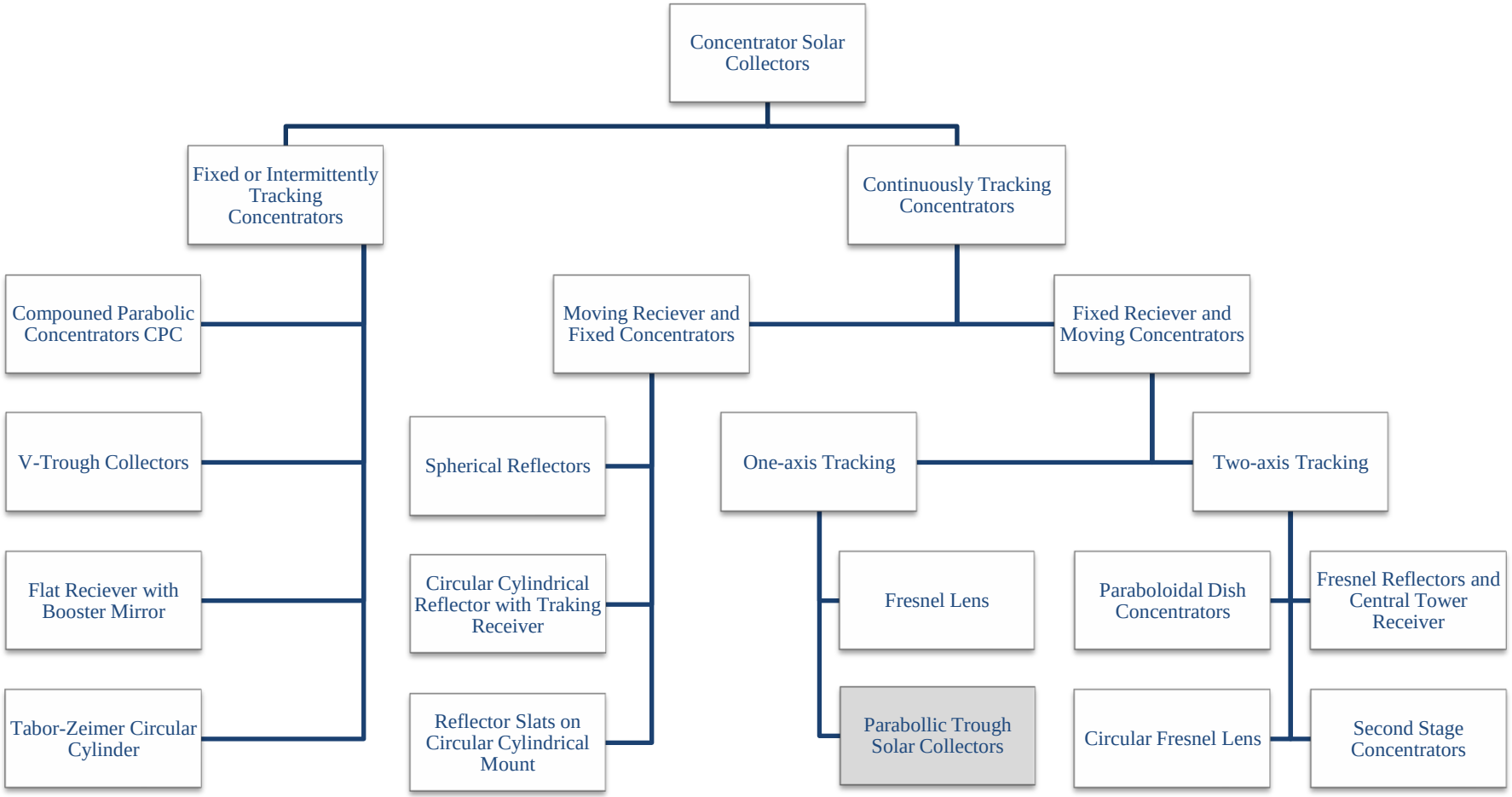

Figure 1.7 Classification the solar concentrator collectors

Compound Parabolic Collectors (CPC): It was developed independently in USA, GERMANY and USSR in 1966. It consists of parabolic reflectors that funnel the radiation from aperture to absorber. The right and left halves belong to different parabolas, expressed by name CPC. For instance the axis of the right branch make an angle θ_c with the collector mid-plane and its focus is at A as we see in figure 1.8.

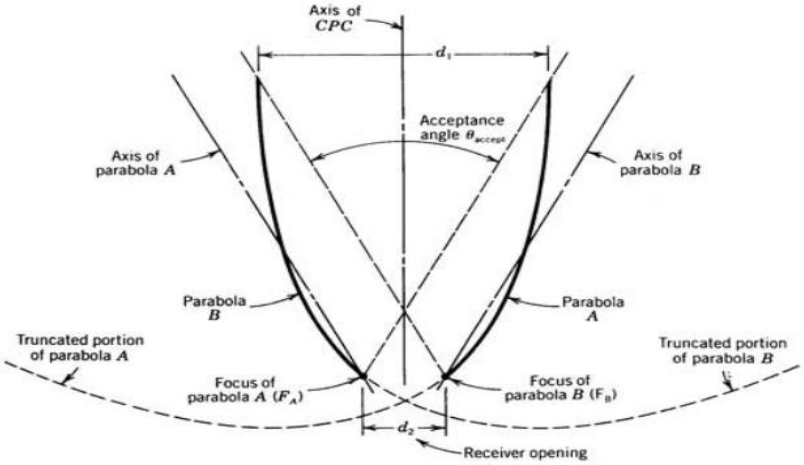

Figure 1.8 Compound parabolic concentrator

Tracing a few sample rays reveals that this device has the following acceptance characteristic; all rays incident on the aperture within the acceptance angle, that is, with $|\theta_{in}| < \theta_{accept}$ will reach the absorber, whereas all the rays with $|\theta_{in}| > \theta_{accept}$ will bounce back and forth between the reflector sides and eventually re-emerge through the aperture as shown in figure 1.9 (Dickinson & Cheremisinoff, 1990).

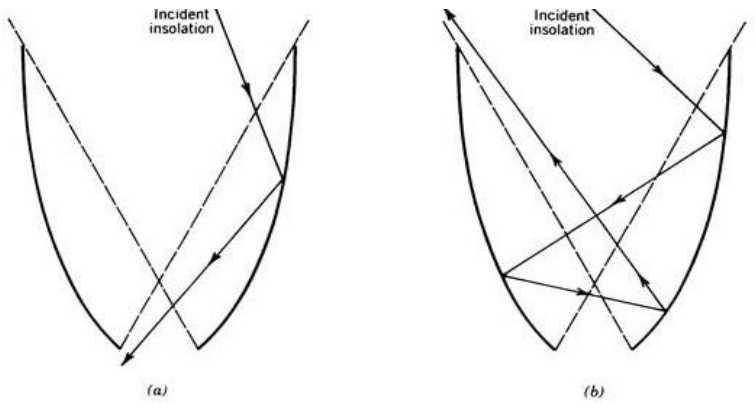

Figure 1.9 Incident beams from the CPC

(a) Incidence angle less than acceptance angle

(b) Incidence angle greater than acceptance angle

V-Trough and Side Reflectors: In figure 1.10 (a) the rays τ_δ and τ_o have angle of incident δ and θ_o, respectively, they pass through the edge of the absorber and are tangential to the reference circle. V-trough concentrators and side reflectors can be considered straight-line approximations to the symmetric CPC, and they are concerned for some applications because of their simple manufacture. The angular acceptance of the V-trough collector in figure 1.10 (a) is shown schematically by the solid line in figure 1.10 (b). Only when the trough angle φ approaches to zero does the acceptance angle approach that of the CPC, however, in this limit the trough becomes too deep and reflection losses become excessive (Dickinson & Cheremisinoff, 1990).

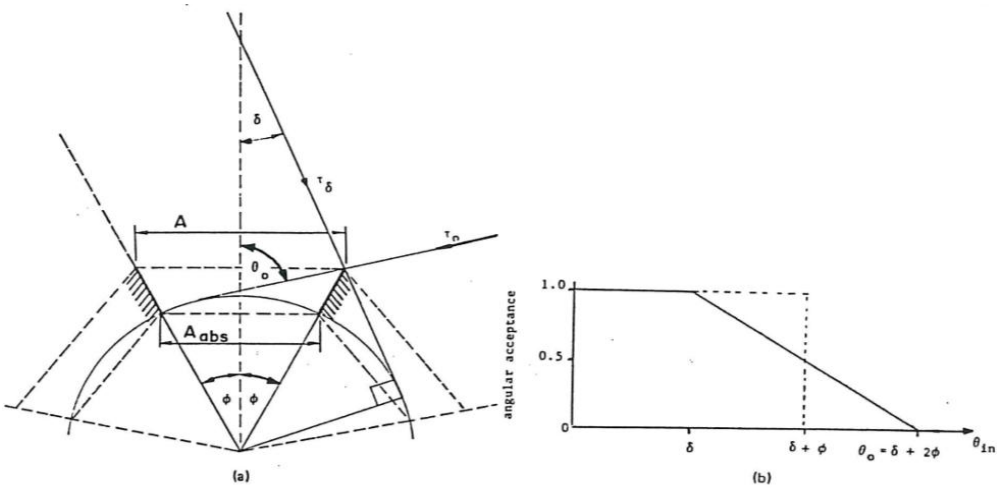

Figure 1.10 V-trough concentrator

(a) With mirror image and reference circle

(b) Angular acceptance

1.2.5.2 Continuously Tracking Concentrators

In order to achieve concentration ratios above 20 for year-round periods of solar collection of 6 hr or more, collectors that track the sun continuously are required. Two types of continuously tracking collectors can be identified:

- *Fixed Receiver and Moving Concentrators*
- *Moving Receiver and Fixed Concentrators*

1.2.5.2.1 Fixed Receiver and Moving Concentrators. They are the common types of the concentrator solar collectors which used in this sector, where can be divided according to their tracking into one and two-axis tracking system, basic concentrating devises are:

Parabolic Trough Solar Collectors: PTSC are made by bending a sheet of reflective surface into a parabolic shape. Typically a single phase fluid circulating through a metal black tube receiver, covered with a glass tube (with vacuum or air in the space between the receiver and cover) to decrease convective heat losses, is placed along the focal line of the receiver. The surface of receiver is typically covered with a selective coating that has a high absorptance for solar radiation, but low emittance for thermal radiation loss. It is sufficient to use a single axis tracking of the sun and thus long collector modules that are supported by pedestals are produced. PTSC with evacuated tubular receivers is the main technology currently used in solar thermal electrical power plants because of considerable experience with the systems and the development of small commercial industry to produce and market these systems.

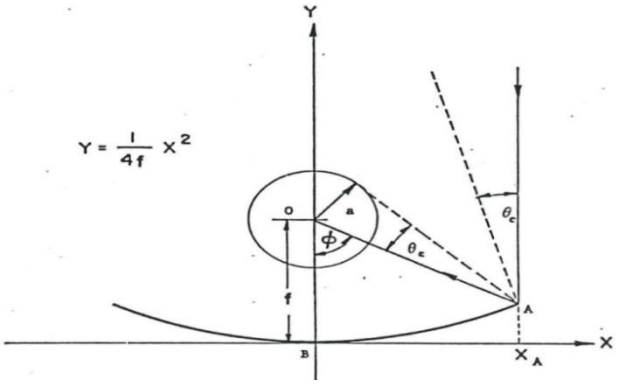

Figure 1.11 Parabolic trough collector with tubular absorber

Fresnel Lenses: Fresnel lenses, shown schematically in figure 1.12 can be used both in line and in point focus system. To minimize accumulation of dirt, the front surface should be smooth. The prism facets need not to be curved if their number sufficiently large (in the order of 100) or if high concentration is not needed. If the incident radiation is not parallel to the optical axis of a Fresnel lens, the focal length shortens and because of aberrations, the size of the focal spot increases.

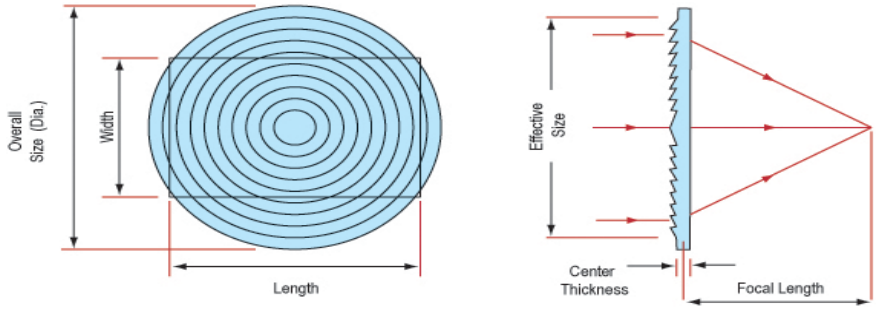

Figure 1.12 Fresnel lens

The most important factor is transmission losses of a Fresnel lens which is represented by reflection losses (unless antireflection coatings are used). The reflection losses at the back surface are larger because of greater incidence angles at the prism faces, and the exact value depends on the number of the lens. Some rays will be lost if the prism faces, as illustrated in figure 1.13a, with some production processes, the later defect can be avoided by the so-called undercut design of figure 1.13b. Additional losses arise from scattering or absorption the lens material. Figure 1.13c indicates typical loss factors encountered in cast acrylic lenses; in practice, overall transmission factors around between (0.85-0.88) are possible (Dickinson & Cheremisinoff, 1990).

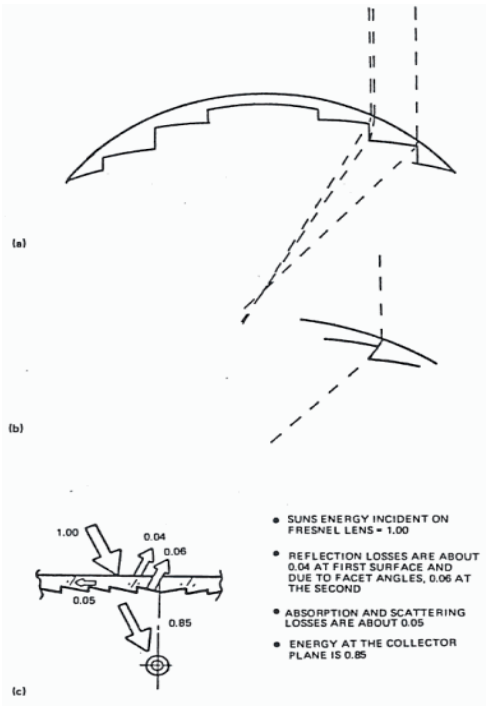

Figure 1.13 Typical losses in Fresnel lens

Paraboloidal Dish Concentrators: A major problem with linear arrays is that it is difficult to achieve the very high concentration that is required for high temperatures. So to achieve high concentration ratio to get high temperature, used paraboloidal dish concentrators there are concave- shaped discs, which remain constantly focused on the sun with the aid of sun-tracking devices. The curve of each dish concentrates make the sun's rays to focus in a small central point, thus reducing heat losses and enabling water (or other fluid) passing through that point to be heated to a high temperature, like it's illustrated in figure 1.14. A component that predicts the receiver aperture diameter and output power from a 2 axis sun-tracking dish collector has dish collector area, rim angle, surface slope error, and mirror reflectivity and percent capture by the receiver specified as parameters.

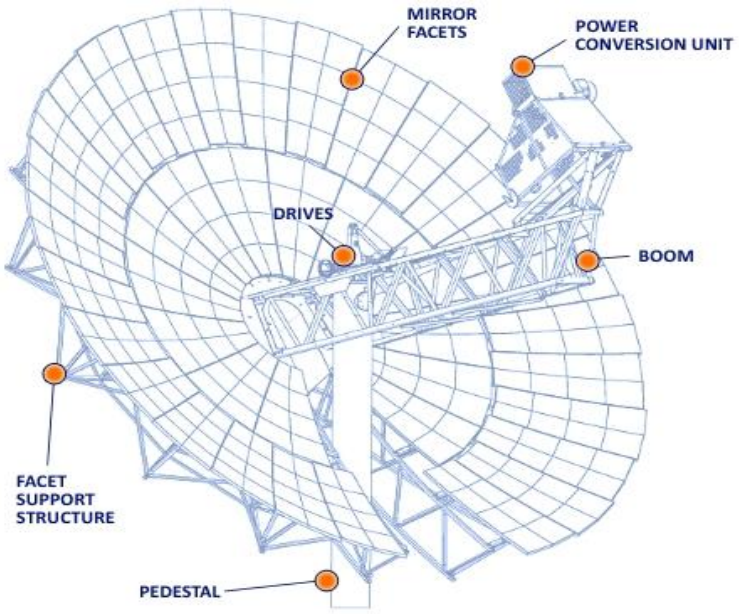

Figure 1.14 Paraboloidal dish concentrators

The direct beams are an input and the outputs are the receiver aperture size needed to achieve the percentage capture (this is fixed by the parameter values) and the power delivered to the receiver (which varies with the dish parameters and the beams radiation level) (Goswami, Kreith & Kreider, 2000).

Power Towers: The smooth optical surface of reflector or lens can be broken into segments, by a method invented by Fresnel. Optically a Fresnel mirror, shown

schematically in figure 1.15 can approximate a focusing parabola. The mirror segments are sufficiently large. Even with flat segments, the number of mirrors need to be large than about 100 meter for line-focus system or 1000 meter for point-focus system, because at that point the aberrations become comparable to the angular width of the sun. A detailed analysis of Fresnel mirrors is complicated shading and blocking effects. Shading occurs if direct sunlight fails to reach a mirror because the mirror fails to reach the absorber because it is intercepted by the back side of another mirror. In the interest of efficient mirror utilization, the reflector segments should be spaced far enough apart to minimize shading and blocking within the constraints of relative cost of total area and reflector area. The use of Fresnel reflectors brings to large installations because of reduced wind loading and simplified manufacture. For linear Fresnel reflectors, the tracking motion can be accomplished by mechanical linkage because all reflector segments undergo the same angular excursion (Rapp, 1981).

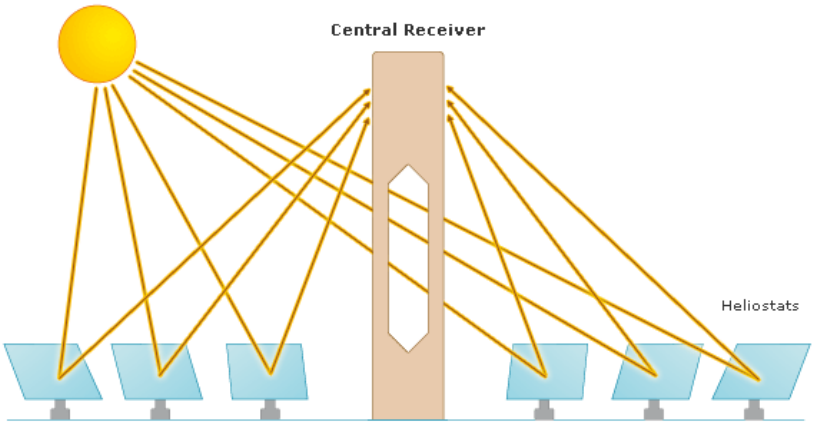

Figure 1.15 Solar tower systems

1.2.5.2.2 Moving Receiver and Fixed Concentrators. As an alternative to move a large reflector, one can design systems in which the reflector is fixed and only a small receiver needs to track the sun. Three such systems are known as follow,

Spherical Reflectors: Collimated radiation incident on a spherical reflector will, after one or several reflections cross the line that extends through the center of this sphere in the direction of the incident direction. Rays close to this line reach the

focus which is on the line, half-way between reflector and center of the sphere, as shown in figure 1.16. Other rays intersect this line between the focus and the aperture. Therefore, a receiver that extends from focus to the aperture will intercept all rays. Because of the spherical symmetry of the reflector, only the receiver needs to track if the radiation source moves. As a solar collector, such a system can attain geometric concentration ratios up to about 270. The flux concentration along the receiver is quite non uniform. Even though the focusing is independent of incidence angle, the affective aperture is not, that is illustrated in figure 1.17 where the reflector portion is inactive for the incidence angles shown (Böer & Duffie 1985).

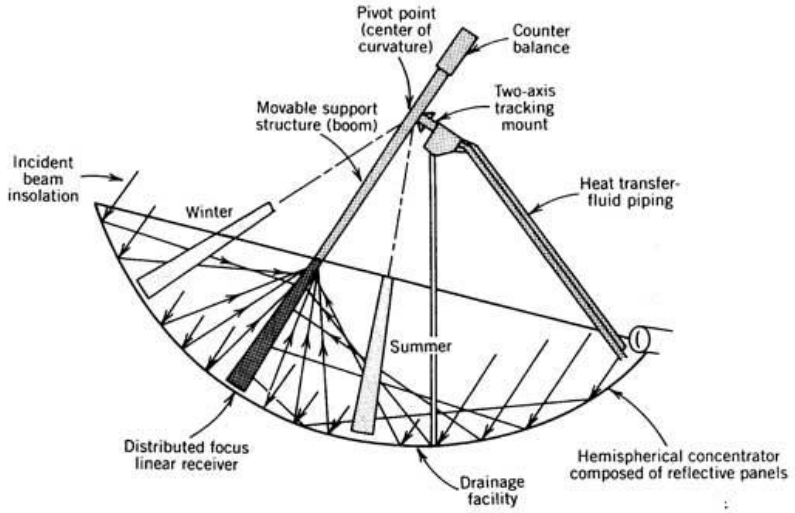

Figure 1.16 Fixed spherical reflectors with tracking receiver

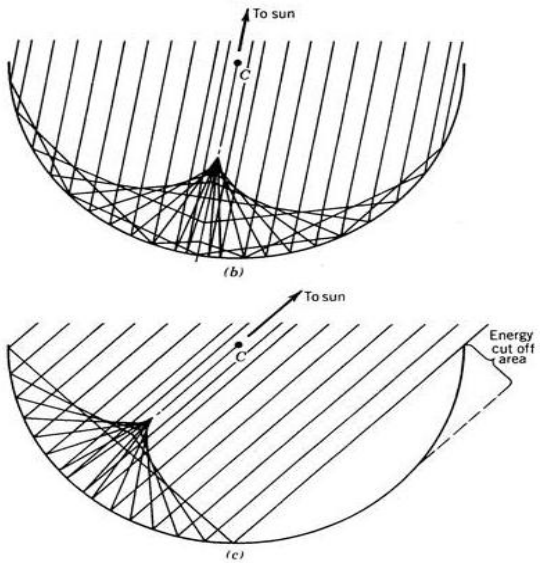

Figure 1.17 Fixed spherical reflectors with tracking receiver at off-normal incidence

Circular Cylindrical Reflector with Moving Receiver: The concentration ratio of such an arrangement is less than 2 and two low to be practical. However, as the ray trace a sufficiently large tubular absorber placed slightly below the focal line can intercept most of the reflected rays (Böer & Duffie 1985).

Reflector Slats on Circular Cylindrical Mount: This type scheme consists of narrow flat reflectors slats that are mounted on a circular cylindrical surface. The cross section is shown in figure 1.18 and 1.19.

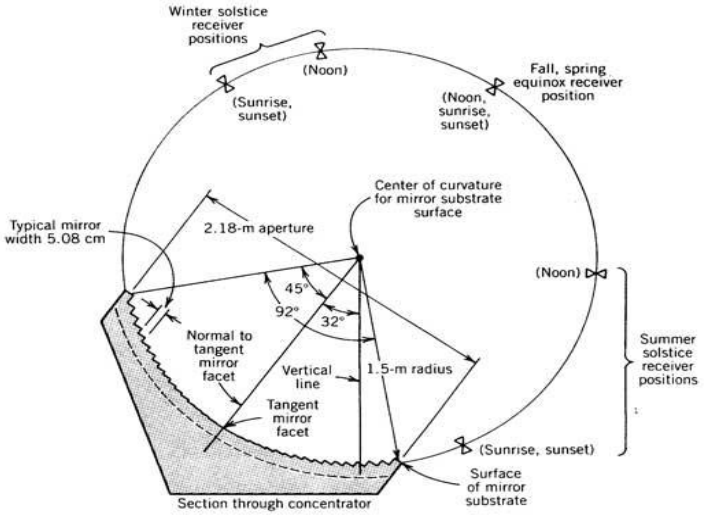

Figure 1.18 Cross section of fixed slat reflectors with tracking receiver

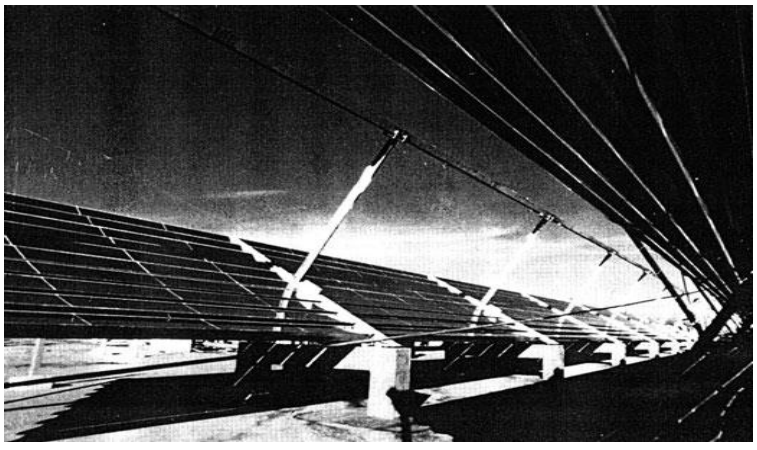

Figure 1.19 Fixed slat reflectors with tracking receiver

If the mirror slats have the correct slope, this system will always produce a perfect line focus (in the limit of infinitely narrow slats), regardless of incidence angle. The focus is on the same circle as the reflector slats (Böer & Duffie 1985).

1.3 Literature Studying in Parabolic Trough Solar Collectors

Concerning the design, construction and simulation of the parabolic trough collectors, there is a large number of publications about it.

Valladares and Velázquez (2008) have performed detailed numerical simulations of thermal and fluid-dynamic behavior of a single-pass and double-pass solar parabolic trough collector. The governing equations inside the receiver tube, together with the energy equation in the tube walls and cover wall and the thermal analysis in the solar concentrator were solved iteratively in a segregated manner. The effects of recycle at the ends on the heat transfer are studied numerically shown that the double-pass can enhance the thermal efficiency compared with the single-pass.

Kumar and Reddy (2008) have presented 3-D numerical analysis of the porous disc line receiver for solar parabolic trough collector. The influence of thermic fluid properties, receiver design and solar radiation concentration on overall heat collection is investigated. The thermal analysis of the receiver is carried out for various geometrical parameters such as angle (h), orientation, height of the disc (H) and distance between the discs (w) and for different heat flux conditions. The receiver showed better heat transfer characteristics; the top porous disc configuration having w = di, H = 0.5di and h = 30. The use of porous medium in tubular solar receiver enhances the system performance significantly.

Özturk (2004) has evaluated experimentally the energy end exergy efficiencies of the collector by design the low-cost parabolic-type solar collector (PTSC) and tested it. The experimental time period was from 10:00 to 14:00 solar time. During this period, it was found that the daily average temperature of water in the PTSC was 333 K and the daily average difference between the temperature of water in the cooking

pot and the ambient air temperature was 31.6 K. The energy output of the PTSC varied between 20.9 and 78.1 kW, whereas its exergy output was in the range 2.9–6.6 kW. The energy and exergy efficiencies of the PTSC were in the range, respectively, 2.8–15.7% and 0.4–1.25%.

Bakos, Ioannidis, Tsagas and Seftelis (2000) have developed and installed a PTSC which has an absorber tube with semi-insulation from the top side of it, and developed a simulation program calculates the outlet temperature and shows the efficiency of the proposed PTSC as a function of the outlet temperature, absorber tube diameter, the intensity of incoming solar radiation and the width of the parabolic collector.

Çolak (2003) has designed and constructed the parabolic solar collector in aim; to get high temperature range in suitable to technique, economic and environmental aspects and tested the beams intercept performance by laser ray testing equipment. Moreover he has performed a simulation program to calculate the performance of the PTSC system and compared it with the experimental results.

Valan Arasu and Sornakumar (2006) have developed a PTSC with fiberglass reinforced parabolic reflector. The total thickness of the parabolic reflector is 7 mm. The concave surface where the reflector is fixed is manufactured to a high degree of surface finish. The fiberglass reinforced parabolic trough was tested under a load corresponding to the force applied by a blowing wind with 34 m/s. Distortion of the parabola due to wind loading was found to be within acceptable limits. The thermal performance of the newly developed fiberglass reinforced parabolic collector was determined according to ASHRAE Standard 1986 method of testing to determine the thermal performance of solar collectors.

Riffelmann, Neumann and Ulmer (2004) have developed two methods of measuring the solar flux in the focal region in order characterize of the optical performance and detection of optical losses of parabolic trough collectors which are very important issues in order to improve the optical efficiency of these systems and

to ensure the desired quality in solar power plants. The parabolic-trough-flux-scanner method is a solar flux density measurement instrument which can be moved along the receiver axis. The sensor registers the flux distribution in front and behind the receiver with high resolution. The resulting flux maps allow to calculate the intercept factor and to analyze the optical properties of the collector at the finally interesting location, i.e. around the receiver. The camera-target-method uses a diffuse reflecting lambertian target and a calibrated camera which takes pictures of it. The target is held perpendicular to the focal line surrounding the receiver. With the resulting images of this fast and easy method it is possible to visualize the paths of the reflected rays close to the receiver and to detect local optical errors.

Rolim, Fraidenraich and Tiba (2007) have developed an analytic model for a solar thermal electric generating system with parabolic trough collectors. The energy conversion of solar radiation into thermal power along the absorber tube of the parabolic collector is studied, taking into consideration the non-linearity of heat losses and its dependence on the local temperature. They simulated the efficiency curves of collectors with evacuated and non-evacuated absorbers and compared with experimental results. Three fields of different collectors were considered, the first field with evacuated absorbers, the second with non-evacuated absorbers and the third with bare absorbers. Finally, the output power of the plant is analyzed as a function of the evaporation temperature of the water-vapor fluid.

Spirkl, Ries, Muschawech and Timinger (1996) have developed parabolic trough solar collectors with a secondary reflectors, which increase the concentration of the solar beams onto the absorber tube. They optimized numerically various secondary concentrators and investigated their performance by means of ray tracing, taking into account reflectivity losses, shading and the effective solar angular distribution. They found that the secondary reflector significantly improves the concentration and is essentially optimal in a wide class of shapes, even at efficiencies close to unity.

Bakos (2005) has performed an experimental study to investigate the effect of using a continuous operation two-axes tracking on the solar energy collected. The

collected energy was measured and compared with that on a fixed surface tilted at 40^{o} towards the South. The results indicate that the measured collected solar energy on the moving surface was significantly larger (up to 46.46%) compared with the fixed surface.

Pfander, Lupfert and Pistor (2004) have performed an experimental study to investigate the temperature distribution on solar trough absorber tubes in order to determines thermal losses and hotspots can lead to material stress and limit absorber tube lifetime. The concentrated solar radiation, however, makes it difficult to determine the temperature on solar absorbers. Temperature sensors that require contact to the measurement object are not appropriate and even pyrometry fails, when external light sources interfere. Only solar-blind pyrometry offers reliable temperature readings without perturbation through reflected solar radiation.

Tyagi et al. (2006) have evaluated the exergetic performance of concentrating type solar collector and studied the parametric using hourly solar radiation. The exergy output is optimized with respect to the inlet fluid temperature and the corresponding efficiencies are computed. Although most of the performance parameters, such as, the exergy output, exergetic and thermal efficiencies, stagnations temperature, inlet temperature, ambient temperature etc. increase as the solar intensity increases but the exergy output, exergetic and thermal efficiencies are found to be the increasing function of the mass flow rate for a given value of the solar intensity. The performance parameters, mentioned above, are found to be the increasing functions of the concentration ratio but the optimal inlet temperature and exergetic efficiency at high solar intensity are found to be the decreasing functions of the concentration ration. On the other hand, for low value of the solar intensity, the exergetic efficiency first increases and then decreases as the concentration ratio is increased. Again it is also observed that the mass flow rate is a critical parameter for a concentrating type solar collector and should be chosen carefully.

Eskin (1998) has performed a study about unsteady, one-dimensional performance analysis of cylindrical parabolic concentrating collectors through the first and second

laws of thermodynamics. These laws, together, help to define the optimum system that satisfies the imposed thermal and economical constraints and minimizes exergy loss. The analysis considers the thermal masses of the absorber pipe, Pyrex envelope and the working fluid of the system individually, in an unsteady state. The instantaneous exergetic and energy efficiencies for the cylindrical parabolic collectors are compared for daily insulation at different flow rates.

Li and Wang (2006) have been used two types of solar evacuated tube to measure their heating efficiency and temperature with fluids of water and N_2 respectively with a parabolic trough concentrator. Experiments demonstrate that both evacuated tubes present a good heat transfer with the fluid of water, the heating efficiency is about 70–80%, and the water is easy to boil when liquid rate is less than 0.0046 kg/s. However, the efficiency of solar concentrating system with evacuated tube for heating N_2 gas is less than 40% when the temperature of N_2 gas reaches 320–460 ^{o}C. A model for evacuated tube heated by solar trough concentrating system has been built in order to further analyze the characteristics of fluid which flow evacuated tube. The characteristics of fluid via evacuated tube heated by solar concentrated system are analyzed under the varying conditions of solar radiation and trough aperture area.

Qu, Archer and Masson (2006) have programmed a performance model for solar thermal collector based on a linear, tracking parabolic trough reflector focused on a surface-treated metallic pipe receiver enclosed in an evacuated transparent tube at steady state, single dimensional model comprises the fundamental radiative and convective heat transfer and mass and energy balance relations programmed in the Engineering Equation Solver, EES. It considers the effects of solar intensity and incident angle, collector dimensions, material properties, fluid properties, ambient conditions, and operating conditions on the performance of the PTSC.

1.4 Aim of Study

We are working to reduce the use of fossil fuel which used in our daily lives by using the renewable energies such as solar radiation which have high energy in most regions of the globe, which we are working to achieve them through the design and development the parabolic trough solar collectors. This system is working to focus the sun's direct beams on the absorber tube thus serve to heat the forced circulation working fluid passing through it to temperatures ranging between 150/180 ^{o}C, which can be used in the absorption refrigeration cycles moreover to used in daily lives.

In this study, An analytic model for parabolic trough collectors was developed. The energy conversion of solar radiation into thermal power along the absorber tube of the parabolic collector is studied, taking into consideration the nonlinearity of heat losses and its dependence on the operating temperature. The PTSC performance model has been programmed for solar thermal collector based on a linear, tracking parabolic trough reflector focused on a selective surface absorber tube (receiver) enclosed in an evacuated transparent glass tube: a Parabolic Trough Solar Collector PTSC. This steady state, single dimensional model comprises the fundamental radiative and convective heat transfer and energy balance relations programmed in the Visual Basic 6.0. It considers the effects of ambiance conditions, design conditions, material properties, fluid properties and operating conditions on the performance of the PTSC. The numerical model has been carefully validated with experimental data obtained by Sandia National Laboratories. Moreover, Depending on the typical meteorological year data for Izmir city and by using the mathematical model, the mean hourly, daily, monthly and annual output power of the PTSC which designed in this study was invistigated.

CHAPTER TWO
SOLAR GEOMETRY AND IRRADIANCE MEASUREMENT

2.1 The Solar Constant

The sun is sphere of intensely hot gaseous matter with a diameter of 1.39 x 10^9 m and is, on the average, 1.5 x 10^{11} m from the earth. As seen from the earth the sun rotates on its axis about once every four weeks. However, it does not rotate as a solid body: the equator takes about 27 days and the Polar Regions take about 30 days for each rotation.

The sun has an effective blackbody temperature of 5777 K. The temperature in the central interior regions is variously estimated at (8 x 10^6 to 40 x 10^6) K and the density is estimated to be about 100 times that of water. The sun is, in effect, a continuous fusion reactor with its constituent gases as the "containing vessel" retained by gravitational forces. Several fusion reactions have been suggested to supply the energy radiated by the sun.

Figure 2.1 shows schematically the geometry of the sun-earth relationships. The eccentricity of the earth's orbit is such that the distance between the sun and the earth varies by 1.7%. At a distance of one astronomical unit, 1.495 x 10^{11} m, the mean earth-sun distance, the sun subtends an angle of 32' (Duffie & Beckman, 1991).

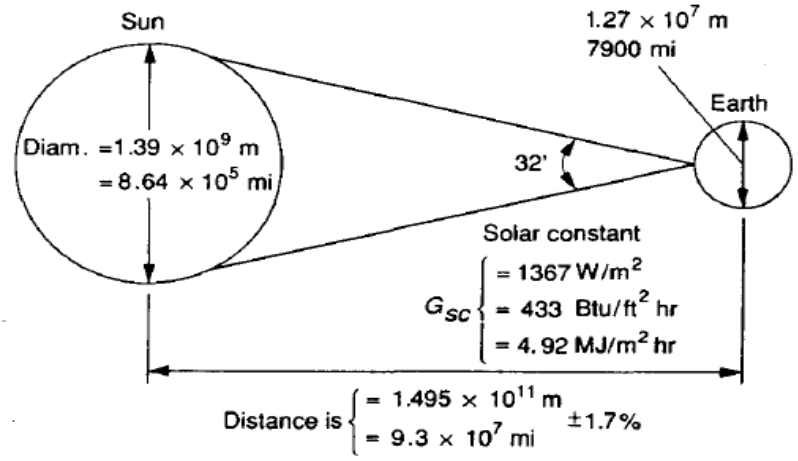

Figure 2.1 Sun-earth relationships

2.2 Motion of the Earth about the Sun

The earth makes one rotation about its axis every 24 hr and completes a rotation about the sun in approximately 365.25 days. The earth moves about the sun in an approximately circular path, with the sun located slightly off center of the circle. This offset is such that the earth is closest to the sun near January 1 and furthest from the sun near July 1. This distance in January is about 3.3% closer, and since the solar intensity is proportional to the inverse square of the distance, the intensity is about 7% higher in January than in July. The earth's axis of rotation is tilted at 23.45° with respect to its orbit plane about the sun. This tilt remains fixed in space and is the cause of the seasons as shown in figure 2.2. (Dickinson & Cheremisinoff, 1990)

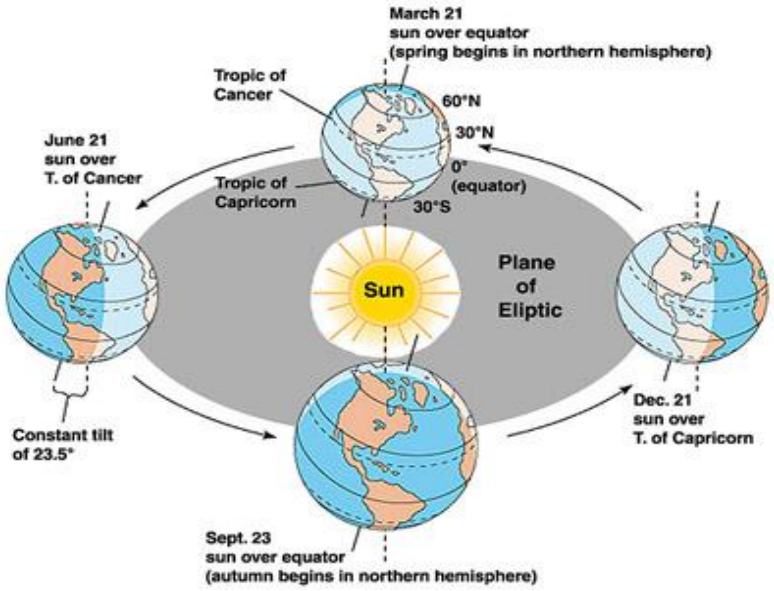

Figure 2.2 Movement of the earth around the sun

2.3 Solar Radiation

The solar constant, which is defined as the average energy flux incident on a unit area perpendicular to the solar beam outside the Earth's atmosphere has been measured to be S = 1367 W/m^2. The solar radiation incident on a collector on the Earth's surface is affected by a number of mechanisms, as shown in figure 2.3. The total radiation consisting of these three components is called **global** radiation.

Although it varies significantly, a solar irradiance value of 1 kW/m^2 has been accepted as the standard for the Earth's surface, in the figure 2.4, we can see the world solar energy distribution.

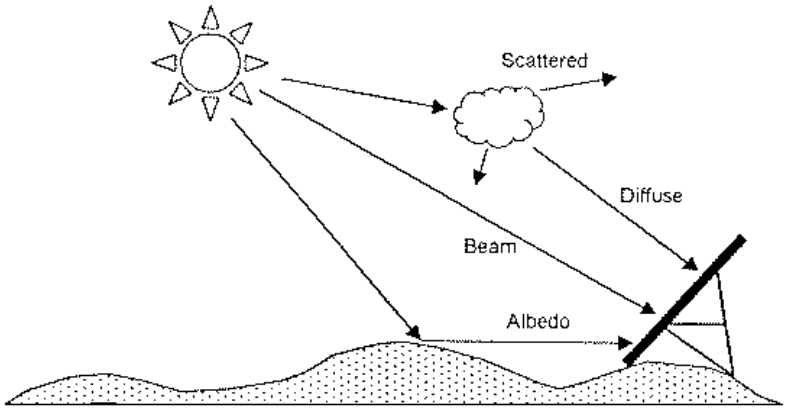

Figure 2.3 The main component of solar radiation in the atmosphere

Calculation of the incident radiation for a particular site from theoretical methods is extremely difficult as it is highly dependent on variables such as local weather conditions, the composition of the atmosphere above the site, and the reflectivity of surrounding land. For this reason, the design of a photovoltaic system relies on the input of experimental data measured as close as possible to the site of the installation. Consequently, the solar beams for the city of Izmir city have measured by using the pyranometers as seen in following sections.

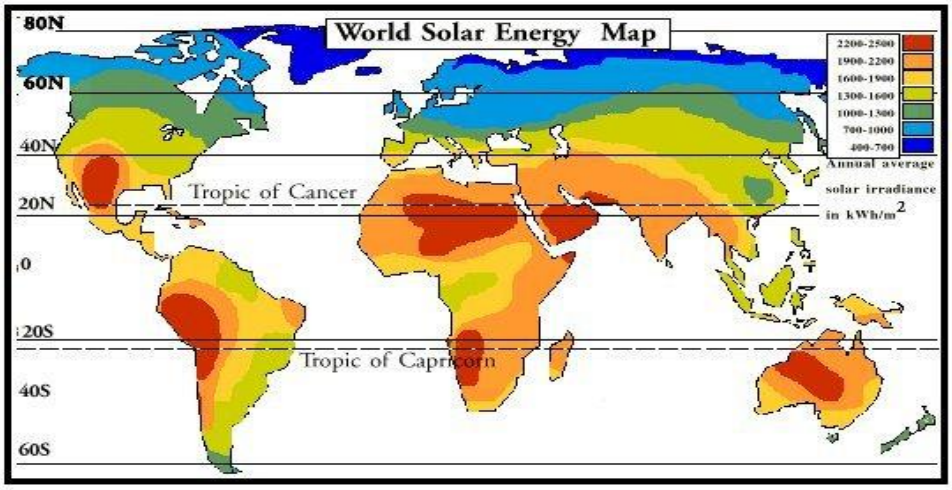

Figure 2.4 The solar irradiance figures indicate the average annual energy available per square meter

This data is generally given in the form of global and beam irradiation on a horizontal surface for each day at a particular location, or for a representative day of every month. According to the concentrator types of solar collectors, the beam radiation is the matter portion of the global irradiation from the diffuser because of the regular irradiance on the earth surface. Therefore, the correct direction of the beam radiation has to determine. So, it must be known some definitions related to directly (beam) radiation, in order to determine their direction on the earth surface (Duffie & Beckman, 1991).

2.4 Direction of Beam Radiation

The geometric relationships between a plane of any particular orientation relative to the earth at any time (whether that plane is fixed or moving relative to the earth) and the incoming beam solar radiation, that is, the position of the sun relative to that plane, can be described in terms of several angles (Benford & Bock, 1939). Some of these angles are indicated in the figure 2.5.

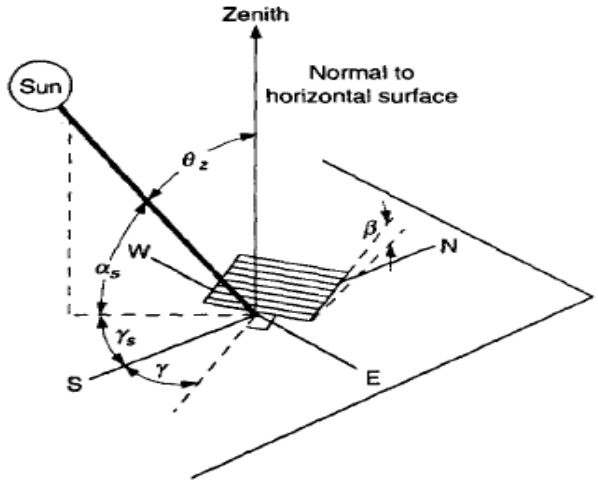

Figure 2.5 The angles related with the direction of solar beam irradiance (Duffie & Beckman, 1991)

The angles are as follows,

- **Latitude [ϕ]**: the angular location north or south of the equator, north positive; ($-90^o \leq \varphi \leq 90^o$).

- **Declination [δ]**: The angle that the sun's rays make with the equatorial plane at solar noon is called the angle of declination. The angle declination varies from 23.45° on June 21, to 0 on September 21, to 23.45° on December 21, to 0 on March 21, north positive. The declination can be found from the equation of (Cooper, 1969).

$$\delta = 23.45 \sin\left(360 \frac{284 + n}{365}\right) \tag{2.1}$$

Where:
n: the day of the year

- **Slope [β]**: the angle between the plane of the surface and the horizontal ($0^o \leq \beta \leq 90^o$).
- **Surface azimuth angle [γ]**: the deviation of the projection on a horizontal plane of the normal to the surface from the local meridian, with zero due souths, east negative.
- **Hour angle [ω]**: the angular displacement of the sun east or west of the local meridian due to rotation of the earth on its axis at 15 per hour, morning negative, afternoon positive.
- **Angle of incidence [θ]**: the angle between the beam radiation on a surface and the normal to that surface.

Additional angles are defined to describe the position of the sun in the sky;

- **Zenith angle [θ_z]**: the angle between the vertical and the line to the sun, i.e. the angle of incidence of beam radiation on a horizontal surface.

$$\cos\theta_z = \cos\phi \cos\delta \cos\omega + \sin\phi \sin\delta \tag{2.2}$$

- **Solar altitude angle [α_s]**: the angle between the horizontal and the line to the sun, i.e. the complement of the zenith angle.

- **Solar azimuth angle [γ_s]**: the angular displacement from south of projection of beam radiation on the horizontal plane, east of south is negative. To calculate γ_s, we must know in which quadrant the sun will be. This is determined by the relationship of the hour angle ω to the hour angle ω_{ew} (when the sun is due east or west). A general formulation for γ_s (Braun & Mitchell, 1983) is written in terms of γ_s' (a pseudo solar azimuth angle in the first of forth quadrant).

$$\gamma_s = C_1 C_2 \gamma_s' + C_3 \left(\frac{1 - C_1 C_2}{2} \right) 180 \tag{2.3}$$

Where,

$$\sin \gamma_s' = \frac{\sin \omega \cos \delta}{\sin \theta_z} \tag{2.4}$$

$C_1 = 1$ if $| \omega | < \omega_{ew}$, -1 otherwise
$C_2 = 1$ if $\phi \ (\phi - \delta) \geq 0$, -1 otherwise
$C_3 = 1$ if $\omega \geq 0$, -1 otherwise

$$\omega_{ew} = \frac{\tan \delta}{\tan \phi} \tag{2.5}$$

The parabolic solar collectors track the sun by moving in prescribed ways to minimize the angle of incidence of beam radiation on their surface and thus maximize the incident beam radiation and those ways are;

- For a plane rotated about a horizontal east-west axis with continuous adjustment to minimize the angle of incidence,

$$\cos \theta = (1 - \cos^2 \delta \sin^2 \omega)^{1/2} \tag{2.6}$$

The slope of this surface become,

$$\tan\beta = \tan\theta_z \left|\cos\gamma_s\right| \tag{2.7}$$

- For a plane rotated about a horizontal north-south axis with continuous adjustment to minimize the angle of incidence,

$$\cos\theta = \left[\cos^2\theta_z + \cos^2\delta \sin^2\omega\right]^{1/2} \tag{2.8}$$

The slope of this surface become,

$$\tan\beta = \tan\theta_z \left|\cos(\gamma - \gamma_s)\right| \tag{2.9}$$

- For plane with a fixed slope rotated about a vertical axis, the angle of incidence is minimized when the surface azimuth and solar azimuth angles are equal, so the angle of incidence is,

$$\cos\theta = \cos\theta_z \cos\beta + \sin\theta_z \sin\beta \tag{2.10}$$

2.5 Measured the Global and Beam Irradiation

2.5.1 Measurement Global Irradiance by Black and White Pyranometers

Black and white Pyranometers is used for measuring global and reflected global radiation and solar radiation on surfaces inclined to the horizontal. The solar radiation coming from the whole sphere and received on a horizontal surface in the spectral range from 0, 3 - 3 μm is called global radiation. These include radiation received directly from the sun (beam irradiance) and also diffuse sky radiation that has been scattered in traversing the atmosphere. The measuring principle of this type of pyranometers is the measurement of the temperature difference between white and black painted sectors. By that means the measuring result is not affected from ambient temperature. A precisely cut dome shields the sensing elements from environmental factors. The black and white pyranometers is shown in figure 2.6. The

sensing element of the instrument consists of a 12 sector star, the sections of which are painted with a special white reflective paint and an absorbing black paint. When exposed to solar radiation the black sectors are heated more than the white ones and this temperature difference is determined by the thermocouples embedded below the star. A precisely cut dome is made of optical glass shields the sensing element from wind and moisture. One threaded ring and two 0-rings clamp the glass of the instrument base providing a watertight seal. A desiccator with Silica gel prevents condensation within the casing. The white painted base shields the desiccator and prevents an overheating of the instrument. A watertight cable outlet prevents intrusion of ambient air. For leveling the instrument is equipped with a spirit level and 3 leveling screws (Meteoclima).

Figure 2.6 The black and white pyranometer

2.5.2 Measurement Beam Irradiance by Pyrheliometer

A pyrheliometer is an instrument designed specifically to measure the direct beam solar irradiance with a field of view limited to 5. This is achieved by the shape of the collimation tube, with precision apertures, and the detector design. The front aperture is fitted with a quartz window to protect the instrument and to act as a filter that passes solar radiation between 200 nm and 4000 nm in wavelength. A pyrheliometer

needs to be pointed at the sun at all times so that the solar disk always falls within the field of view of the instrument. A two-axis tracking mechanism is incorporated to maintain the sun's disc within the acceptance cone of the instrument thus the direct solar irradiance can be measured very accurately during the whole day. This device, shown in figure 2.7 is essentially a thermopile pyranometer placed at the end of a long tube which is aimed at the sun.

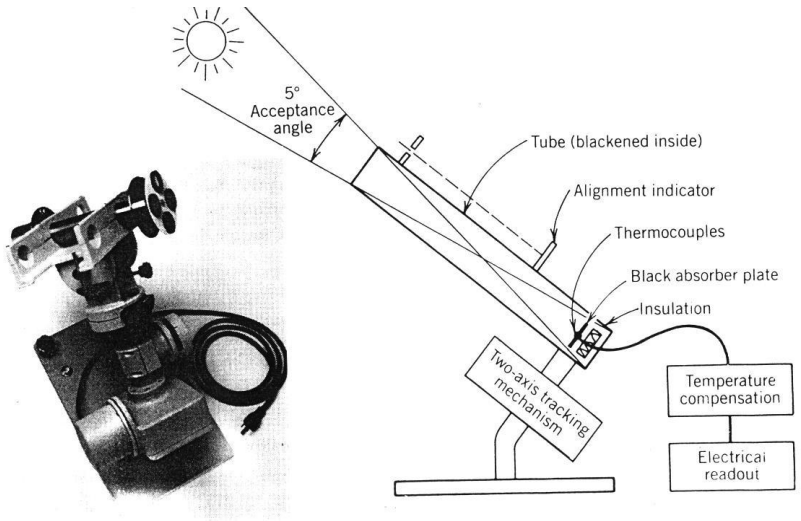

Figure 2.7 The pyrheliometer

Since the sun's disc is approximately 0.5 degree from limb to limb, the normal incidence pyrheliometer not only measures the direct radiation coming from the disc, but also most of the circumsolar radiation. As discussed in the following paragraphs, the circumsolar component becomes significant in atmospheres with considerable aerosols, where this instrument may measure more energy than is available to most concentrating collectors. It appears, however, that the 5-degree acceptance angle, is needed to eliminate the need for an extremely accurate normal incidence pyrheliometer orientation and tracking system, and is therefore an operational minimum for this type of instrument (Kipp & Zonen).

CHAPTER THREE
THE MATHEMATICAL MODEL, THE OPTICAL AND THERMAL ANALYSES FOR THE SUN TRACKER PARABOLIC TRUOGH SOLAR COLLECTOR

In this section, according to the structure of the parabolic solar collector systems, mathematical equations which define the optical and heat transfer was derived. To identified and minimized the various optical and thermal losses, the deriving equations were used with the prepared computer programs, and the detailed simulations analyses for the optical and thermal performance behavior of the system were done. By comparing the simulation model results with the measurement results which take from the literature, the derived mathematical model was verified.

3.1 The Energy Balance and System Structure for the Parabolic Solar Collector

The parabolic solar collector systems structure which is type of the concentrate solar collectors that is gone to design it in this study given below by the schematically figure 3.1.

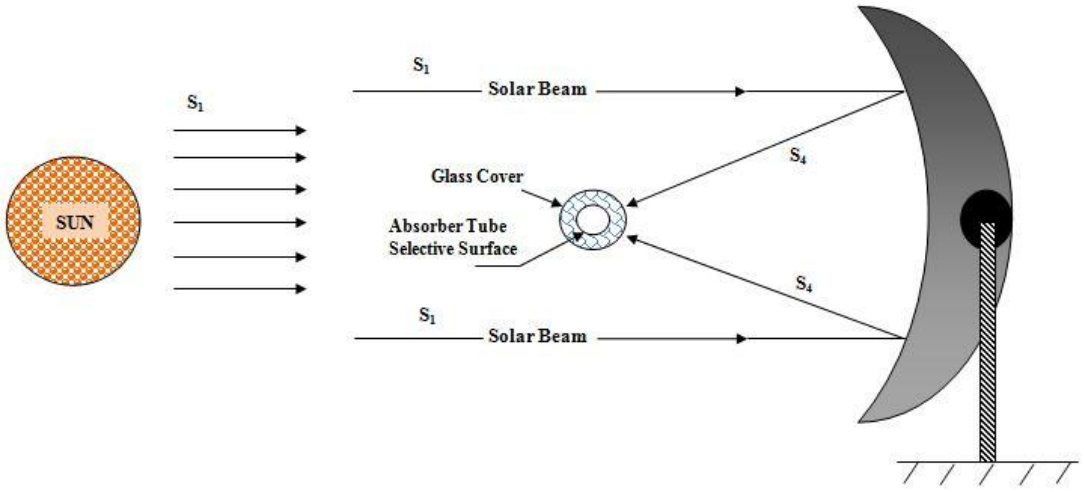

Figure 3.1 A schematic for the parabolic trough solar collector

The energy flow on the collector which is accepted as one-dimensional and steady is defined in two parts. In the first part, the solar beams losses which are determining

the collector optical performance were investigated. These losses consist of the following types.

i. The beam losses arise by not track the sun in full (1-K).
ii. The beam reflection losses which are depending on the surface property of the coating reflecting surface ($1-\rho_{ref}$).
iii. The intersection losses arise by not focus of the beam in full on the absorb tube which is caused by structural and operational reasons of the reflective surface of the collector ($1-\gamma$).
iv. The beam-transmission losses that depends on the material property of the glass cover of the absorb tube ($1-\tau_{gl}$).
v. The beam losses resulting from lack of absorption of the full beam that depend on the property of the material properties of the selective coated surface for the absorber tube ($1-\alpha_{abs}$).

In the second part, the thermal losses (Q_L) of the collector which is defining the thermal performance and occurring from the selective surface of the absorber tube to the environment which depends on operational and environmental factors were investigated.

The beams-heat energy flow that related with the concentrator type solar collectors as shown in the figure 3.2, after removing the atmospheric radiation losses from the constant flow of the solar beams at the entrance of the atmosphere S, the solar beams will reach the collector location is S_1. When the beams losses resulting from tracking the sun (1-K) are removed, the amount of the solar beams reaching the reflective surface is S_2, and when the reflection losses ($1-\rho_{ref}$) are removed, the rest is the amount of the beams which direct to the focal point is S_3, when the intersection losses ($1-\gamma$) have removed, the amount of the beams which reach to the glass cover is S_4. After removing the transmission losses ($1-\tau_{gl}$) from the last amount, the beams on the absorber tube remain is S_5. After removing the losses resulting from lack of absorbing of the full beam ($1-\alpha_{abs}$), the solar thermal energy that is stored in the absorber tube $S_6 = Q_G$ remains. This heat is transferred to the working fluid which is

passing through the absorber tube by the convection. The solar heat which doesn't transferred to the working fluid form the collector is the thermal losses (Q_L).

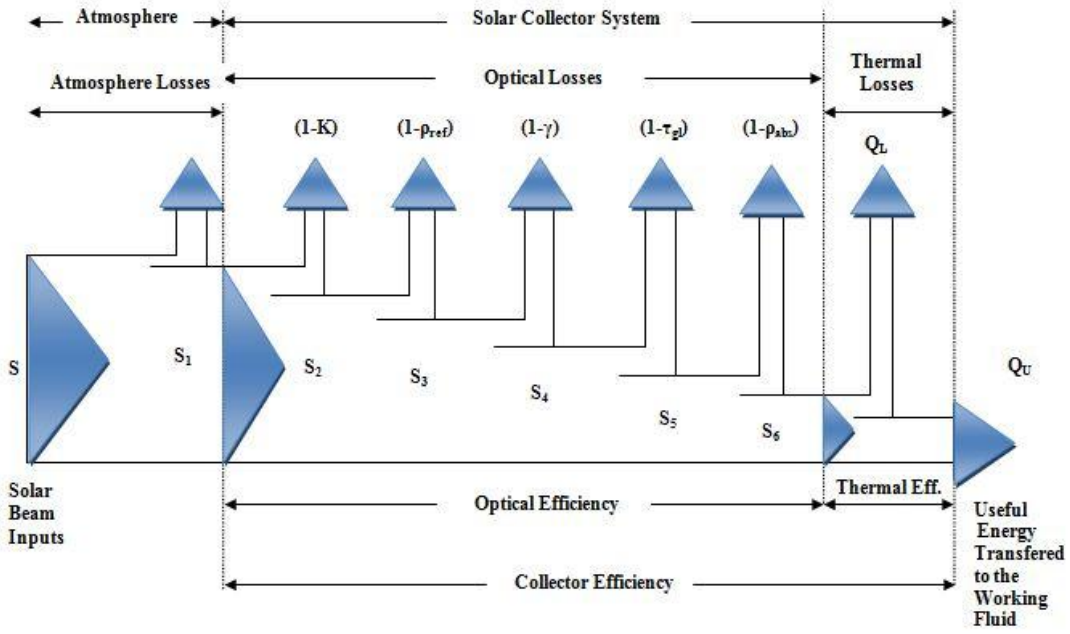

Figure 3.2 A schematic of the beams-heat energy flow that related with the concentrator type solar collectors (Çolak, 2003)

The convection and radiation heat losses (Q_L) from the collector to the environment depend on many variables. The most important of these are, solar radiation intensity, ambient temperature, wind speed, the diameter and location of the absorber tube and glass cover, transparent glass cover features, absorber surface's absorpttance and emissivity value, the thermal conductivity of the air which fills the space between the glass cover and the absorber tube, the wall thickness of the pipes, the heat transfer capability of the working fluid. By keeping all these variables into consideration the thermal analysis of the collector was made.

The net amount of the heat which transfers into the fluid by the collector (Q_U) is founded by removing the heat losses (Q_L) from the gross energy which is transformed from the solar radiation on the absorber surface (Q_G). The net amount of the heat which transfers into the fluid by the collector is;

$$Q_U = m.c.\Delta T \tag{3.1}$$

The gross energy which absorbed by the absorber tube is calculated according to the PTSC optical efficiency as illustrated above to be,

$$Q_G = S_1.\eta_{op} \tag{3.2}$$

$$Q_U = Q_G - Q_L \tag{3.3}$$

3.2 The Beam Transfer and the Optical Losses Analyses for the Sun Tracker Parabolic Trough Solar Collectors

The primary solar radiation input S_1 which falls on the solar collector (Refer to figure 3.2) is determined by removing the atmospheric losses from the solar constant (S=1367 W/m^2) (Duffie & Beckman, 1991) which defined at the entrance of the atmosphere. And this value S_1 is determined by the direct beam measurement at the collector place.

Optical analysis is the computation of the optical losses in the reflective surface, glass cover and selective absorption surface, As was discussed in the figure 3.2, the solar beams that reach on the elements of the collector system are listed below.

S_1: Direct radiation measured in the collector position.
S_2: The solar beams which is falling on the reflective surface.
S_3: The redirected solar beams from the reflective surface into the focal point.
S_4: The solar beams which intersection the glass cover.
S_5: The solar beams which falling on the absorber tube surface.
S_6: The stored solar heat resulting from absorbing the heat energy by the absorber tube.

The optical performance is the ratio of the solar heat which is transformed from the solar beams in the absorber tube ($S_6 = Q_G$) into the primary solar radiation input to the entrance of the solar collector S_1 and it can be defined as follows.

$$\eta_{op} = \frac{S_6}{S_1} = \prod_{i=1}^{n=5} \eta_{op_i} = \eta_{op_1}.\eta_{op_2}.\eta_{op_3}.\eta_{op_4}.\eta_{op_5} \tag{3.4}$$

Here,

$$\eta_{op_i} = \frac{S_{i+1}}{S_i} \tag{3.5}$$

The optical performances which are generally defined in the equation 3.4 are described below.

$\eta_{op_1} = \frac{S_2}{S_1} = K$: It is the Incident Angle Modifier Factor which describes the optical efficiency of the solar tracking mechanism

$\eta_{op_2} = \frac{S_3}{S_2} = \rho_{ref}$: Describes the optical performance of the reflected surface, show the surface reflective value

$\eta_{op_3} = \frac{S_4}{S_3} = \gamma$: Depends on the reflected surface deformations and the surface pollution and etc factors. Describes reflected surface focus efficiency

$\eta_{op_4} = \frac{S_5}{S_4} = \tau_{gl}$: Describes the transmission feature of the glass cover, and give the optical efficiency of the beams transmission

$\eta_{op_5} = \frac{S_6}{S_5} = \alpha_{abs}$: Show selective surface absorber tube’s beam absorptance value and describes the optical efficiency of the beams absorption

So, the overall optical efficiency which is defined in equation 3.4 can be written as below.

$$\eta_{op} = K.\rho_{ref}.\gamma.\tau_{gl}.\alpha_{abs} \tag{3.6}$$

Solar beams can be condensed by using focused spot lens or an axial-oriented parabolic reflector. The parallel solar beams condense in both focal point and linear axis. Concentrated solar beams are collected ideally at a focal spot in the three-dimensional concentrators and at a focal linear axis in two-dimensional concentrators. The absorber surfaces which define as receiver in the literature are placed in focal spot or linear axis in suitable geometry.

One of the most important concepts in the solar collectors is the concentration ratio, in the literature two different definitions are used for concentration ratio. These are, geometric and solar beams intensity concentration ratio. Geometric concentration ratio can be defined as the ratio of the collector's aperture area A_{ref} to the absorbing surface area A_{abs}, so the geometric concentrate ratio is:

$$C = \frac{A_{ref}}{A_{abs}} \tag{3.7}$$

And solar beams intensity concentration ratio is the ratio of the solar beams intensity to the solar beams intensity which is falling on the collector surface. In general, the solar beams intensity concentration ratio is used for solar cells, and the geometric concentration ratio is used for solar collectors.

Concentrate ratio of the circle receiver surface for paraboloidal concentrator's reflector which is shown in figure 3.3 can be given as below (Kılıç & Öztürk, 1983).

$$C = \frac{A_{ref}}{A_{abs}} = \left(\frac{D}{d}\right)^2 \tag{3.8}$$

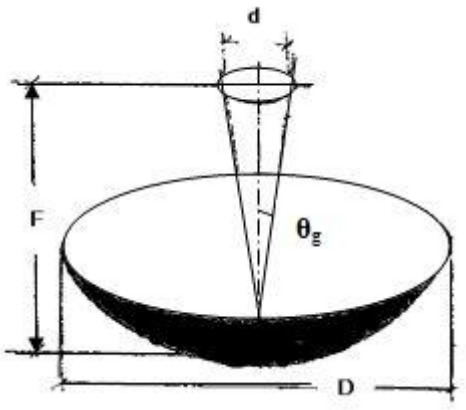

Figure 3.3 The paraboloidal dish concentrators

And the concentration ratio of cylinder concentrators which is shown in figure 3.4 can be given as below (Kılıç & Öztürk, 1983).

$$C = \frac{W_{ref}}{\pi D_{absOu}} \tag{3.9}$$

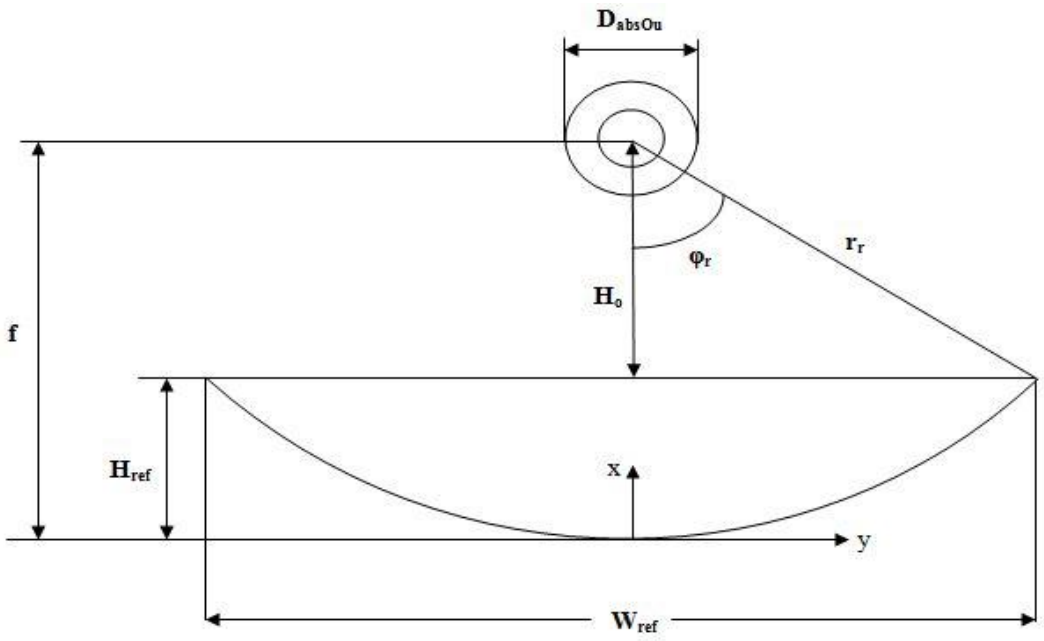

Figure 3.4 The cylindrical parabolic collector

To increase concentrator collector efficiency, the solar beams must be falling parallel to the optical axis in the three-dimension collectors or perpendicular to the

optical plane in the two dimension collectors. And that can be achieved by good tracking to the sun. The variation between the solar heat which is transferred to the working fluid and the concentrate ratio can be seen in figure 3.5 (Kılıç & Öztürk, 1983).

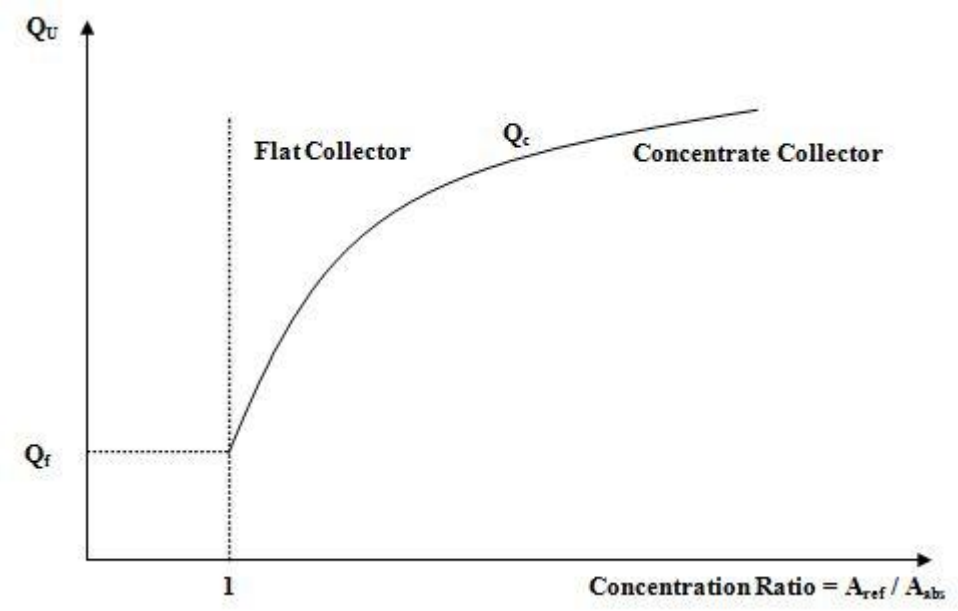

Figure 3.5 The variation of the concentration ratio with the solar heat which transferred to the working fluid

As seen above the efficiency can increase as the concentration ratio increases on condition that the heat losses decrease. The main factors that affect the collector efficiency are the reflector surface, selective absorbing surface and glass cover dimensions, optical features and the geometry of the receiver.

The solar beams transfer mechanism for the parabolic solar collector according to the investigated optical analyses above can be seen in figure 3.6. In this analysis the direct solar beams are given as $S_1 = I_d$ at the collector position.

The optical balance at the reflector surface: $\alpha_{ref} + \rho_{ref} = 1; \tau_{ref} = 0$ (3.10)

The optical balance at the glass cover: $\alpha_{gl} + \rho_{gl} + \tau_{gl} = 1; \rho_{gl} \approx 0; \alpha_{gl} + \tau_{gl} = 1$ (3.11)

The optical balance of selective surface absorber tube: $\alpha_{abs} + \rho_{abs} = 1; \tau_{abs} = 0$ (3.12)

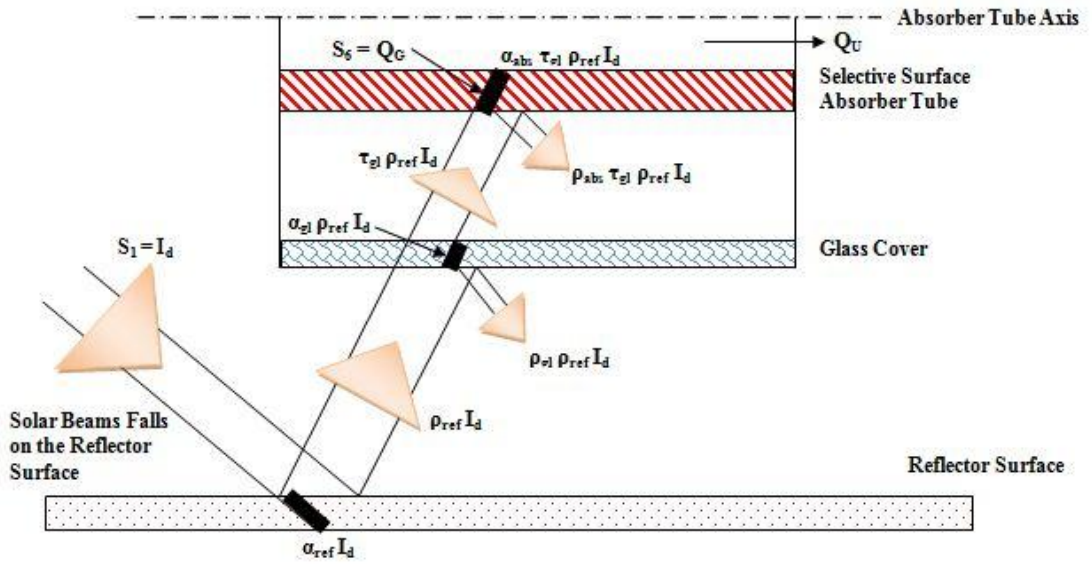

Figure 3.6 The beams transfer and optical losses in the parabolic trough solar collector

The direct beam which falls on the reflector surface I_d;

The reflecting part from the reflector surface = $\rho_{ref} I_d$ (3.13)

The part which takes in by the glass cover = $\tau_{gl}\rho_{ref} I_d$ (3.14)

The absorption part by the selective surface absorber tube = $\alpha_{abs}\tau_{gl}\rho_{ref} I_d$ (3.15)

Accordingly, the solar radiation which absorbs by the selective absorbing surface (Q_G) (see figure 3.2) can be defined as (Duffie & Beckman, 1991).

$$Q_G = I_d.\eta_{op} = I_d.\prod_{i=1}^{5}\eta_{op_i} \tag{3.16}$$

$$Q_G = I_d.\rho_{ref}.\gamma.(\tau_{gl}.\alpha_{abs})_e.K \tag{3.17}$$

Where,

I_d : The direct solar beams which fall on the reflector surface; for the solar collectors which have got concentrate ration larger than 10 the direct solar beams only affects, and the diffuse solar radiations are negligible.

ρ_{ref} : Reflective value for the reflector surface.

γ : Intercept factor; refers to the part of the solar beams which are reflected by the reflector and absorbed by the absorbing surface.

K : Incident angle modifier factor.

$(\tau_{gl}.\alpha_{abs})_e$: Multiplying the effective transmittance of the glass cover by the absorptance of the absorbed tube under the effect of the thermal insulation of the glass cover.

The $\gamma \geq 0.9$ is given in the literature (Duffie & Beckman, 1991). γ can be increased by increasing the absorbing tube diameter as shown in figure 3.7 (Duffie & Beckman, 1991). but the thermal losses are increased at the same time. Accordingly, the optimum absorbing tube diameter must be determined to define the maximum intercept factor. And this factor is affected by 8% in a negative way when the surface has been dusty. So, the reflected surface should always be clean. Therefore, the soft water and air lines must be mounted on the ground which the collector is designed and installed on it too. In the evenings when the collector has been closed, it is recommended to wash the collector by using the pressurized soft water and dry up it by using the air. There, the using water must be free of lime and it is aimed to prevent its particle from making stains on the surface.

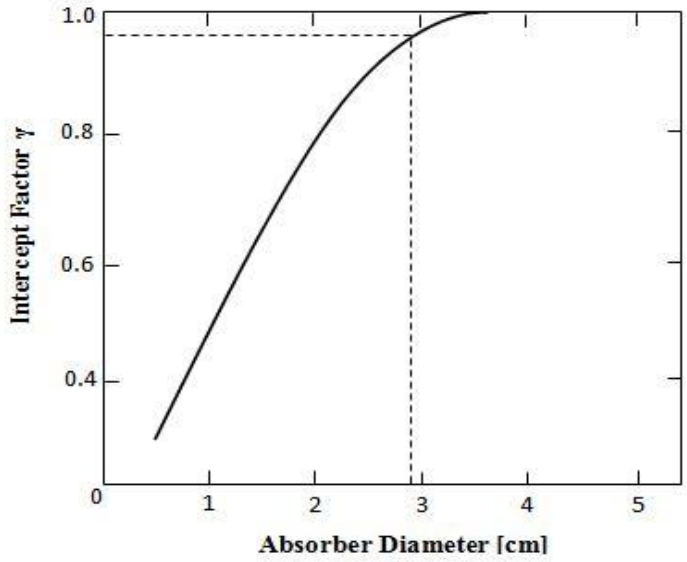

Figure 3.7 The variation of the intercept factor with the absorber tube diameter

Incident angle modifier factor K is the rate of the optical efficiency for the solar beams fall on the reflector in particular angle of incidence ($\eta_{op}(\theta>0)$) to the optical efficiency for solar beams which is falling on the reflector in perpendicular state ($\eta_{op}(\theta=0)$) as shown in equation 3.8 (Gilett & Moon, 1985). Incident angle modifier is function of incident angle of the solar beams which fall on the reflector surface, and it is used to fix the deviations from the perpendicular to the surface.

Incident angle modifier factor, $K = K(\theta) = f(\theta)$

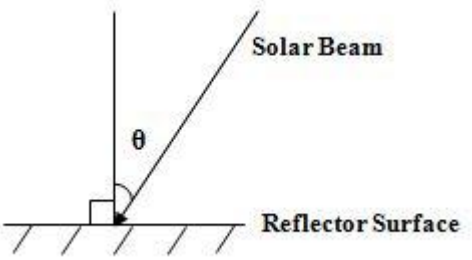

Figure 3.8 The definition of the direct solar beam incident angle θ

Incident angle modifier factor K(θ) is defined as below [Gilett & Moon, 1985].

$$K(\theta) = \frac{\eta_{op}(\theta > 0^o)}{\eta_{op}(\theta = 0^o)} = \cos\theta \tag{3.18}$$

The rate of the solar beams losses at the tip point of the collector to the total reaching solar beams increase as the length of the collector decreases. Therefore, the incident angle modifier factor gains importance at the short collectors tests. So, the effect of the solar beams losses at the tip point of the short collectors is developed by (Rabl, 1985) to give the next correlation. So, the incident angle modifier factor K(θ) for short solar collector is:

$$K(\theta) = 1 - \frac{f}{L_{ref}}\left(1 + \frac{W_{ref}^2}{48 f^2}\right)\tan\theta \tag{3.19}$$

Where,

f : Focus distance [m]

W_{ref}: Reflector width [m]

L_{ref} : Reflector length [m]

θ : Incident Angle [Degree]

The parabolic reflector surface profile (figure 3.9) can be defined by the parabolic curve function as given below (Duffie & Beckman, 1991):

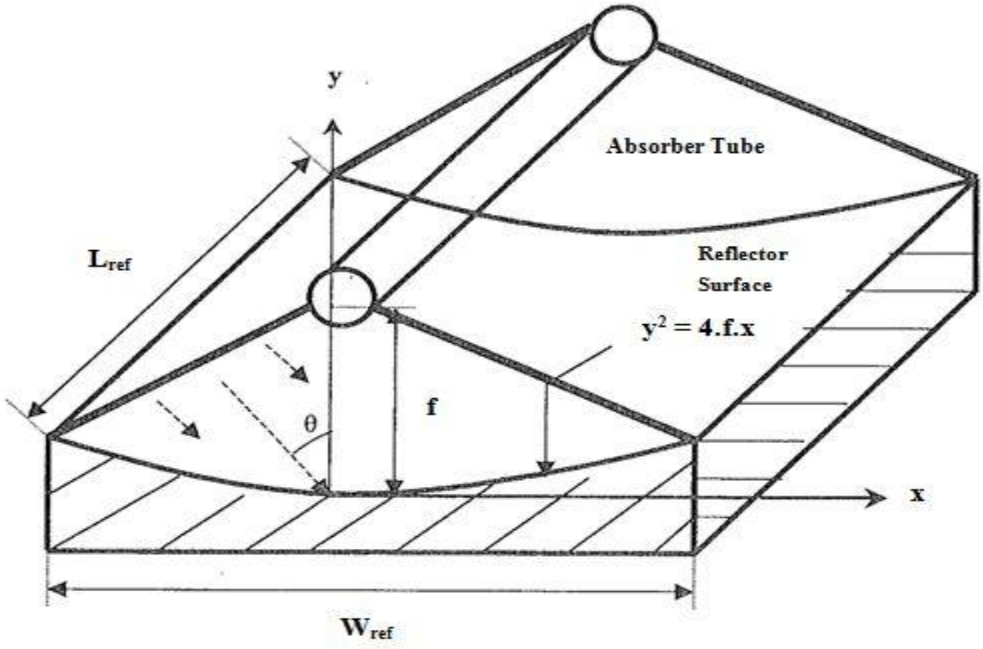

Figure 3.9 The schematic of the parabolic trough solar collector

$$y^2 = 4.f.x \tag{3.20}$$

The collector length has restriction in order to keep the focus losses in certain range which occur as a result of the twist of the reflector surface which caused by structural and environmental effects. The large capacity collectors are achieved by arranged the short solar collectors alongside. Considering to alongside arranging short collector's overall losses, the delocalization of the solar beams on the absorber tube which extends along the spaces between the collectors and the shading which is happened as a result of the structural elements must be considered.

In relation to the glass cover thermal insulation, multiplying the effective transmittance of the glass cover in the absorptance of the absorbed tube (equ. 3.17). All of the solar radiation that is absorbed by a glass cover is not lost, since this absorbed energy tends to increase the glass cover temperature and consequently reduce the thermal losses from the plate. This definition which includes the glass cover transmission τ_{gl} can be defined as below if only the absorption and transmission of the glass cover are accepted (Duffie & Beckman, 1991).

$$\tau_{gl} = \frac{I_{takein}}{I_{fall}} = \exp(-\frac{K_{gl} t_{gl}}{\cos\theta}) \qquad (3.21)$$

Where,

θ : The direct beams incident angle on the glass cover

t_{gl} : Glass cover thickness [m]

K_{gl}: The glass cover transmission τ_{gl} coefficient, and it's taken as 4 m^{-1} for low Iron glass and 32 m^{-1} for ordinary glass (Duffie & Beckman, 1991)

When the total heat transfer (thermal losses) coefficient U_L between the selective absorbing surface and the environment is determined, the glass cover is accepted as not absorber to the solar beam. But in fact, amount of the solar beams have absorbed by the glass cover. And the consequence of absorbing the glass cover to the solar beam is increase the temperature of the cover as a result of the impact of heat stored. Therefore, the thermal losses decreases and as a result the solar heat energy have increased. In order to apply the last effect on the optical performance equation, the concept of multiplying the effective transmittance of the glass cover in the absorptance of the absorbed tube $(\tau_{gl}.\alpha_{abs})_e$ has developed. $(\tau_{gl}.\alpha_{abs})_e$ is always greater than the $(\tau_{gl}.\alpha_{abs})$ value in small amount. To show the difference between the $(\tau_{gl}.\alpha_{abs})_e$ and $(\tau_{gl}.\alpha_{abs})$, the both cases of solar beams, unabsorbed (I) and absorbed (II) by the glass cover are shown as schematic in figure 3.10. In case of $(\tau_{gl}.\alpha_{abs})_e$, $\Delta T'$ is reduced so the thermal losses to the environment are reduced too (Duffie & Beckman, 1991).

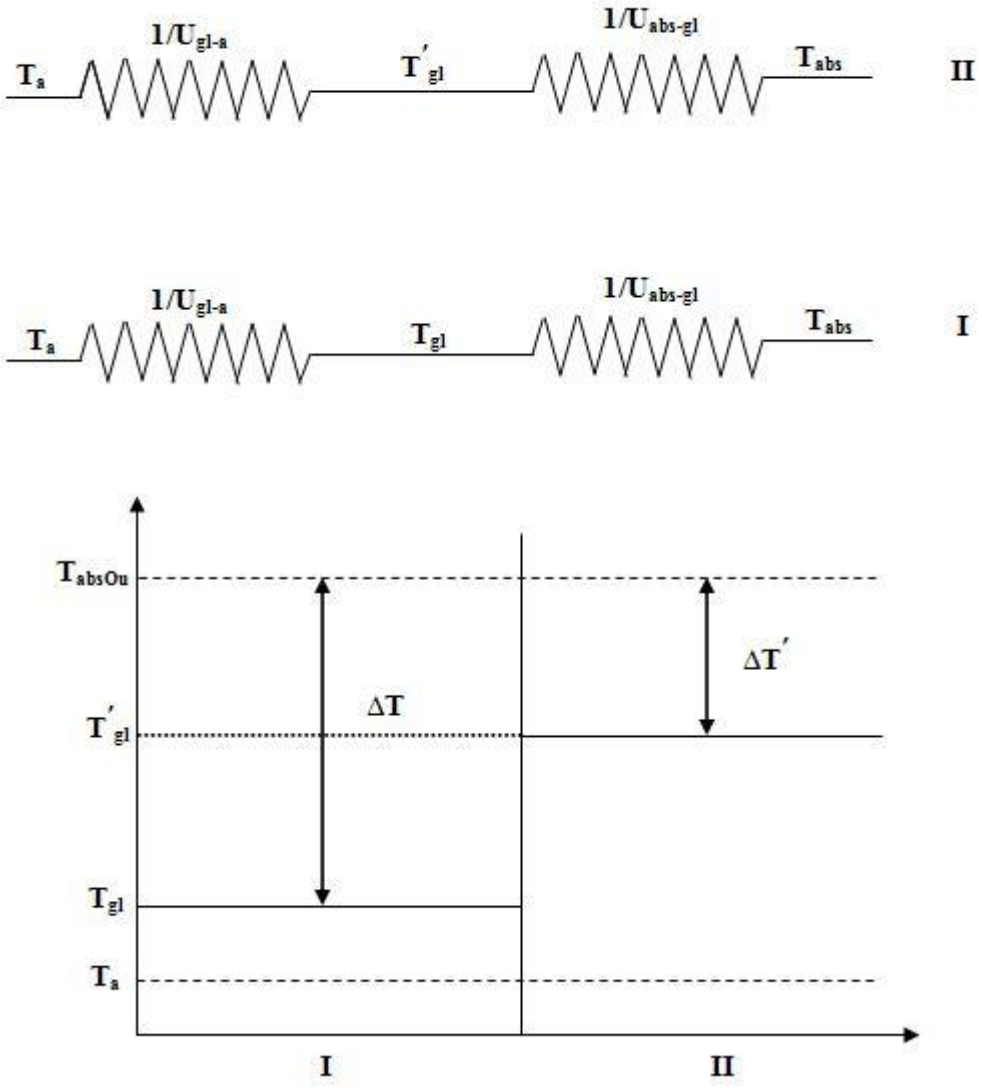

Figure 3.10 The heat transfer electrical analogy between the absorber tube and the environment

If the cases (I) and (II) are investigated;

(I) In this case, the glass cover doesn't absorbed the solar beams is accepted, so the T_{gl} is small. Therefore, the $\Delta T = T_{abs} - T_{gl}$ is large. Based on this the thermal losses is large as well.

$$Q_{LI} = U_{abs-gl}(T_{abs} - T_{gl}) \tag{3.22}$$

(II) In this case, amount of the solar beams have absorbed by the glass cover is accepted, so the T'_{gl} is higher than the last case, and the $\Delta T' = T_{abs} - T'_{gl}$ is decreasing. Consequently, the thermal losses are smaller than the first case.

$$Q_{LII} = U_{abs-gl}(T_{abs} - T'_{gl}) \tag{3.23}$$

The effect of the partial increase in the glass cover temperature on the heat transfer coefficient $U_{abs\text{-}gl}$ and $U_{gl\text{-}a}$ can be negligible.

To show the thermal losses difference between the cases (I) and (II):

$$\Delta Q_L = U_{abs-gl}[(T_{abs} - T_{gl}) - (T_{abs} - T'_{gl})] \tag{3.24}$$

Where,

$$T_{abs} - T_{gl} = \frac{U_{abs-a}(T_{abs} - T_a)}{U_{abs-gl}} \tag{3.25}$$

$U_{abs\text{-}a}$: the heat transfer coefficient between the absorber tube and the environment.

$$U_{abs-a} = \frac{U_{abs-gl}.U_{gl-a}}{U_{abs-gl} + U_{gl-a}} \tag{3.26}$$

From this equations,

$$T_{abs} - T'_{gl} = \frac{U_{gl-a}(T_{abs} - T_a) - I_T(1-\tau_{gl})}{U_{abs-gl} + U_{gl-a}} \tag{3.27}$$

$$\Delta Q_L = \frac{I_T U_{abs-a}(1-\tau_{gl})}{U_{gl-a}} \tag{3.28}$$

Here,

ΔQ_L: represent the effect of the glass cover insulation on the collector thermal losses reduce and it is added to the collector equation. Thus, the thermal energy which is transferred to the working fluid is:

$$q_U = F_R\left[q_G + \frac{I_T U_{abs-a}(1-\tau_{gl})}{U_{gl-a}} - U_L(T_{abs} - T_a)\right] \tag{3.29}$$

I_T is defined in the form of $I_T = f(I_d, I_{dif}, I_{ref})$ which depends on the direct beams I_d, the diffuse beams I_{dif} and the reflection beams I_{ref}, that all fall on the glass cover. In the mathematical model for the parabolic solar collector the $I_T = I_d$ is accepted because the parabolic solar collector is working on this basis.

So, equation 3.29 becomes,

$$q_U = F_R\left[I_d(\tau\alpha) + \frac{I_d U_{abs-a}(1-\tau_{gl})}{U_{gl-a}} - U_L(T_{abs} - T_a)\right] \tag{3.30}$$

$$(\tau\alpha)_e = (\tau\alpha) + (1-\tau_{gl})\frac{U_{abs-a}}{U_{gl-a}} \tag{3.31}$$

As seen in equation 3.31, the glass thermal insulation effect can be determined as $(1-\tau_{gl})U_{abs-a}/U_{gl-a}$. For ordinary glass cover $(\tau\alpha)_e = 1.02\ (\tau\alpha)$, and for white low Iron glass cover $(\tau\alpha)_e \approx 1.01\ (\tau\alpha)$ is taken (Duffie & Beckman, 1991). For the mathematical modeling calculations of the solar collector which is designed and developed, the used materials properties are taken from the information given by the manufactures company.

The overall optical efficiency η_{op} which is found in the consequence of the optical performance analyses for the parabolic solar collector can be the maximum collector performance $\eta_{max} = \eta_{op}$ ($\Delta T \rightarrow 0$) when it is accepted that there is no thermal losses.

And the total thermal efficiency is reduced as increase the thermal losses which transfer from the selective absorber surface to the environment which depend directly on $\Delta T = T_{abs} - T_a$ (figure 3.11).

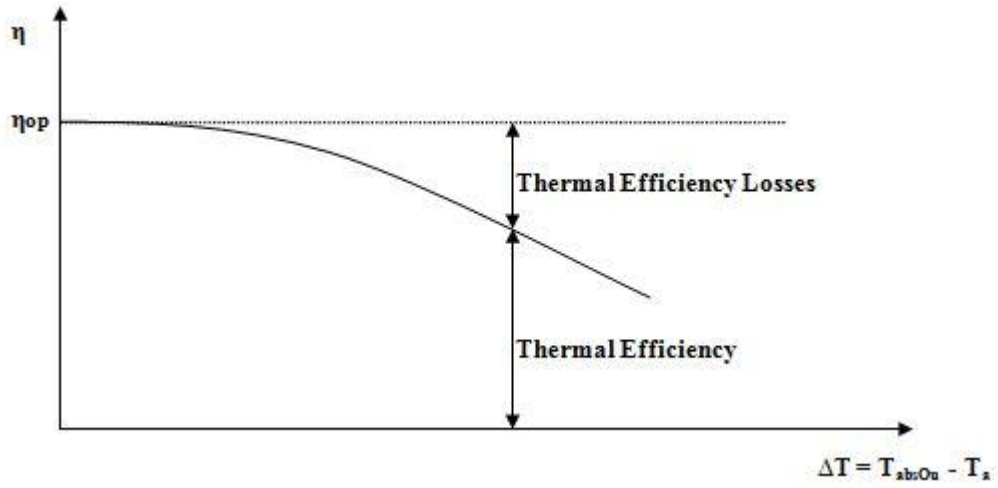

Figure 3.11 The variation of the thermal performance of the parabolic trough solar collector with the temperature difference

3.3 The Heat Transfer and the Thermal Losses Analyses for the Sun Tracking Parabolic Solar Collector

An amount of the solar beams which are absorbed and stored as a solar heat by the selective absorbed surface are going to the environment by heat convection, conduction and radiation. All these heat losses are defined by the value of the effective overall heat transfer (thermal losses) coefficient U_o. Thermal losses increase as the difference between the absorber surface mean temperature T_{abs} and the environment temperature T_a increases as shown in figure (3.11). Depending on the application field, the thermal losses can be reduced by the technical optimization at the design, manufacturing and operation stages. The optical and thermal losses in the glass cover adversely affect the overall thermal performance of the system. Although the glass cover reduces the thermal losses but it increases the optical losses. The total thermal losses coefficient U_L is defined based on the absorber surface mean temperature. At the definition of the thermal losses the working fluid mean temperature is used in lieu of the absorber surface mean temperature because of the

measurement difficulty. The working fluid mean temperature is taken as the arithmetic mean of the inlet and outlet temperature. The effective overall thermal loss coefficient U_o is equal to the multiplication of collector performance factor F_E in the total thermal losses coefficient U_L. The collector efficiency factor which will explain in section 3.4.1 is defined as below.

$$F_E = \frac{U_o}{U_L} \tag{3.32}$$

The thermal losses which take place in the concentrate types of the solar collector depend on many factors as a zone, environmental, structural and operational. The thermal losses to the environment are affected by many factors as the radiation intensity, wind speed, ambient temperature, collector dimension, the dimension and the properties (absorption value, emissivity value, thermal conductivity and thickness) of the absorber tube, the dimension and properties (transmittance, emissivity, thickness and glass Iron-rate) of the glass cover and the working fluid properties (temperature, pressure, specific heat capacity, viscosity, thermal conductivity and prandl number).

The thermal system of the parabolic trough solar collector which consists of absorber tube and glass cover is given in figure 3.12. The heat transfer is accepted as one dimensional and steady state in this mathematical model to determine the thermal losses to the environment.

The thermal efficiency which defines the performance of the parabolic trough solar collector is a function of the parameters which is illustrated below and given at the beginning of this study in the list of symbols.

$$\eta_{th} = f(I_d, T_a, V_W, \dot{m}, L_{ref}, W_{ref}, T_{in}, T_{ou}, t_{abs}, t_{gl}, \varepsilon_{abs}, \varepsilon_{gl}, \alpha_{abs}, \tau_{gl}, k_{abs}, D_{absOu}, D_{glOu}, \gamma, K, \rho_{ref}, wf)$$

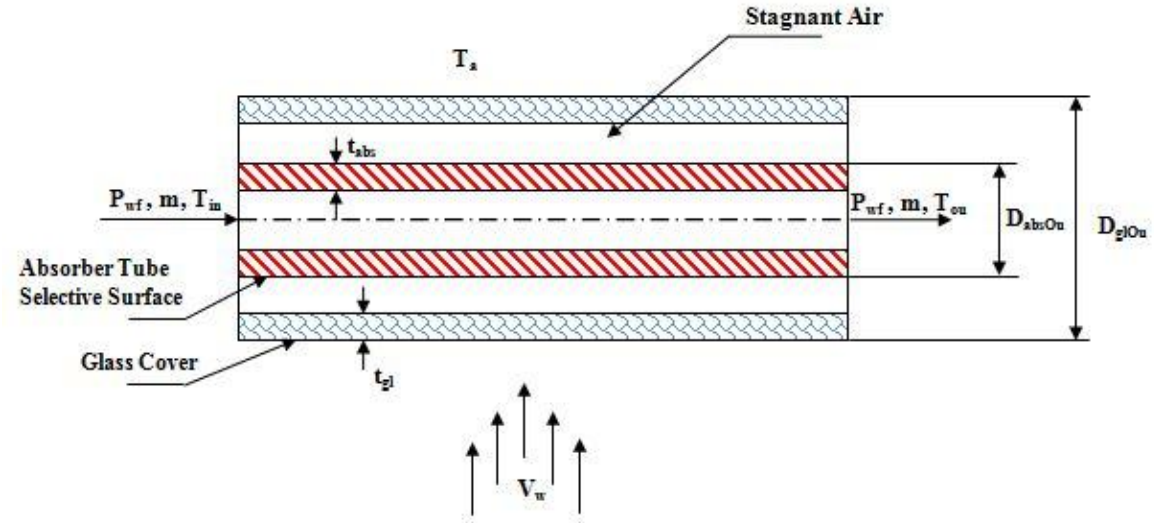

Figure 3.12 The Schematic of the selective surface absorber tube and glass cover

Before start thermal calculations, the heat transfer coefficients of the thermal system in absorber tube and glass cover of the parabolic trough solar collector (figure 3.13) have to define.

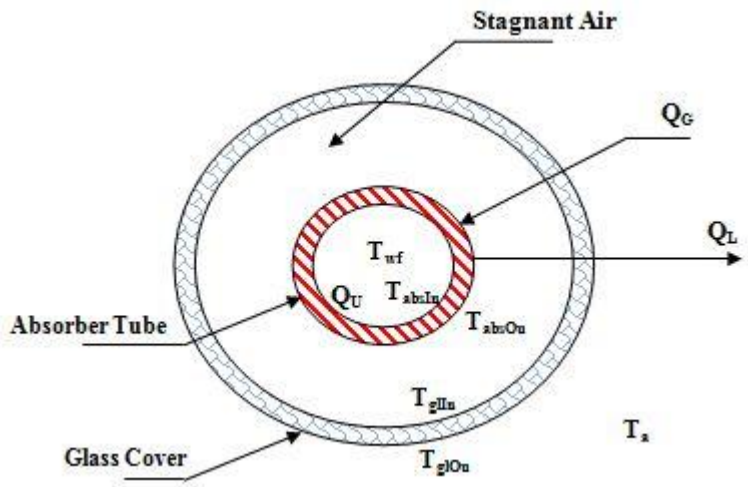

Figure 3.13 Thermal System schematic of the absorber tube and glass cover

The electrical analogy of the heat transfer system between the working fluid temperature T_{wf} and the environmental temperature T_a is given below. In this analogy, the glass cover thickness t_{gl} can be neglected when it is compared with the

other dimension. Therefore, the glass cover temperature can be accepted constant ($T_{glIn} \approx T_{glOu}$).

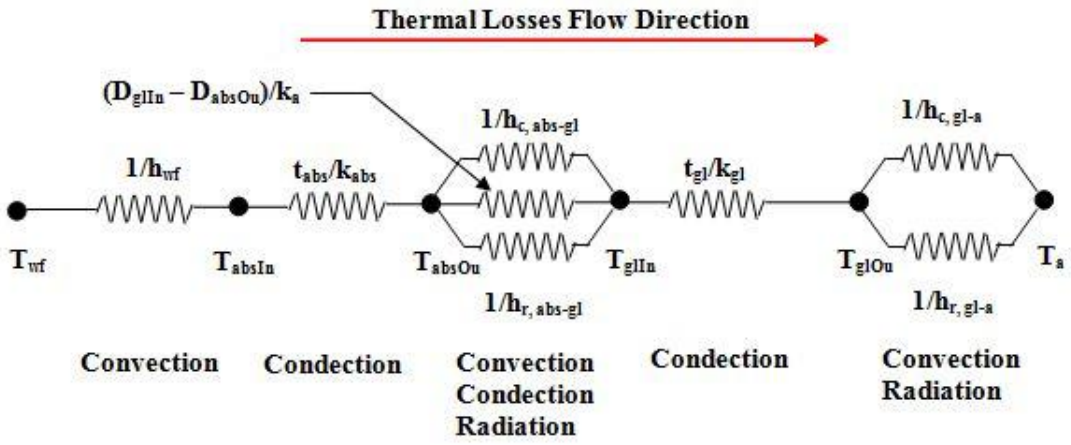

Figure 3.14 Electrical analogy of the heat transfer system between the working fluid temperature and the environmental temperature

This leads to neglect the thermal gradient in the glass wall. Therefore, the electrical analogy which is given in figure 3.14 can be taken the new form by removing the thermal conductivity term t_{gl}/k_{gl} as given below.

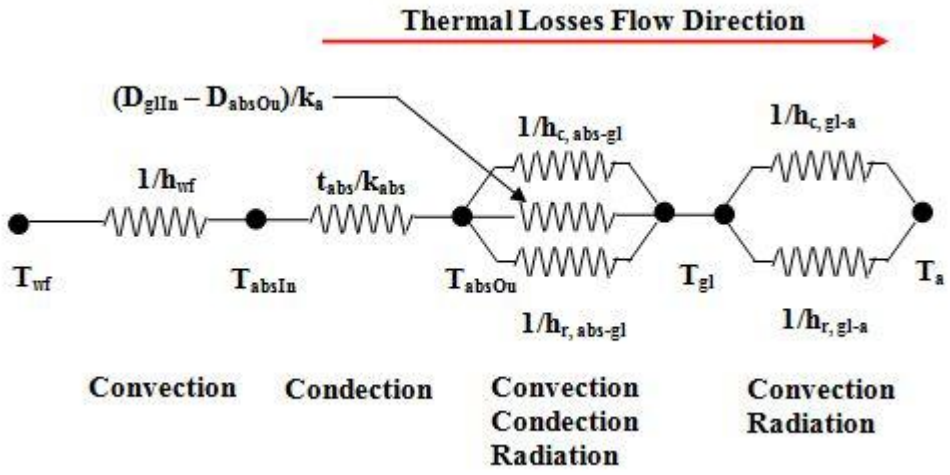

Figure 3.15 Electrical analogy of the heat transfer system between the working fluid temperature and the environmental temperature after removing the temperature gradient in the glass wall

If the energy balance at the selective surface absorber tube is written as shown in the figure 3.16;

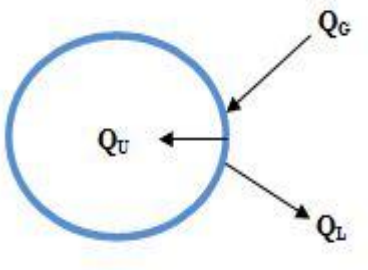

Figure 3.16 The energy balance at the selective surface absorber tube

$$Q_U = Q_G - Q_L \tag{3.33}$$

$$Q_U = \dot{m}.c_{wf}.\Delta T_{wf} \tag{3.34}$$

Here;

Q_U : The useful energy which transfers to the working fluid.

Q_G : The solar absorbed energy which is absorbed by the selective surface absorber tube from the reflected solar beam by the unshaded reflector area after particular optical losses of the collector, and it can be defined as below.

$$Q_G = \eta_{op}.I_d.A_{UnSh} \tag{3.35}$$

Here;

A_{UnSh} : Unshaded reflector area [m^2]

Unshaded reflector area is the net area which obtains by subtracting the glass cover shaded projection area from the reflector surface projection area (Duffie & Beckman, 1991) as shown in the figure 3.17 below.

$$A_{UnSh} = A_{ref} - A_{sh} = L_{ref}.W_{ref} - L_{ref}.D_{glOu} = L_{ref}(W_{ref} - D_{glOu}) \quad (3.36)$$

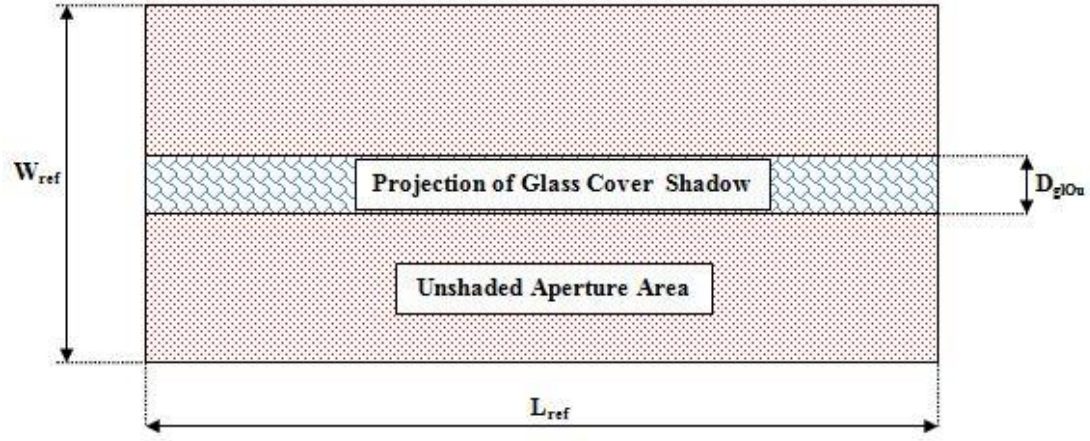

Figure 3.17 The unshaded reflector area in the parabolic trough solar collector

Q_L : Represent the convection and radiation heat losses from the selective surface absorber tube outside surface to the environment.

$$Q_L = U_L.A_{absOu}.(T_{absOu} - T_a) \quad (3.37)$$

Here;

A_{absOu} : The outside surface area of the selective surface absorber tube.

T_{absOu} : The outside temperature of the selective surface absorber tube.

U_L : The total thermal losses coefficient from the selective surface absorber tube outside surface to the environment (figure 3.18), and it can determined as shown below from the equation 3.39 (Duffie & Beckman, 1991).

Figure 3.18 The total thermal losses coefficient U_L

$$\frac{1}{U_L.A_{absOu}} = \left[\frac{1}{h_{C,abs-gl} + h_{R,abs-gl} .A_{absOu}} + \frac{1}{h_{C,gl-a} + h_{R,gl-a} .A_{gl}} \right] \tag{3.38}$$

$$U_L = \left[\frac{1}{h_{C,abs-gl} + h_{R,abs-gl}} + \frac{A_{absOu}}{A_{gl}} \frac{1}{h_{C,gl-a} + h_{R,gl-a}} \right]^{-1} \tag{3.39}$$

The $h_{C,abs-gl}$, $h_{R,abs-gl}$, $h_{C,gl-a}$ and $h_{R,gl-a}$ which are used in last equations represent the convection heat transfer and radiation heat transfer coefficients between the absorber tube-glass cover and glass cover-environment respectively. Their definitions and calculation methods are explained below.

(a) $h_{C,abs-gl}$: The convection heat transfer coefficient between the absorber tube surface-glass cover.

The convection heat transfer doesn't occur if the space between the two tubes is evacuated. But in the literature, if it isn't completely discharged from the air the conduction heat transfer is more effective than the convection heat transfer (Holman, 1976). Therefore, in this case the conductive heat transfer coefficient k_a should be use but it should be taken into consideration the effect of the natural convection. So, the effective conductive heat transfer coefficient k_{ea} is used and it can determine from the equations as shown below (Holman, 1976).

$$h_{C,abs-gl} = \frac{2.k_{ea}}{D_{absOu} \ln D_{gl} / D_{absOu}} \tag{3.40}$$

Here, to calculate the effective conductive heat transfer coefficient for horizontal cylindrical tubes, the derived empirical equation is used (Holman, 1976). According to this equation;

If (Gr.Pr) < 10^3, $K_{ea} = K_a$ is taken. Here, "K_a" is the conductive heat transfer coefficient for the air which is between the tubes at mean temperature. "Gr" is Grashof number and "Pr" is Prandl number.

If (Gr.Pr) > 10^3, the following empirical equation is used;

$$k_{ea} = k_a.C.\ Gr.\Pr^{\ n}.\left(\frac{L}{D}\right)^m \tag{3.41}$$

Here, for the natural convection in the horizontal cylindrical tube the following values are taken (Holman, 1976).

C = 0.11
n = 0.29
m = 0

Accordingly, the equation 3.41 returns to the form below.

$$k_{ea} = k_a.(0.11).\ Gr.\Pr^{\ 0.29} \tag{3.42}$$

Here, Gr value is found from the following equation (Holman, 1976).

$$Gr = \frac{g\beta\ \ T_{absOu} - T_{gl}\ \ \delta^3}{\nu_a^2} \tag{3.43}$$

Here;

δ : Space between the two tubes. [m] $\left(\delta = \frac{D_{glIn} - D_{absOu}}{2}\right)$ (3.44)

β : Volumetric expansion coefficient. [K^{-1}] $\left(\beta = \frac{1}{T_{m,abs-gl}}\right)$ (3.45)

Here, K_a, ν_a and Pr values are found from the tables at the mean temperature between the tubes $T_{m,abs\text{-}gl}$ which can be calculated as below,

$$T_{m,abs-gl} = \frac{T_{absOu} + T_{gl}}{2} \quad [K] \tag{3.46}$$

(b) $h_{R,abs\text{-}gl}$: The radiation heat transfer coefficient between the absorber tube surface-glass cover.

The derived equation for the radiation heat transfer coefficient between two cylindrical surfaces is given below (Holman, 1976).

$$h_{R,abs-gl} = \frac{\sigma \left(T_{gl}^2 + T_{absOu}^2 \right) \left(T_{gl} + T_{absOu} \right)}{\frac{1-\varepsilon_{abs}}{\varepsilon_{abs}} + \frac{1}{F_{abs-gl}} + \frac{1-\varepsilon_{gl}}{\varepsilon_{gl}} \frac{A_{absOu}}{A_{gl}}} \tag{3.47}$$

Here, the shape factor is taken as $F_{abs\text{-}gl} = 1$ because the all radiation which move out from one of the surfaces reach to the other surface. And the other variables are;

A_{absOu}: Area of the selective tube exterior surface. [m^2] $A_{absOu} = \pi D_{absOu} L_{ref}$

A_{gl} : Area of the glass cover surface. [m^2] $A_{gl} = \pi D_{gl} L_{ref}$

If the $\left(\frac{A_{abs}}{A_{gl}} = \frac{D_{abs}}{D_{gl}} \right)$ is written in this form and placed in the equation 4.47, the below equation can be obtained.

$$h_{R,abs-gl} = \frac{\sigma \left(T_{gl}^2 + T_{absOu}^2 \right) \left(T_{gl} + T_{absOu} \right)}{\frac{1}{\varepsilon_{abs}} + \frac{D_{abs}}{D_{gl}} \left[\frac{1}{\varepsilon_{gl}} - 1 \right]} \tag{3.48}$$

(c) $h_{C,gl-a}$: The convection heat transfer coefficient between glass cover-ambient.

The convection heat transfer of the air over the glass can be natural, forced or mixed convection. Therefore these dominates can be determined from the relative magnitudes of the Grashof and Reynolds number squared (Gr/Re^2). If this ratio is greater than one forced convection can be neglected otherwise the natural convection can be neglected, but if the ratio is approximately one both forced and natural convection (mixed convection) need to be taken into account. Where, Grashof and Reynolds numbers can be found as follow,

$$Gr = \frac{g\beta\ \ T_{gl} - T_a\ \ D_{glOu}^3}{\nu_a^2} \tag{3.49}$$

$$\mathrm{Re} = \frac{\rho_a . V_w . D_{glOu}}{\mu_a} = \frac{V_w . D_{glOu}}{\nu_a} \tag{3.50}$$

And the general equation of the convection heat transfer coefficient is,

$$h_{C,gl-a} = \frac{k_a}{D_{glOu}} Nu \tag{3.51}$$

So,

For $Gr/\mathrm{Re}^2 > 1$, the Nusselt Number for the natural convection can be determined from the next equation (Churchill, 1983).

$$\sqrt{Nu} = \sqrt{Nu_o} + \left[\frac{\frac{Gr.\mathrm{Pr}}{300}}{\left(1 + \left(\frac{0.5}{\mathrm{Pr}}\right)^{9/16}\right)^{16/9}} \right]^{1/6} \tag{3.52}$$

Where, $Nu_o = 0.36$ for the horizontal cylinder case, and

$$\beta = \frac{1}{T_{m,gl-a}} \tag{3.53}$$

$$T_{m,gl-a} = \frac{T_{gl} + T_a}{2} \tag{3.54}$$

For $Gr/\mathrm{Re}^2 < 1$, the Nusselt Number for the forced convection which depends on the wind speed can be determined from the next equation (Duffie & Beckman, 1991).

$$Nu = 0.4 + 0.54\,\mathrm{Re}^{0.52} \qquad 0.1 < \mathrm{Re} < 1000 \tag{3.55}$$

$$Nu = 0.3\,\mathrm{Re}^{0.6} \qquad 1000 < \mathrm{Re} < 50000 \tag{3.56}$$

For $Gr/\mathrm{Re}^2 \approx 1$, the Nusselt Number for the mixed convection can be determined from the next equation (Churchill, 1975).

$$\sqrt{Nu} = \sqrt{Nu_o} + \frac{0.387\,Ra^{1/6}}{\left(1 + \left(\frac{0.559}{\mathrm{Pr}}\right)^{9/16}\right)^{8/27}} \tag{3.57}$$

Where, Rayleigh Number is,

$$Ra = \frac{g\beta\ \ T_{gl} - T_a\ \ D_{glOu}^3}{\nu_a^2 . \alpha_a} \tag{3.58}$$

k_a, ρ_a, ν_a, α_a, μ_a and Pr are the properties of the ambient air which is flowing on the glass cover surface at the mean temperature $T_{m,gl\text{-}a}$.

(d) $h_{R,gl-a}$: The radiation heat transfer coefficient between the glass cover-ambient (Duffie & Beckman, 1991).

$$h_{R,gl-a} = 4.\sigma.\varepsilon_{gl}.T_{m,gl-a}^{3} \tag{3.59}$$

In fact the ambient temperature which is used here must be taken as the sky temperature T_s. The sky temperature can be found from the below equation which is derived by (Berdahl & Martin, 1984).

$$T_s = T_a\left[0.711 + 0.0056T_{dp} + 0.000073T_{dp}^{2} + 0.013\cos(15*t)\right]^{1/4} \tag{3.60}$$

Here;

T_s and T_a : Sky and ambient temperature. [K]

T_{dp} : Dew Point temperature. [^oC]

t : The time which lasts from the midnight to that moment [hour].

However, the difference between T_s and T_a in the hot humid climate doesn't exceed the 5 ^oC. So, using T_a doesn't change or affect the collector performance (Duffie & Beckman, 1991).

Right now the temperature distribution in the selective surface absorber tube hasn't taken in the calculation. The resistance which happens because of the heat capacity of the selective surface absorber tube during the heat transfer from the outside surface of the tube to the working fluid can be higher in the concentrate solar collector system. So, based on the tube outside surface, the overall heat transfer coefficient from the working fluid to the environment U_o is defined rather than the total heat transfer coefficient from outside of the absorber tube to the environment U_L. The electrical analogy for U_o is given below.

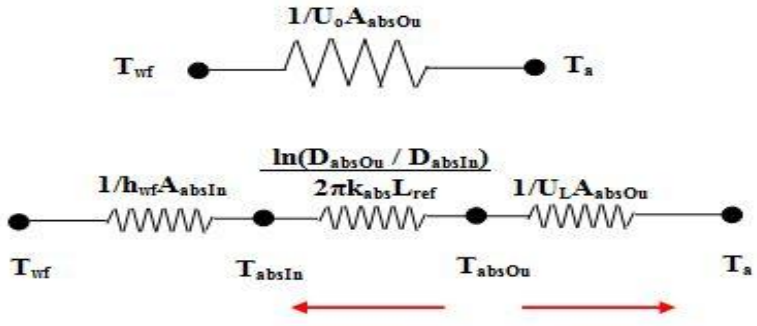

Figure 4.19 The electrical analogy of the overall heat transfer coefficient

$$U_o = \left[\frac{1}{U_L} + \frac{D_{absOu}}{h_{wf} D_{absIn}} + \frac{D_{absOu} \ln(D_{absOu} - D_{absIn})}{2k_{abs}} \right]^{-1} \tag{3.61}$$

The convection heat transfer coefficient of the working fluid h_{wf} depends on the working fluid's physical properties, temperature and flow velocity. The convection heat transfer coefficient of the working fluid is changing between (100-1500) W/m^2 depending on the flow type (laminar or turbulent). And the flow type is defined by determining the Reynolds Number. If the Re $\leq$ 2300 the flow is laminar and if the Re $\geq$ 2300 the flow is turbulent. The convection heat transfer coefficient of the working fluid h_{wf} is determined from determining the Nusselt Number for the turbulent flow in a flat surface tube which is given below from the empirical equation found by Dittus Boelter (Mc Adams, 1954).

$$Nu = 0.023 \,\mathrm{Re}^{0.8} \,\mathrm{Pr}^{n} \tag{3.62}$$

In this equation, for heating and cooling application n is taken as 0.4 and 0.3 respectively. So, since the collector system is heating system the last equation can be written as below.

$$Nu = 0.023 \,\mathrm{Re}^{0.8} \,\mathrm{Pr}^{0.4} \tag{3.63}$$

To calculate the Reynolds and Prandl Number for this equation, the following equations are used (Holman, 1976).

$$\mathrm{Re} = \frac{V.D_{absIn}}{\nu_{wf}} = \frac{\rho_{wf}.V.D_{absIn}}{\mu_{wf}} \tag{3.64}$$

$$\mathrm{Pr} = C_{wf}\,\frac{\mu_{wf}}{k_{wf}} \tag{3.65}$$

$$V = \frac{\dot{m}}{\mu_{wf}\pi D_{absIn}} \tag{3.66}$$

$$\mathrm{Re} = \frac{4m}{\mu_{wf}\pi D_{absIn}} \tag{3.67}$$

$$Nu = \frac{h_{wf}D_{absIn}}{k_{wf}} \tag{3.68}$$

$$h_{wf} = \frac{Nu.k_{wf}}{D_{absIn}} \tag{3.69}$$

The variables in these equations are expressed by; the flow rate m, velocity V, viscosity μ_{wf}, density ρ_{wf}, specific heat C_{wf} and Prandl Number Pr for the working fluid. Excepting the flow rate and the velocity, all of the rest variables are taken from the table at the mean flow temperature T_{wf}.

$$T_{wf} = \frac{T_{in} + T_{Ou}}{2} \tag{3.70}$$

3.4 The Thermal Performance Analyses for the Parabolic Trough Solar Collector

Form the energy balance of the absorber tube, the useful solar heat energy which transfers to the working fluid per unit area of the collector q_u, can be expressed in

terms of the outside temperature of the absorber tube T_{absOu}, ambient temperature T_a, unshaded reflector area A_{UnSh}, direct solar beams I_d, optical performance of the collector η_{op} and the total thermal losses coefficient U_L as follows;

$$q_u = \frac{A_{UnSh} I_d \eta_{op}}{L_{ref}} - \frac{A_{abs} U_L}{L_{ref}} \left(T_{absOu} - T_a \right) \tag{3.71}$$

Because of the absorber tube outside temperature T_{absOu} is unknown and the difficulty of determining it, the working fluid mean temperature T_{wf} or inlet temperature T_{In} can be used instead of the absorber tube outside temperature T_{absOu} to simplify the analyses. For this, it should be defined the collector efficiency factor F_E or the heat removal factor F_R and the flow factor F_F.

3.4.1 The Determination of the Collector Efficiency Factor F_E

The heat transfer between the absorber tube outside surface and the working fluid per unit area of the collector can be written as below,

$$q_u = \frac{A_{absOu} / L_{ref} \quad T_{absOu} - T_{wf}}{\frac{D_{absOu}}{h_{wf} D_{absIn}} + \left(\frac{D_{absOu}}{2k_{abs}} \ln\left(\frac{D_{absOu}}{D_{absIn}} \right) \right)} \tag{3.72}$$

To eliminate unknown absorber tube outside temperature T_{absOu} from the equations and using the mean working fluid temperature T_{wf} in order to simplify the calculations and obtain an expression for the useful gain in terms of known parameters, we substitute equation 3.68 into equation 3.67, and solving the result for the useful gain, to obtain

$$q_u = F_E \frac{A_{UnSh}}{L_{ref}} \left[I_d \eta_{op} - \frac{A_{absOu}}{A_{UnSh}} U_L \left(T_{wf} - T_a \right) \right] \tag{3.73}$$

But the mean working fluid temperature T_{wf} is different from the absorber tube outside temperature T_{absOu}. So, with using the collector efficiency factor F_E, it can be calculated the useful solar energy which transferred to the working fluid with using the mean working fluid temperature T_{wf}. The physical interpretation for F_E is the ratio of the actual useful energy gain to the useful energy gain that would result if the collector absorbing surface had been at the mean fluid temperature, so the collector performance factor can be written as follow (Duffie & Beckman, 1991).

$$F_E = \frac{q_u \ \ \Delta T = T_{absOu} - T_a}{q_u \ \ \Delta T = T_{wf} - T_a} \tag{3.74}$$

$$F_E = \frac{1/U_L}{\frac{1}{U_L} + \frac{D_{absOu}}{h_{wf} D_{absIn}} + \left(\frac{D_{absOu}}{2k_{abs}} \ln\left(\frac{D_{absOu}}{D_{absIn}} \right) \right)} \tag{3.75}$$

As a result the collector performance factor is defined as follow.

$$U_o = F_E . U_L \tag{3.76}$$

3.4.2 The Determination of the Heat Removal Factor F_R and Flow Factor F_F

The useful energy gain above is expressed in terms of the absorber tube outside temperature T_{absOu} and mean working fluid temperature T_{wf}. But, because of the changing of the working fluid temperature with the flow direction and the difficulty to determine the mean working fluid temperature T_{wf}, the useful energy gain to the working fluid can be expressed in term of the working fluid inlet temperature T_{in}. The heat removal factor can be defined as the ratio of the actual useful energy gain to the maximum useful energy gain which occurs when the whole absorber tube outlet surface were at the working fluid inlet temperature, so the thermal losses to the surroundings are then at minimum (Duffie & Beckman, 1991).

$$F_R = \frac{q_u \ \Delta T = T_{absOu} - T_a}{q_u \ \Delta T = T_{In} - T_a} \tag{3.77}$$

$$F_R = \frac{m\, C_{wf}}{A_{absOu} U_L} \left[1 - \exp\left(- \frac{A_{absOu} U_L F_E}{m\, C_{wf}} \right) \right] \tag{3.78}$$

And the flow factor F_F is defined as the ratio of the heat removal factor F_R to the collector efficiency factor F_E as below (Duffie & Beckman, 1991).

$$F_F = \frac{F_R}{F_E} = F_R = \frac{m\, C_{wf}}{A_{absOu} U_L F_E} \left[1 - \exp\left(- \frac{A_{absOu} U_L F_E}{m\, C_{wf}} \right) \right] \tag{3.79}$$

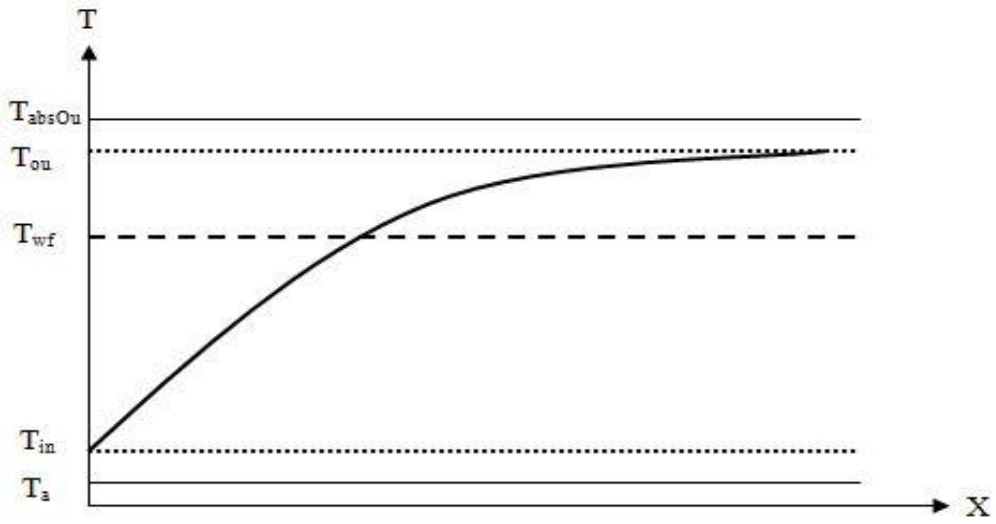

Figure 3.20 The changing of the working fluid temperature with the flow direction in the absorber tube

If there is no increasing in the working fluid temperature with the flow direction, then $F_R = F_E$ is taken. The heat energy transfers from the absorber tube surface to the working fluid at steady state condition can be determined from the next equation.

$$Q_U = F_R \left[q_G . A_{UnSh} - U_L . A_{absOu} \ \ T_{In} - T_a \ \right] \tag{3.80}$$

$$Q_U = F_R.A_{UnSh}\left[q_G - \frac{A_{absOu}}{A_{UnSh}} U_L \ \ T_{In} - T_a \ \right] \tag{3.81}$$

The q_G can be written as follow in this equation.

$$q_G = I_d.\eta_{op} \tag{3.82}$$

3.4.3 The Determination of the Working Fluid Outlet Temperature

The difference between the working fluid inlet and outlet temperature is changed depending on the unshaded reflector area, absorber tube outside surface area, direct solar beam, flow rate and the thermal losses from the absorber tube outside surface. And the working fluid outlet temperature T_{Ou}, can be founded by substituting equation 3.34 into 3.76.

$$T_{Ou} = T_{In} + \frac{F_R\left[q_G.A_{UnSh} - U_L.A_{absOu} \ \ T_{In} - T_a \ \right]}{\dot{m}.C_{wf}} \tag{3.83}$$

3.4.4 The Determination of the Glass Cover Temperature

To determine the heat losses from the glass cover to the surrounding, the glass cover temperature has to determine. If the absorbed energy of the glass neglected (which is taken into considiration in the optical performance calculation see Equ. 3.17), the energy balance on the glass cover can be defined as $Q_{abs\text{-}gl} = Q_{gl\text{-}a}$, so, the next equation can be written.

$$A_{absOu} \ \ h_{C,abs-gl} + h_{R,abs-gl} \ \ T_{absOu} - T_{gl} \ = A_{gl} \ \ h_{C,gl-a} + h_{R,gl-a} \ \ T_{gl} - T_a \tag{3.84}$$

Here, if we defined h_1 and h_2 as;

$$h_1 = h_{C,gl-a} + h_{R,gl-a} \tag{3.85}$$

$$h_2 = h_{C,abs-gl} + h_{R,abs-gl} \tag{3.86}$$

$$T_{gl} = \frac{A_{absOu} h_2 T_{absOu} + A_{gl} h_1 T_a}{A_{gl} h_1 + A_{absOu} h_2} \tag{3.87}$$

If T_{absOu} is known, the T_{gl} is assumed, and then h_1 and h_2 are determined, and then T_{gl} is calculated by iterative method and compared with the first guess. If the difference between them more than 0.1 ^{o}C, the T_{gl} calculated again until satisfied the condition (Duffie & Beckman, 1991).

3.4.5 The Determination of the Critical Direct Solar Beam Level

The critical direct beam level should be determined to determine the operation condition for the parabolic trough solar collector system. The direct beam becomes critical direct beam when the useful heat gain which transfers to the working fluid become zero, so based on this the critical direct solar beam can be determined as follow (Duffie & Beckman, 1991).

$$Q_U = F_R A_{UnSh} I_d \eta_{op} - F_R U_L A_{absOu} \quad T_{In} - T_a \tag{3.88}$$

So, if the $Q_U = 0$, then $I_d = I_{cd}$ and the equation 3.84 become,

$$I_{cd} = \frac{U_L A_{absOu} \quad T_{In} - T_a}{A_{UnSh} \eta_{op}} \tag{3.89}$$

$$Q_U = A_{UnSh} F_R \quad I_d - I_{cd} \quad \eta_{op} \tag{3.90}$$

So, if $I_d > I_{cd}$, then $Q_U > 0$ and on the other hand it means the absorbed useful heat energy by the absorber tube is more than the thermal losses from it. If $I_d < I_{cd}$ the thermal losses become more, then the working fluid is unintentionally cooled. And to prevent this, the working fluid flow must be stopped automatically by the collector control system.

3.4.6 The Determination of Thermal Performance of the PTSC

The thermal performance can be defined as the ratio of the useful energy transferred to the working fluid to the direct solar beam energy falls on the reflector aperture. The mathematical model for the thermal performance of the PTSC which is affected by designer, operation and environmental factors is given below. The parameters of the this equation is investigated very thoroughly and discussed in the previous sections.

$$\eta = \frac{Q_U}{I_d A_{ref}} = \frac{\left[F_R \;\; q_G A_{UnSh} - U_L A_{absOu} \;\; T_{In} - T_a \;\; \right]}{I_d A_{ref}} \tag{3.91}$$

The daily average thermal performance of the PTSC is defined as the ratio of the total useful heat gain transferred to the working fluid which depends on the intensity of the direct beam along the day to the total direct solar energy along the day too, and it can written as below.

$$\eta_{Daily} = \frac{\sum Q_U}{\sum I_d A_{ref}} = \frac{\sum q_u}{\sum I_d} \tag{3.92}$$

3.5 The Development Computer Program for the Mathematical Simulation of the Thermal Performance Behavior of the PTSC and Proven Its Validity by Comparing It with Sample Application

Based on the analyses and discussions that have studied in the former sections, and by using the equations which obtained as a result of these analyses, a computer program was developed by using the Visual Basic 6 program. The sketchy flow chart for this package is given in the figure 3.21, and the detailed flow chart is given in the Appendix-A while the program's code and form are given respectivily in the Appendix-B and Appendix-C. And the sample thermal performance calculation of the PTSC which is designed in this study is given in Appendix-D in form of print outputs of the package.

In order to prove the accuracy and validity of the package, it is required to compare it with experimental test results. So, on the basis of this objective literature has been scanned and the thermal performance test results of the PTSC for IST laboratory in the Sandia, America was obtained (Dudley, Evans & Matthews, 1995). The design, operation, environmental and the test results of the obtained PTSC are applied on the mathematical model program.

In the IST test, the thermal oil SYLTHERM 800 is used as working fluid which using in the high temperature applications. The thermophysical properties of the oil which needed in the calculations is given in the Appendix-E. And the design properties and dimensions data for the PTSC parameters which used in test is given in the next table 3.1.

Table 3.1The properties and dimensions of the Sandia PTSC parameters

PTSC Parameters	**Properties and Dimensions**
Collector Length L_{ref} [m]	6.100
Collector Width W_{ref} [m]	2.300
Rim Angle φ_r [Degree]	72
Absorber Tube Selective Surface Diameter D_{absOu} [mm]	50.8
Absorber Tube Selective Surface Wall Thickness t_{abs} [mm]	1.6
Absorber Tube Selective Surface Absorptance α_{abs}	0.94
Absorber Tube Selective Surface Emissivity ε_{abs}	0.18
Glass Cover Diamter D_{glOu} [mm]	75
Glass Cover Wall Thickness t_{gl} [mm]	1.25
Glass Cover Transmittance τ_{gl}	0.91
Glass Cover Emissivity ε_{gl}	0.88
Reflector Reflective Value ρ_{ref}	0.93
Aperture Area A_{apr} [m^2]	13.2
Working Fluid	Syltherm 800
Operation Temperature range [^oC]	100 - 300

The incident angle modifier factor K and the intercept factor γ for the obtained test results which important to make the analyses aren't given. So, to prove the validity of the mathematical simulation model the value of the both unknown value is taken as $K = 0.95$ and $\gamma = 0.95$.

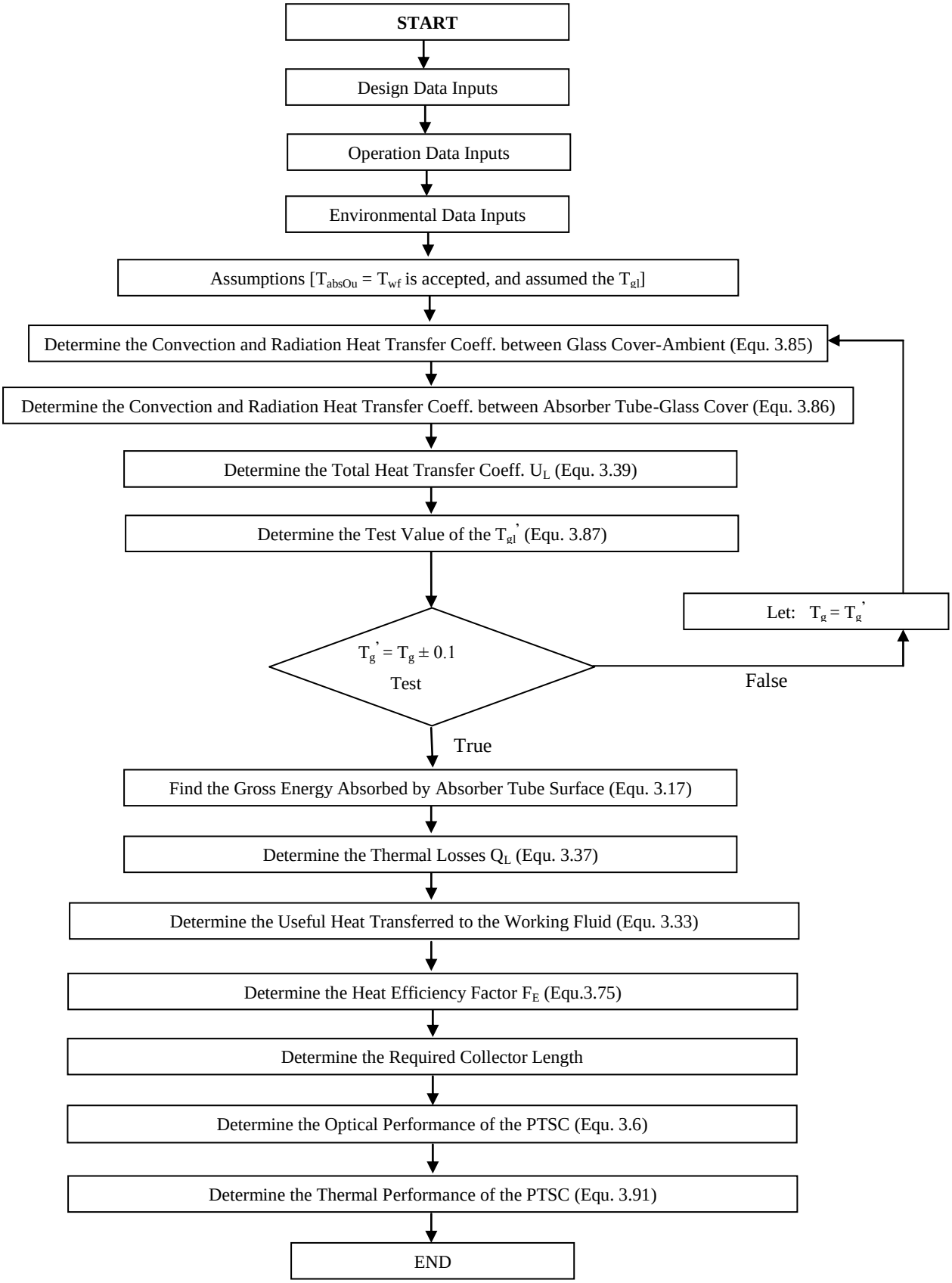

Figure 3.21 The flow chart for the PTSC thermal performance analyses program

By entering the properties and dimensions of the PTSC parameters which is given above in the table 3.1, and the operation and environmental condition of the IST test which is given in the next table 3.2 in the mathematical simulation model program which is derived in this study, the thermal performance results is obtained and its given with the test thermal performance results in the next table 3.2. In addition to the deviation ratio between the model and test results which given in the next table also. As a result of comparison when the test results are based, found that the maximum deviation is 6.21 % and the minimum deviation is 0.12 %, and the average deviation for the sixteen data is 0.1 % and the standard deviation is 2.17 %. Hereby it is proving the validity and accuracy of the developed thermal model for the PTSC system. The thermal performance results of the IST test and model are compared in form of curve which is given in figure 3.22.

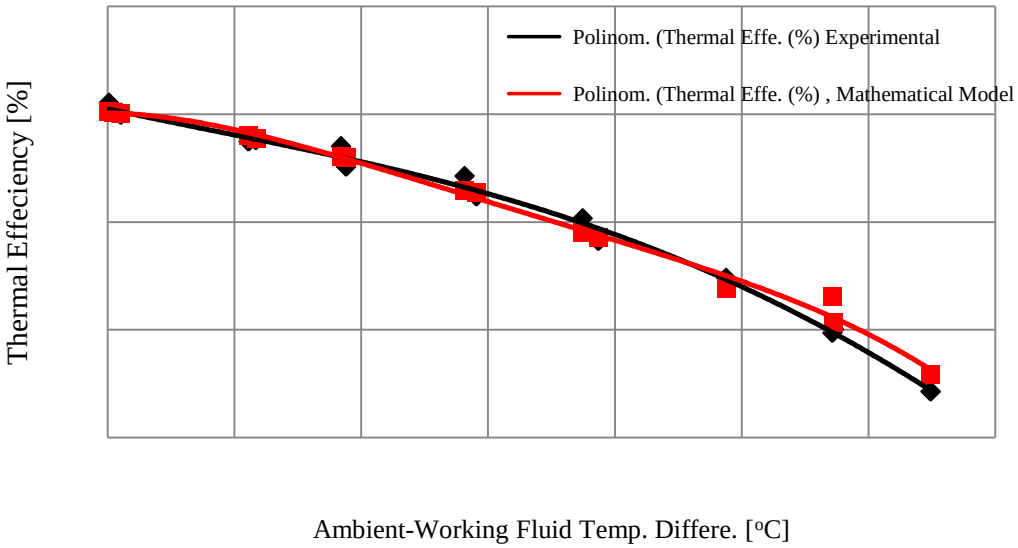

Figure 3.22 The approach curves of the Sandia IST test and mathematical model results

It is seen that the IST test and mathematical model results approach with each other by 0.1 % deviation. The deviation and deviation approach curves between the Sandia IST test and mathematical model results at the measurement points is given in the next figure 3.23.

Table 3.2 The operation, environmental conditions and the performance results for the IST sandia test laboratory and the model program

Test Date 1993	Direct Beam I_d [W/m^2]	Wind Speed V_w [m/sec]	Ambient Temperature T_a [^oC]	Inlet Temperature T_{In} [^oC]	Outlet Temperature T_{Ou} [^oC]	Flow Rate [lt/min]	Test Themal Performance [%]	Model Themal Performance [%]	Deviation Ratio [%]
25/08	940.7	1.8	31.4	29.25	34.40	24.7	71.07	70.14	1.308
25/08	936.0	2.1	29.6	29.18	34.26	24.6	70.20	70.08	0.171
03/09	987.1	0.1	25.4	27.88	33.23	24.6	69.93	70.03	-0.143
03/09	991.2	0.3	25.4	27.93	33.31	24.6	70.10	70.01	0.128
20/10	995.1	2.9	11.8	100.2	107.38	48.2	67.01	65.89	1.671
20/10	1005.7	3.9	14.1	151.38	158.09	50.4	64.26	62.76	2.334
20/10	875.5	1.8	16.1	200.65	206.16	51.0	60.35	58.79	2.584
21/10	927.2	3.7	10.2	251.34	256.69	51.9	54.82	53.6	2.225
21/10	994.9	4.1	14.0	297.75	303.11	52.5	50.04	50.4	-0.719
21/10	977.1	4.4	16.0	338.16	342.86	53.0	43.27	45.59	-2.981
22/10	920.3	1.2	11.4	63.27	70.35	45.5	67.46	67.88	-0.622
27/10	927.9	3.1	7.8	62.76	69.87	45.9	67.60	67.52	0.118
27/10	969.6	2.4	8.8	99.47	106.25	48.4	65.12	65.77	-0.998
27/10	972.7	2.5	10.2	152.42	158.73	50.3	62.37	62.58	-0.336
27/10	933.0	3.1	11.4	202.14	207.74	51.7	58.24	58.32	-0.137
01/11	1001.3	1.5	15.5	298.57	303.95	52.3	49.73	52.82	-6.213

The deviation between the Sandia IST test and mathematical model results stems from Sandia IST test results measurement error, the unknown value of some material properties, the one dimensional and steady state accepting of the thermal losses analysis for the mathematical model, the possible errors in the empirical equations which is used in the calculation of the heat transfer coefficients, the accepting of the incident angle at the solar noon is 18^{o} (K = 0.95) and the accepting of the intercept factor $\gamma = 0.95$.

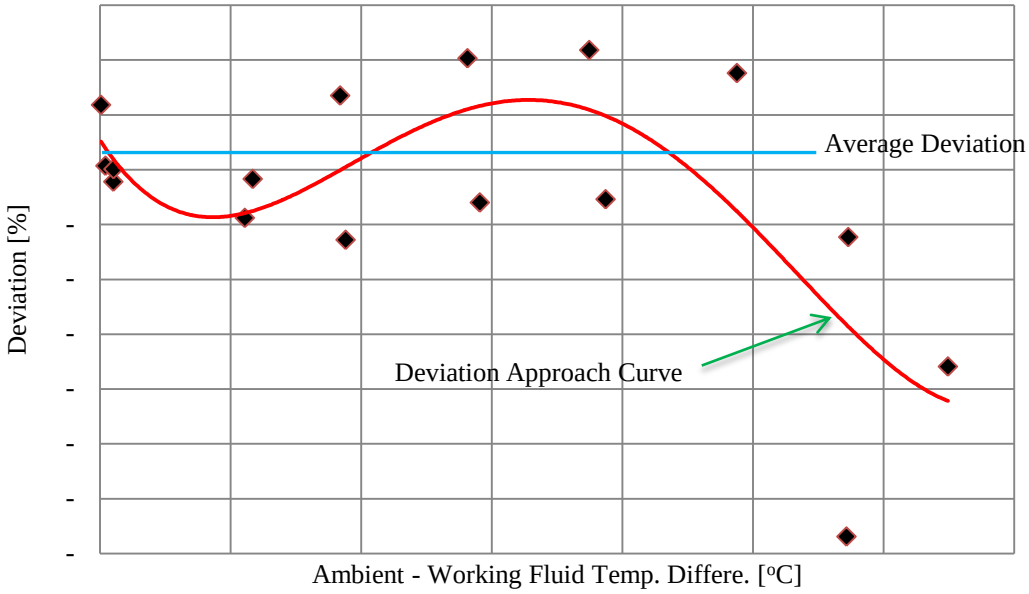

Figure 3.23 The deviation and deviation approach curves between the Sandia IST test and mathematical model results at the measurement points.

The mathematical model for PTSC which its validity proven can be used reliably in the thermal performance and design calculation and it can be used as basis in the study which is done on this issue in the future. Especially if the K and intercept factor enter in the mathematical model as variable, and taken into consideration the two dimensional and unsteady state conditions of the heat transfer which is taken in the thermal losses analyses.

CHAPTER FOUR
THE DESIGN OF THE PARAPOLIC TROUGH SOLAR COLLECTOR

The main aim of the solar collector design in the high temperature industrial applications are, produce high temperature working fluid which is required in these applications, develop a system around medium concentration ratio (C = 10–30) with economically acceptable investment (suitable recycling period), minimize the thermal losses areas to the maximum suitable extent and finally ensure customer satisfaction in the technical and economic aspects.

The PTSC is the most and easiest applied collector type. The thermal losses of this type is low because of the receiver surface area is small, but the optical losses is high because it depends on the direct beams only. Generally, the PTSC is used in middle and high temperature applications. The main applications are, residential heating using the solar energy, steam generation in the industrial process, absorbing cooling system applications and in the solar power stations which used to produce the electricity.

This collector consists from parabolic reflector coated with high reflective material, and the reflected solar beams concentrate on the absorber tube which installed along the parabolic focus line. The absorber tube is covered by glass with low reflectivity, high transmittance and high temperature and shock resistant glass, which works to minimize the thermal losses from the absorber tube to the environment. The high temperature difference between the absorber tube surface and the environment is one of the important factors which led to increase the thermal losses. The working fluid temperature can be increase to reach more high temperature level by in case of insufficient flow. Here, the flow rate of the working fluid should be controlled to keep the working fluid temperature under the upper level of the temperature for the design conditions. In case of uncontrolled working fluid temperature, the absorber tube deformations are concerned. These deformations can cause an optical deviation of the absorber tube which leds to increse the optical losses and break the glass cover and explode the system.

The four main parameters which affect the economics of the sun tracking PTSC are given below (Karaduman, 1989).

- The operation condition of the collectors (direct beam intensity, sun track type and technique, working fluid temperature and flow rate etc.),
- The design parameters of the collector system (concentration ratio, rim angle and collector dimensions etc.),
- The properties of the reflector and glass cover (reflectivity, transmittance, emittance and resistance etc.),
- The properties of the selective surface absorber tube (absorber tube geometry, absorptance, emittance, thermal conductivity and resistance etc.).

This design is aimed to transfer 25 kW of useful heat to the working fluid per collector. The thermal performance of the collector is about 70 % which changes depending on the environmental and operation factors. Accordingly, if the direct beams intensity which fall on the aperture area is 900 W/m^2, the useful heat gain which can transfers to the working fluid per unit area is 630 W/m^2. So, it is need to aperture area about 40 m^2 to get 25 kW of useful energy.

As a result of design calculations, the collector aperture area is determined as 40 m^2, and the dimension is determined in accordance with operation and technique condition as seen below. This assessment is taken into consideration the deformation which may occur in the reflector as a result of the wind load, that's led us to accept the intercept factor $\gamma = 0.96$. Accordingly;

L_{ref} = 8.0 m (Collector Length)
W_{ref} = 5.0 m (Collector Width)

4.1 The Design of the PTSC Reflector

4.1.1 Determination the Material of the PTSC Reflector Surface

The reflector is one of the most important parts of the PTSC system, the weatherproof thin sheet of aluminum material which have high reflected ratio 88 % is selected. This sheet (Alanod, see table 4.1) can be imported and its width equal to 1 m and thickness is 0.5 mm where it can be pasted on local sheet to install it. The reflective properties for some types of materials which are used as reflector surface of the concentrator collectors are compared in table 4.1 (Kılıç & Öztürk, 1983). In this design plan, the Alanod aluminum material is planned to use and the main reasons for this are, the silver is too expensive and the mirror is hard to give shape.

Table 4.1 The reflectivity of the some reflector surface materials

Reflector Surface Material	Reflectivity
Silver	0.94 ± 0.02
Gold	0.76 ± 0.03
Acrylic-coated aluminum	0.86
Aluminum	0.82 ± 0.05
Copper	0.75
Mirror	0.88
Custom polished aluminum thin film (Alanod)	0.88

4.1.2 The Dimension of the PTSC Reflector Surface

The parabolic reflector surface profile can be defined by the parabola curve function as given below (Duffie & Beckman, 1991). The definition of this equation is aimed to reflect the all direct beams which fall on the reflector toward the receiver. In this equivalent, the f term is defined the focal length. The basic design parameters of PTSC are given in the next figure (Duffie & Beckman, 1991).

$$y^2 = 4.f.x \tag{4.1}$$

In this figure, a = W_{ref} collector width, and φ_r is the rim angle, and r_r is the maximum reflector radius. The rim angle is defined as equation as shown below in terms of focal length, collector width and the maximum reflector radius (Duffie & Beckman, 1991).

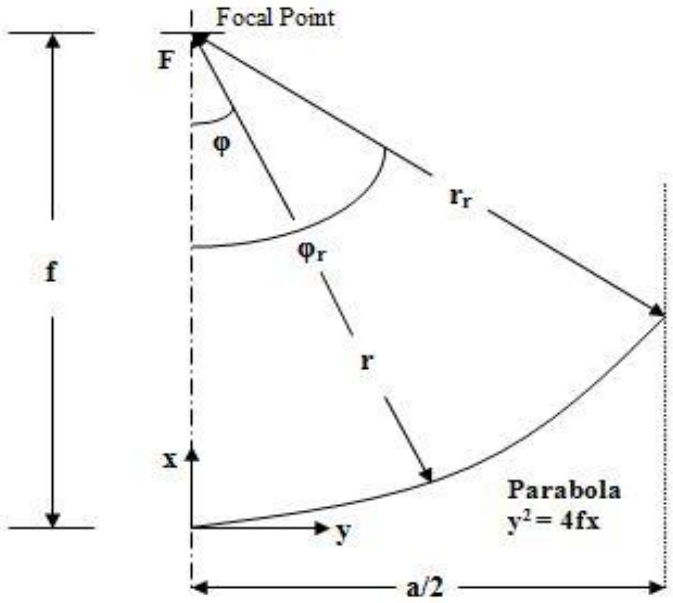

Figure 4.1 Section of a PTSC showing major dimensions and the x,y,z, coordinates

$$\varphi_r = \tan^{-1}\left[\frac{8.\ f/a}{16.\ f/a^{\ 2}-1}\right] = \sin^{-1}\left[\frac{a}{2.r_r}\right] \tag{4.2}$$

For any point of the parabolic reflector the reflector radius r is defined in equation 4.3 (Duffie & Beckman, 1991).

$$r = \frac{2.f}{1+\cos\varphi} \tag{4.3}$$

In order to design compact system the rim angle is taken as $\varphi_r = 70^o$, and to determine the focal length the next calculations are done. The parameters which are used in the calculations are defined in the figure 4.1 and 4.2.

$$H_o = \frac{W_{ref}/2}{\tan\varphi_r} = \frac{5000/2}{\tan 70} = 910\ \text{[mm]} \tag{4.4}$$

$$r_r = \frac{W_{ref}/2}{\sin\varphi_r} = \frac{5000/2}{\sin 70} = 2660\ \text{[mm]} \tag{4.5}$$

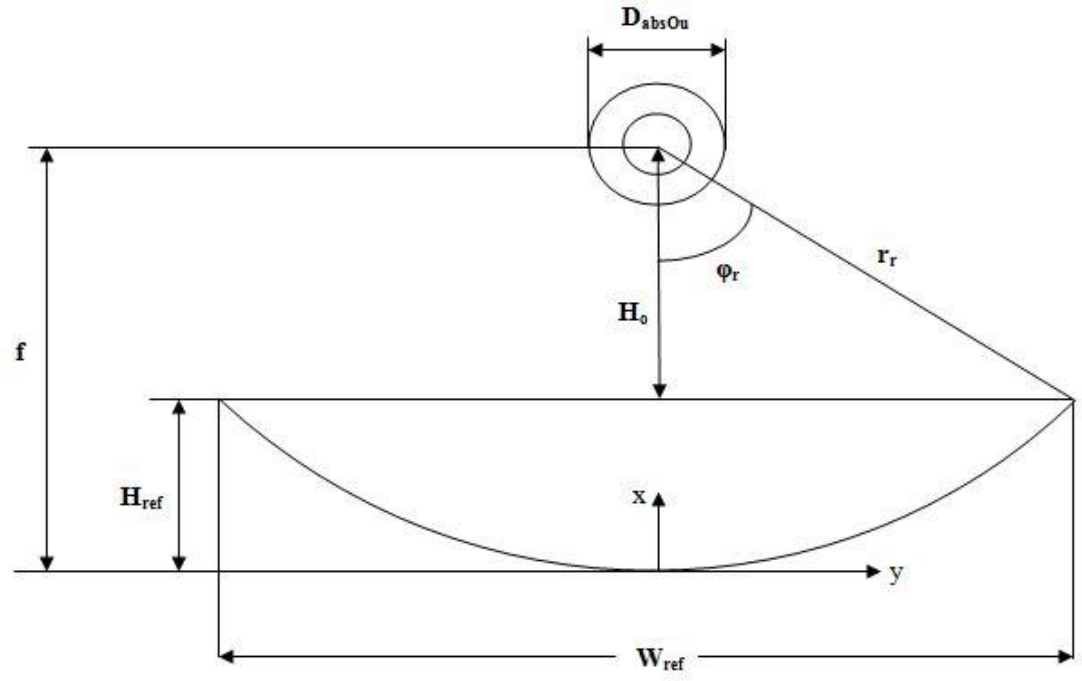

Figure 4.2 The basic geometry parameters of the PTSC system

And by substituting the r_r and φ_r in equation 4.3, the focal length f = 1.785 [m] in the last figure can be obtained. By substituting the last in equation 4.1, the reflector parabola equation can be determined as below.

$$y^2 = 7140.x \ \ [\text{mm}] \tag{4.6}$$

And the H_{ref} value can be defined and determined from the figure 4.2 as shown below.

$$H_{ref} = f - H_o = 1785 - 910 = 875 \ [\text{mm}] \tag{4.7}$$

After determining the H_{ref} value, the length of the parabola length W_p can be determined from the next equation to be equal to W_p = 5.383 [m].

$$W_p = 2\left[W_{ref}/4 \sqrt{1+ 4H_{ref}/W_{ref}}^2 + W_{ref}^2/16H_{ref} \ \ln\left(\sqrt{1+ 4H_{ref}/W_{ref}}^2 + 4H_{ref}/W_{ref}\right)\right] \tag{4.8}$$

According to this dimensions which obtained in the calculations above the collector is aimed to design. Accordingly, the reflector which has length 8 m can be designed from 8 pieces (1000 x 5383 x 0.5) mm of the Alanod which can pasted on local Aluminum sheet to install it.

4.2 The Design of the PTSC Glass Covered Selective Surface Absorber Tube

4.2.1 The Selective Surface Absorber Tube

The design of the selective surface absorber tube is limited by two opposite factors, where the diameter of the absorber tube should be large as much as possible in order to increase the optical performance by increasing the intercept factor, and on the other hand the diameter of the absorber tube should be small as much as possible in order to make the working fluid flow in turbulent state and reduce the thermal losses which depend on the outer surface area of the absorber tube. Accordingly, from the optical performance side the absorber tube diameter should be increased and from the thermal performance side the absorber tube should be decreased. This is an optimization problem which used to select the suitable diameter by taking into consideration the heat capacity aimed of the collector, the temperature difference of the working fluid at the operation conditions and the concentration ratio.

The absorber tube is the part of the PTSC which absorbed the direct solar beam and turned it to solar heat transferred to the working fluid. The absorber tube primarily should be had a high absorber rate to the short wave and low emittance rate as much as possible to the long wave. In order to achieve good heat transfer from the absorber tube surface which is heated by absorbed the direct beam to the working fluid, the high thermal conductivity materials and the thin wall thickness should be selected. In order to increase the forced convection heat transfer coefficient of the working fluid, the turbulence of the working fluid flow should be increased which be provided by decreasing the absorber tube diameter, increasing the working fluid flow rate or by using the nuzzle if the diameter can’t decrease because of the optical losses. Generally, the copper, aluminum and stainless steel are used to produce the

absorber surface. Although the high thermal conductivity of the copper, it is expensive comparing to other metals. Where the steel can be easily obtained but it is inclined to corrosion. On the other hand, the soldering and welding for the materials should be taken into consideration. The soldering and welding of the copper is easy but expensive, whereas the aluminum is difficult to solder or weld with other material. In the opaque absorber surface the transmittance is equal to zero ($\tau_{abs} = 0$), and the sum of the reflectivity and absorption rates for specific wavelength are equal to one ($\rho_{abs} + \sigma_{abs} = 1$).

According to Kirchhoff law, the opaque absorber surface absorption and emittance rates are equals for specific wavelength at the thermal equilibrium. The black painted surface has high absorption rate, but it has high emittance rate too. In the black surface absorber tube absorption rate to the direct solar beam and emittance rate to the long wave are ranged between (0.90-0.95). The absorption rate of the surface depends on the incident angle of the direct beam on the surface. The absorption rate to the direct solar beam and emittance rate to the long wave for some materials are shown in table 4.2 [Kılıç & Öztürk, 1983]. The given (σ/ε) ratio in the table 4.2 is scale to the solar heat gain. At the design of the absorption tube, the high (σ/ε) ratio should be selected.

Table 4.2 Spectral properties of some materials [Kılıç & Öztürk, 1983].

Surface	**Spectral Properties**		
	σ	**ε**	**σ /ε**
White painted aluminum	0.20	0.91	0.22
Water	0.94	0.95-0.96	0.98
Black painted (polished)	0.90	0.90	1.00
Black painted (opaque)	0.94-0.98	0.88	1.07-1.11
Galvanized steel	0.65	0.13	5.00
Aluminum	0.15	0.05	3.00
Chrome	0.49	0.08	6.13
Polished zinc	0.46	0.02	23.0

The black body is really absorber to the solar beam. It absorbed the all solar beams which fall on the surface, while the grey body reflected some of the solar beams depending on the incident angle of them on the absorber surface. The ideal black body has a high emittance rate at the same time. The ideal black body is the surface which absorbed all short waves and not emit to any long waves. Physically,

this situation is impossible. Here, the selective surface can be defined as the surface which approximately absorbed the all short waves and doesn't emit as much as possible to the long wave. The cross-sectional view of the beam losses mechanism for the normal surface and selective surface which plays an important role in increasing the thermal performance of the PTSC is compared in the figure 4.3. The processing stages of the selective surface absorber tube consisting of cleaning the tube surface which will be coated and then immersed in an acid tub. It is coated by a film of a material which has a high emittance rate to the long waves and high absorptance rate to the short waves. The coating is achieved by a chemical tub, spraying or by electrolysis plating. The coating by electrolysis plating isn't difficult but it is a bit expensive because it is needed to continuo attention and care to control the electrolysis tub and its homogeneity. In this process, the absorption and emittance rate of the selective surface is changing with the pH value of the solution, the solution temperature and the current intensity and its period which given to the solution.

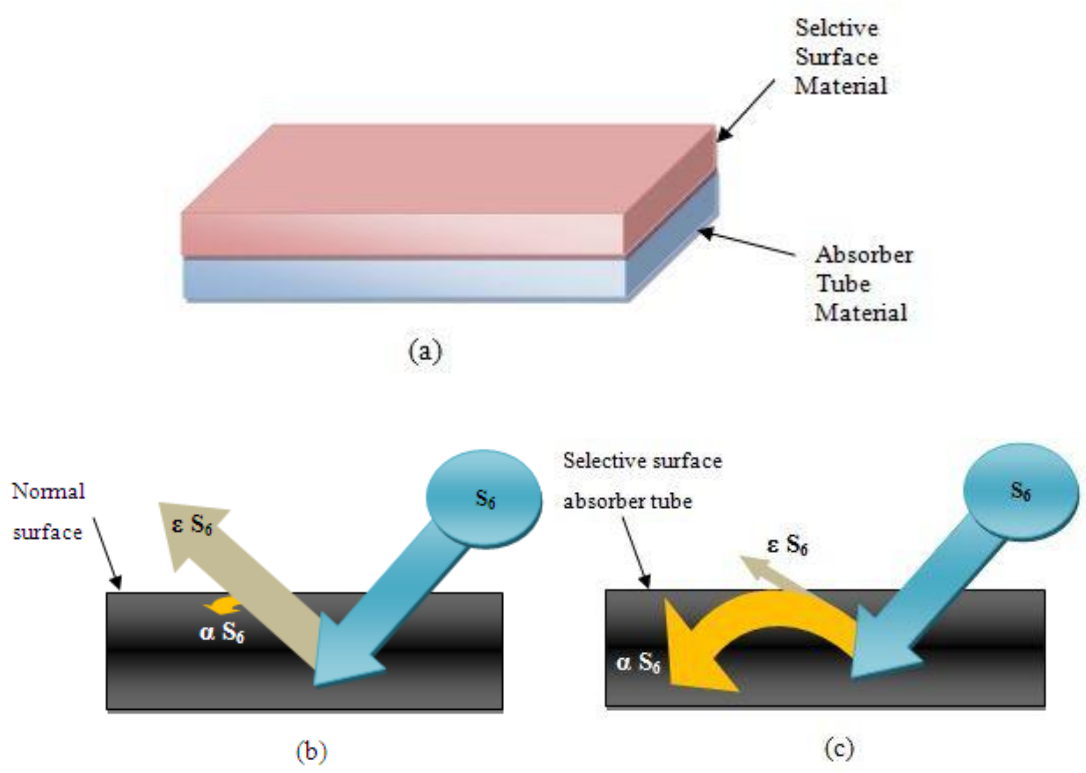

Figure 4.3 (a) Cross sectional view of selective surface absorber tube
(b) Beam losses mechanism at the normal surface
(c) Beam losses mechanism at the selective surface absorber tube

The spectral properties of some types of selective surface absorber tube are given in table 4.3 (Kılıç & Öztürk, 1983). As mentioned earlier the (α/ε) ratio is scale to the solar heat gain. Generally, the (α/ε) ratio is more than 4 for the selective surface. Practically, the absorptance rate decreases with decreasing the emittance rate. Therefore, the high (α/ε) ratio it doesn't mean that it's the best. In the application, the highest absorption rate which compatible with the operation and economic conditions is selected. The aim in the design of the absorber tube is making the all reflected direct beams which reflected from the reflector to focus on the absorber tube. The solar beams fall on the ground in a cone shape with apex angle 0.53^o or $32'$ (Duffie & Beckman, 1991).

Table 4.3 Spectral properties of some selective surface absorber tube [Kılıç & Öztürk, 1983].

Selective Surface (Upper Layer)	**Absorber Tube (Lower Layer)**	**Spectral Properties**		
		α	**ε**	**α/ε**
Nickel	Galvanized steel	0.93	0.08	13.6
Cobalt	Galvanized steel	0.91	0.12	7.6
Chrome	Steel	0.95	0.16	5.9
Iron oxide	Steel	0.83	0.06	13.8
Cobalt	Aluminum	0.92	0.13	7.1
Copper oxide	Aluminum	0.93	0.11	8.5
Lead sulfide	Aluminum	0.89	0.20	4.5
Nickel	Zinc coated-aluminum	0.94	0.10	9.4
Chrome	Zinc	0.91	0.08	11.4
Zinc oxide	Zinc	0.95	0.08	11.9
Chrome	Copper	0.92	0.08	11.5

This angle is known as the constant sun beams incidence angle. So, the angle between the cone axis and its rim is ($\theta_s = 0.53^o / 2$), which has 0.267^o or $16'$ value (Duffie & Beckman, 1991). The direct beam which falls in a cone shape on the rim of the reflector which is the most critics point on it is reflected and focuses on the absorber tube in specific angular aperture. This angle is the constant sun beams incidence angle as shown in the figure 4.4 below. In order to focus all the reflected solar beams on the selective surface absorber tube, the diameter of the absorber tube should be at least equal to the cone base circle of the beams which collected on the absorber tube.

$$r_{absOu} = r_r . \sin\theta_s \tag{4.9}$$

By substituting equation 4.5 in the last equation, the absorber tube outer diameter becomes;

$$D_{absOu} = \frac{W_{ref}}{\sin \varphi_r} \sin \theta_s \tag{4.10}$$

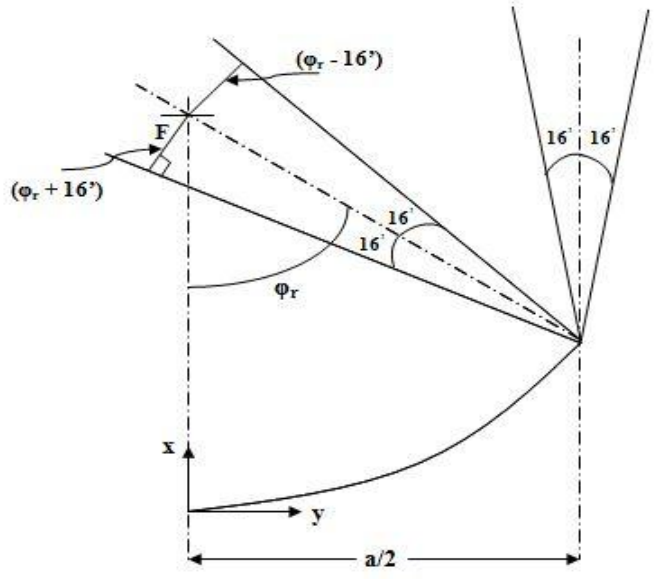

Figure 4.4 View of the solar beam which fall on the PTSC and reflected into the absorber tube in solar intercept angle, and the angular aperture of it.

By substituting the design parameters value (W_{ref} = 5000 mm and $\varphi_r = 70^o$) and the half solar intercept angle angle ($\theta_s = 0.267^o$), the minimum selective surface absorber tube outer diameter (D_{absOu} = 24.8 mm) can be determined. But this situation is valid only for the ideal reflector surface which doesn't have any imperfections in the shape of parabola. Therefore, the cone angle aperture for the reflector surface is bigger than the ideal situation by the dispersion angle value δ as shown in the figure 4.5 (Duffie & Beckman, 1991). The dispersion angle which derived from the imperfections in the shape of parabola can be determined by adding it to the solar intercept angle angle to derive the next equation.

$$D_{absOu} = \frac{W_{ref}}{\sin \varphi_r} \sin(\theta_s + \delta/2) \tag{4.11}$$

The dispersion angle of the PTSC which is designed in this steady is taken as δ=1 for safety, so the minimum selective surface absorber tube determined to be (D_{absOu} = 71.2 mm).

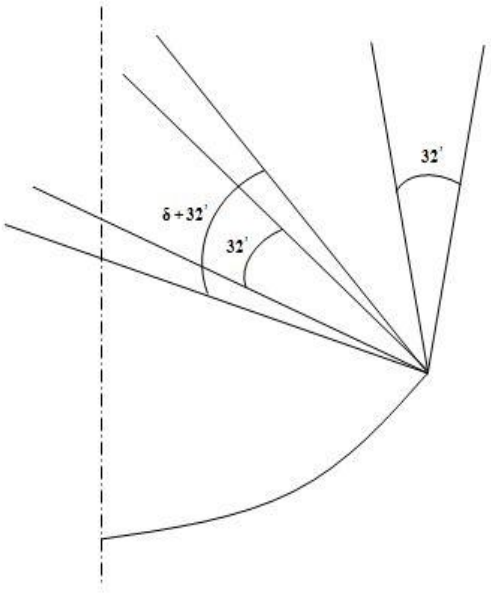

Figure 4.5 Schematic of a portion of a reflector with a dispersion angle δ added to the solar intercept angle.

4.2.2 The Glass Cover

The main aim in the design of the glass cover is reduce the thermal losses from the selective surface absorber tube to the environment and reduce the glass cover diameter in order to increase the unshaded area of the reflector which leads to increase the useful heat gain which transferred to the working fluid. Here, to reduce the unshaded area the glass cover diameter should decrease, but the thermal losses reducing is achieved by increasing the glass cover diameter in order to increase the space between the selective surface absorber tube. This condition requires making the thermal losses equal to zero $dQ_G / dr = 0$ and this condition leads to adversely affect the η_{op4}. By taking into consideration these conditions, the glass cover should design. Particularly, in the windy areas where the thermal losses become too much. So, the glass cover should be used in the windy areas where the convection heat

transfer coefficient (thermal losses coefficient) between the absorber tube and the environment is too much. This leads to divide the convection heat transfer coefficient above to free convection heat transfer coefficient between the absorber tube and glass cover and forced heat transfer coefficient between the glass cover and the environment. Now, in aim to reduce the forced heat transfer coefficient between the glass cover and the environment the glass cover temperature should be decreased. In order to achieve that, the space between the glass and tube should be evacuated to make vacuumed space between them. And that's leads to reduce the thermal losses in significant portion.

In addition, the glass cover protects the selective surface absorber tube from the external influences as the rain, hail and dust. The glass cover should be a good transmittance to the short solar wave which coming from the reflector (0.3 – 3.0) μm and has a low transmittance to the long solar wave (3.0 – 50) μm which coming from the absorber tube. And should be cheap, be easy to supply, not be affect from the ultraviolet solar beams, be lightweight and be break and scratch resistant. Generally, the glass and plastic based materials are used to produce the glass cover. The glasses are; transmittance to a large portion of the short solar waves (0.3 – 3.0) μm and prevent and the transmittance of the long solar wave (3.0 – 50) μm, and it's a good resistant to the high temperature and not be affect from the solar beams, but whereas it is difficult to transportation and difficult to processing.

The transmittance rate of the glass decreases with increasing the rate of the iron-oxide. Thus, the glasses which have an iron-oxide rate less than 0.05 % should be selected; these types have a transmittance rate to the short solar beams more than 0.83 %. The ordinary glasses which have a green color when viewed from the side and the windows glasses have an iron-oxide rate more than 0.10 %; these types have a transmittance rate to the short solar beams at about 0.70 % (Kılıç & Öztürk, 1983). The reflectivity of the glass is important as the transmittance. The antireflection materials are used to coat the one or two surfaces of the glass, to reduce the reflectivity rate and make it to approach zero (Kılıç & Öztürk, 1983). The plastic-based glass covers have a high transmittance rate for the short solar wave but it also

has a high transmittance rate for the long solar wave. Thus, it leads to increase the thermal losses to the environment. It's cheap, easy to supply, easy to processing, but whereas non-resistant to high temperature and affected from the solar beams. Some types of them are resistant to high temperature but it's expensive. The spectral properties, thickness and the high temperature resistance for the some types of the glass and plastic based glass is given in the table 4.4 (Kılıç & Öztürk, 1983) and table 4.5 (Karaduman, 1989).

Table 4.4 The structure and spectral properties of some types of glass (Kılıç & Öztürk, 1983).

Material Type	**Thickness [mm]**	**Refractive Index**	**Normal Transmittance Value**		**High Temperature Resistance [^{o}C]**
			Solar Beams	**Diffuse Beams**	
Leksan	3.20	1.586	0.73	0.02	120-130
Acrylic	3.20	1.490	0.80	0.02	80-90
Teflon	0.13	1.340	0.90	0.26	200
Tedlar	0.10	1.450	0.88	0.21	110
Sunlit	0.64	1.540	0.75	0.08	90
Smooth Glass	3.20	1.520	0.79	0.02	730
Temper Glass	3.20	1.520	0.79	0.02	230-260
Water-White Glass	3.20	1.500	0.92	0.02	200

Table 4.5 The spectral properties of some types of glass (Karaduman, 1989).

Glass Type	**Spectral Properties**		
	Transmittance (τ)	**Absorptance (α)**	**Reflectivity (ρ)**
Pyrex	0.90	0.02	0.08
Window Glass	0.87	0.04	0.09
Cast Glass	0.77	0.16	0.07
Heat Absorptance Cast Glass	0.41	0.53	0.06
Low-Iron Borosilicate Glass	0.92	0.02	0.06

4.3 The Design of the PTSC Tracking System

The optical performance of the PTSC is developed by improving the reflected solar beams focus on the absorber tube. Thus, the PTSC has to track the sun accurately. This tracking system of the PTSC can be tracked the sun in a single-axis or dual-axis. The performance and properties for the four types of the tracking system which are used in PTSC systems are compared in the table 4.6 [Singh & Cheema, 1976]. The east-west direction tracking system is planned to use in the PTSC system which designed in this study. The following system properties are needed to achieve the aimed tracking system.

- Movement Range: The PTSC positioned horizontally in north-south axis direction. To track the sun all day, the reflector has to revolve around the north-south axis from sunrise to sunset in 180^o. Further, for the sleeping mode at nights and sudden load emergency cases for instance strong wind, hail etc., the rotation angle should be selected as 270^o.

- Tracking accuracy: In the PTSC systems, the single-axis solar tracker system which provides the possibility to track the sun by one axis with high tracking accuracy of up to ± 0.01 degree.

- Torque of the reflector on the carcass system: The single-axis solar tracker system should be able to make the collector closing and coming to sleeping mode in emergency cases. Accordingly, it needs to 750 N.m torque to close the collector system which has 40 m^2 aperture area when the wind speed is 15 m/sec.

- Maximum angular rotation rate: The angular rotation rate is very slow in the normal case. But to protect the collector from the bad weather conditions and bring it to the sleeping mode, the collector has to return the 270^o at most in 10 minutes. So, the maximum angular rotation rate should be at least $270^o/600$ sec = 0.45 [^{o}/sec].

The continuous tracking to the sun in east-west direction in the horizontal north-south axis is satisfied by using software developed to track the sun depending on the application coordinate, date and time and this software controlled by two photocells supported on the collector. These photocells measured the direct solar beams on the collector and depending on the difference between them the deviation information from the optimum collector position sent to the computer which in turn directs the collector on the right position. Further, the manual control system should be found in aimed to bring the collector system to the sleeping mode in the bad weather conditions or any other emergency cases.

Table 4.6 The performance and properties for the four types of the tracking system which are used in PTSC systems (Singh & Cheema, 1976)

No.	Definition	Sun Tracking Performa-nce	Properties
1	Continuous tracking to the sun in north-south and east-west direction in both north-south and east-west axis.	100 %	a. The hourly or seasonal tracking performance doesn't change because of the continuity tracking to the sun, b. Precise computer control is required, c. Expensive, d. The wind effect creates problems, e. The pipe installations are difficult.
2	Continuous tracking to the sun in east-west direction in the north-south polar axis.	96 %	a. Although the tracking performance doesn't show a significant change hourly, but seasonally depending on the application region latitude it shows some change, b. Computer control is required, c. The collector should installed inclined at an angle equal to the latitude angle in the application region, d. The wind effect creates big problems.
3	Continuous tracking to the sun in east-west direction in the north-south horizontal axis.	77.3 %	a. Although the tracking performance doesn't show a significant change hourly, but it shows a big change seasonally. b. Common photocell and software control are required, c. It has high investment costs because of the large angular path to track the sun.
4	Continuous tracking to the sun in north-south direction in the east-west horizontal axis.	67.2 %	a. Although the tracking performance doesn't show a significant change seasonally, but it shows quite big changes hourly, d. Common photocell and software control are required, b. The collector will have the same track angle at sunrise and sunset.

Taking into consideration the operation conditions of the collector which consist of 25 kW thermal capacity, 30 ^{o}C difference between the inlet and outlet temperature of the working fluid (Syltherm 800) under 12 atm. The vacuumed glass cover selective surface absorber tube is selected to have (70 mm diameter, 1.25 mm wall thickness, 0.96 absorptance rate, 0.09 emittance rate of the selective surface absorber tube and 115 mm diameter, 2 mm wall thickness, 0.96 transmittance rate, 0.88 emittance rate of the glass cover with 4.060 m length) as it can be imported from a particular companies.

In order to satisfy the collector length from the absorber tube, 2 number of the selective surface absorber tube can be welding alongside to have 8 m length in total. The thermal conductivity of selective surface absorber tube is (k = 27 W/m.K). Now, after determined the selective surface absorber tube dimensions, the concentration ratio which is the most important criterion of PTSC can be determined as below.

$$C = \frac{A_{ref}}{A_{absOu}} = \frac{W_{ref}}{\pi D_{absOu}} = \frac{5000}{\pi.(70)} = 22.73 \tag{4.12}$$

Now, the dimensions and properties of the PTSC which designed in this study can be given in the next table 4.7.

Table 4.7 The dimensions and properties of the designed PTSC

PTSC Parameters		Dimension and Properties
Reflector	Material	Aluminum (Alanod)
	Thickness	0.5 [mm]
	Reflectivity Value	0.88
	Intercept Factor	0.96
	Width	5 [m]
	Length	8 [m]
	Parabola Length	5.383 [m]
	Parabola Equation	$y^2 = 7140\ x$
Vacuumed Glass Covered Selective Surface Absorber Tube	Tube Material	Stainless Steel
	Selective Surface	Cermet
	Tube Absorptance Value	0.96
	Tube Emittance Value	0.09
	Tube Thermal Conductivity	27 [W/m.K]
	Tube Diameter	70 [mm]
	Tube Wall Thickness	1.25 [mm]
	Glass Material	Low-Iron Borosilicate glass
	Glass Transmittance Value	0.96
	Glass Emittance Value	0.88
	Glass Diameter	2 [mm]
	Glass Wall Thickness	2 [mm]
	Length	4.060 [m]
	Collector Tubes Number	2
Tracking System	Tracking Type	Single-axis
	Tracking Direction	East-West
	Rotation Angle	270^o
	Angular Rotation Rate	0.45 [^{o}/sec]
	Rotation Torque	750 [N.m]
	IAMF	0.96
Geometric Parameters	Concentration Ratio	22.73
	Rim Angle	70^o
	Focal Length	1785 [mm]
	Reflector Rim Radius	2660 [mm]

CHAPTER FIVE
GRAPHICAL ANALYSIS AND ASSESSMENT

Based on the mathematical simulation program which developed in this study depending on the analyses and discussions those have studied in the chapter 3, and by using the designed parameters which given in chapter 4, with a simple operation and environmental conditions which will given later, several sets of calculations were carried out in the first part of this chapter. In the second part, the mean daily and monthly net collect energy by the PTSC (which designed in current study) in the Izmir city were determined by using the typical meteorological year data of this city which given in Appendix-F (Turkish State Meteorological Service, European Commission:Joint Research Center).

5.1 The Effect of the Desgin, Operation and Environment Parameters on the PTSC Thermal Performance

The thermal losses from the collector receiver are functions of operating temperature. The thermal losses through PTSC are changed in different ways depending on the receiver's configuration and operational conditions. The thermal losses are always existing (if there is a temperature difference between receiver and ambient) whenever solar radiation is available or not. In order to understand the PTSC performance, several sets of calculations were carried out. These studies help us to make the sensitivity analysis for the design and operation parameters which affect the collector performance. The main design, environmental and operation parameters which affect the PTSC performance are obtained from the preliminary simulation studies.

Those parameters are; Ambient temperature, Direct solar beams, Selective surface absorber tube diameter, Mass flow rate of the working fluid, Emittance value of the selective surface absorber tube, Absorptance value of the selective surface absorber tube, Reflectivity value of the reflector, Reflector width, Transmittance of the glass cover, Wind speed, The inlet temperature of the working fluid and Incident angle.

The variation of the PTSC thermal performance with the parameters which refer above is simulated and calculated using the mathematical simulation model. In order to study the effect of specific parameter on the thermal performance of the PTSC graphically and make the sensitivity analysis of it, the other parameters should keep constant. The environmental and operation conditions taken as follow; direct beam 900 W/m^2, ambient temperature 30 ^{o}C, and working fluid working temperature 150/180 ^{o}C with 0.45 kg/sec mass flow rate and wind speed is 4 m/sec.

5.1.1 The Effect of the Operating Temperature on the PTSC Thermal Performance

When the operating temperature increases, the temperature of collector has enhanced. The thermal losses to ambient are functions of the collector temperature. As known, the convection has a linear relationship with the temperature and the radiation has the forth power of the collector temperature. Therefore increased collector operating temperature induces more thermal losses. Figure 5.1 shows that the collector efficiency drops with operating temperature increasing.

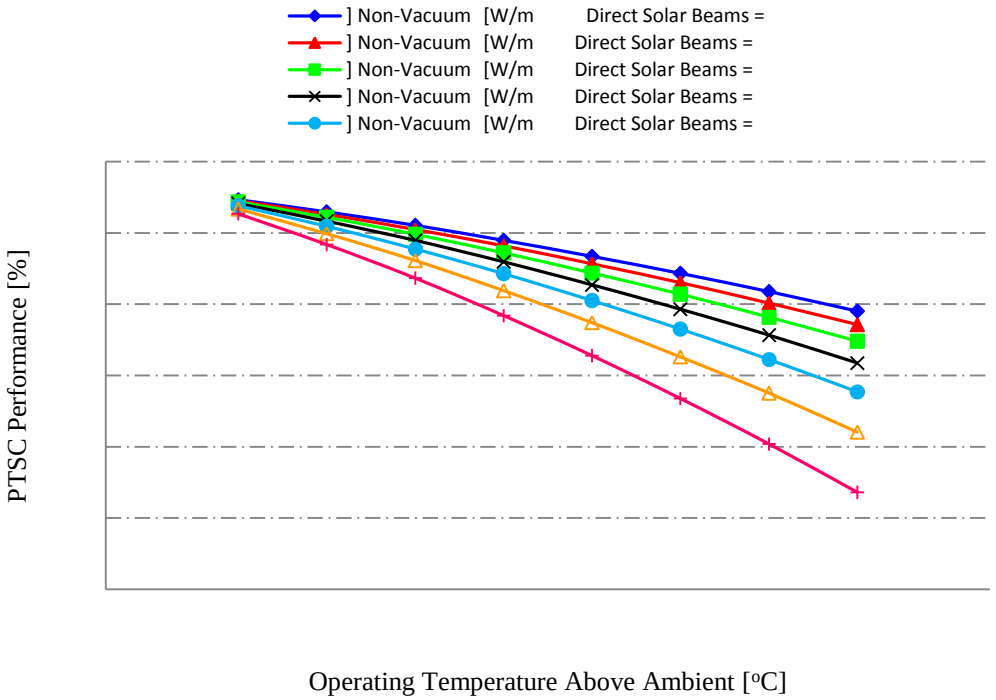

Figure 5.1 The variation of the PTSC performance with the operating temperature

5.1.2 The Effect of the Ambient Temperature on the PTSC Thermal Performance

Excluding the ambient temperature, the all rest design, environmental and operation parameters kept constant, and the variation of the PTSC thermal performance with the ambient temperature which given in the next figure was studied using the mathematical simulation model.

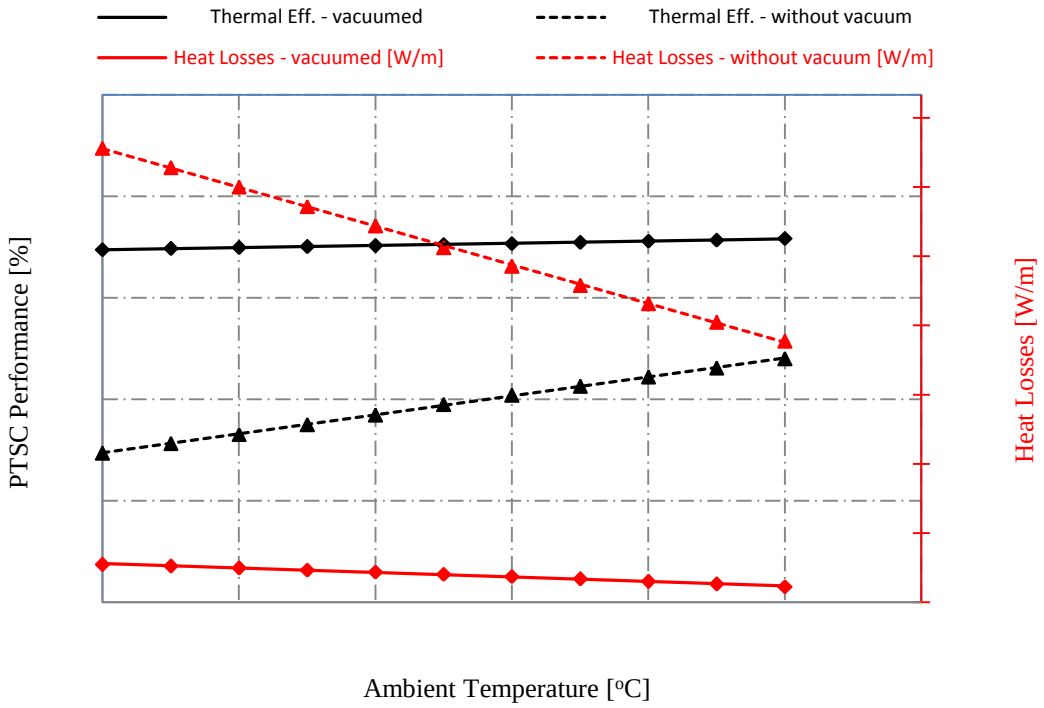

Figure 5.2 The variation of the PTSC performance and heat losses with the ambient temperature

In both cases vacuumed and non-vacuum the thermal performance increases linearly with increasing the ambient temperature, but they range between (71.97 – 72.14) % and (68.13 – 69.62) % for application region of the first and second case respectively, when the heat losses range between (36 - 46) W/m and (143 – 227) W/m respectively for application region too. The increasing in the ambient temperature leads to reduce the temperature difference between the mean working temperature and the ambient temperate, so reduce the heat losses as shown in the figure which leads to increase the PTSC thermal performance.

5.1.3 The Effect of the Selective Surface Absorber Tube Diameter on the PTSC Thermal Performance

The effect of only the selective surface absorber tube diameter is shown in the figure 5.3 below. As shown in the figure the PTSC thermal performance decreases by increasing the selective surface absorber tube diameter. That's can be explained by the increasing of the thermal losses as a result of increase the absorber tube exterior area.

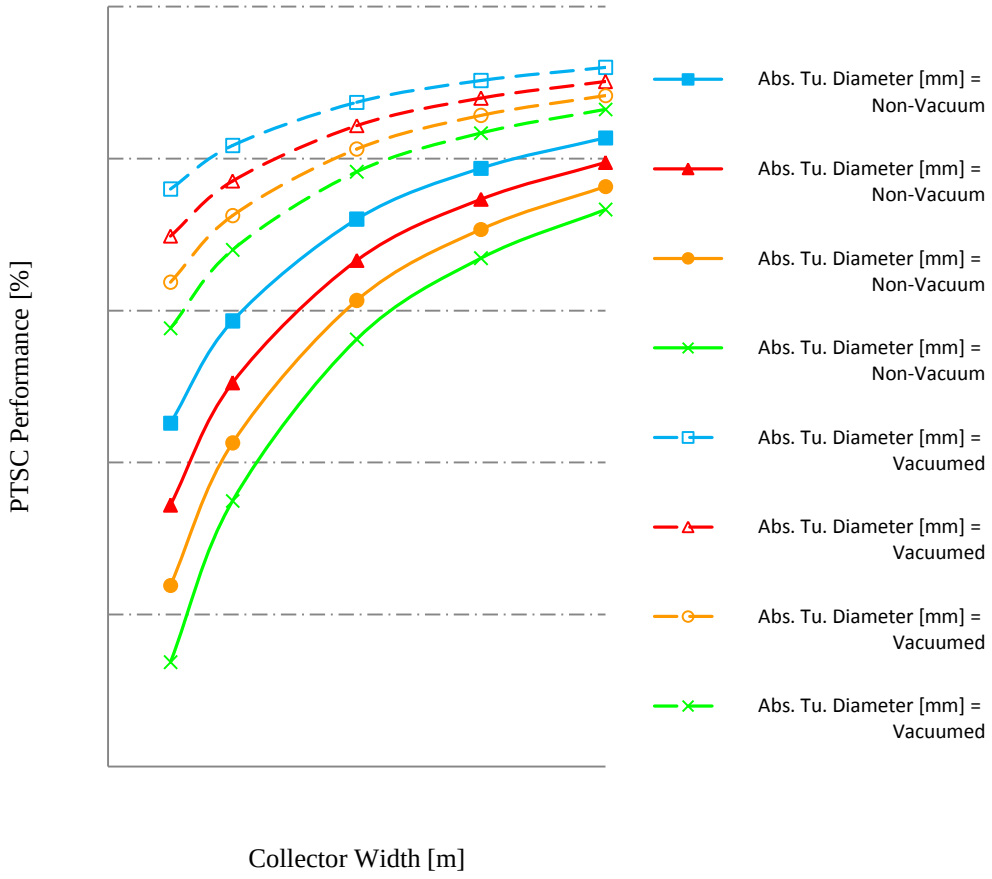

Figure 5.3 The variation of the PTSC performance with the selective surface absorber tube diameter

5.1.4 The Effect of the Direct Beams on the PTSC Thermal Performance

Solar collector absorbed more energy along with solar intensity increasing. Although the thermal losses also increase due to the increased absorber tube

temperature, it is much smaller than the enhanced absorbed solar energy. As shown in figure 5.1 and 5.4, PSTC performance increases with the solar intensity increasing. The increasing in the thermal performance is based on the high concentration ratio of the PTSC.

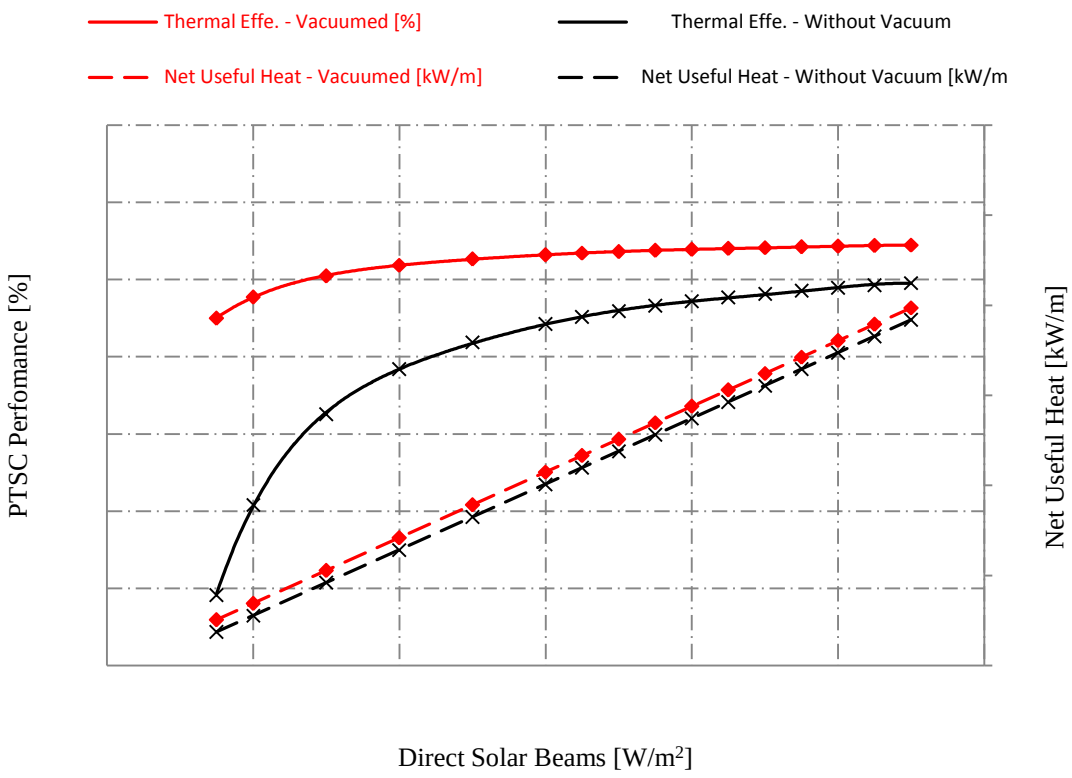

Figure 5.4 The variation of the PTSC performance and net useful heat with the direct beams intensity

So, the direct beams collected from the reflector area which is very large compared with the absorber tube surface area that the heat losses based on it. In this graphic the vacuumed and without vacuum cases thermal performance curves are intersected with the x-axis to be zero at 11.2 and 48.1 [W/m^2] respectively which represent the critical direct beams intensity of the two cases. In this critical intensity the heat losses are equal to the gross solar heat energy which collects on the absorber tube surface. The both vacuumed and without vacuum cases thermal performance values range between (70.9 –72.1) % and (64.2 – 69.4) % for application region of the first and second case respectively, when the net useful energy range between (1.4 – 3.6) kW/m and (1.2 – 3.4) W/m respectively for application region too.

5.1.5 The Effect of the Working Fluid Mass Flow Rate on the PTSC Thermal Performance

The results under different flow rate show that flow rate does not impact on the PTSC performance as shown in figure 5.5. The small sectional area of the absorber tube makes the flow always turbulence (even at low velocities). The thermal performance in the turbulent flow region is increased in very low linearly form with increasing the mass flow rate.

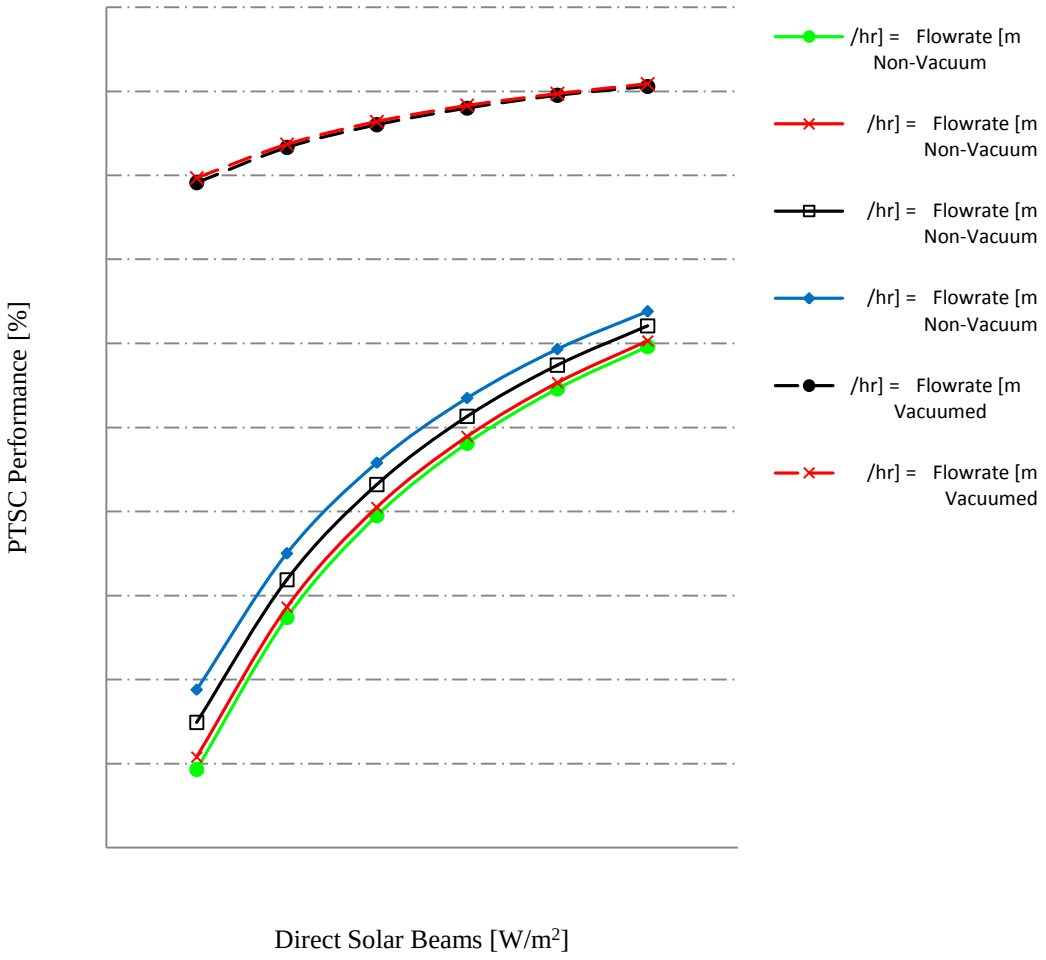

Figure 5.5 The variation of the PTSC performance and direct solar beams with the working fluid mass flow rate

5.1.6 The Effect of the Selective Surface Absorber Tube Emittance on the PTSC Thermal Performance

The effect of the selective surface absorber tube emittance on the PTSC performance is shown in the figure 5.6 below. As seen in the figure the PTSC performance decreases with increase the emittance of the selective surface absorber tube.

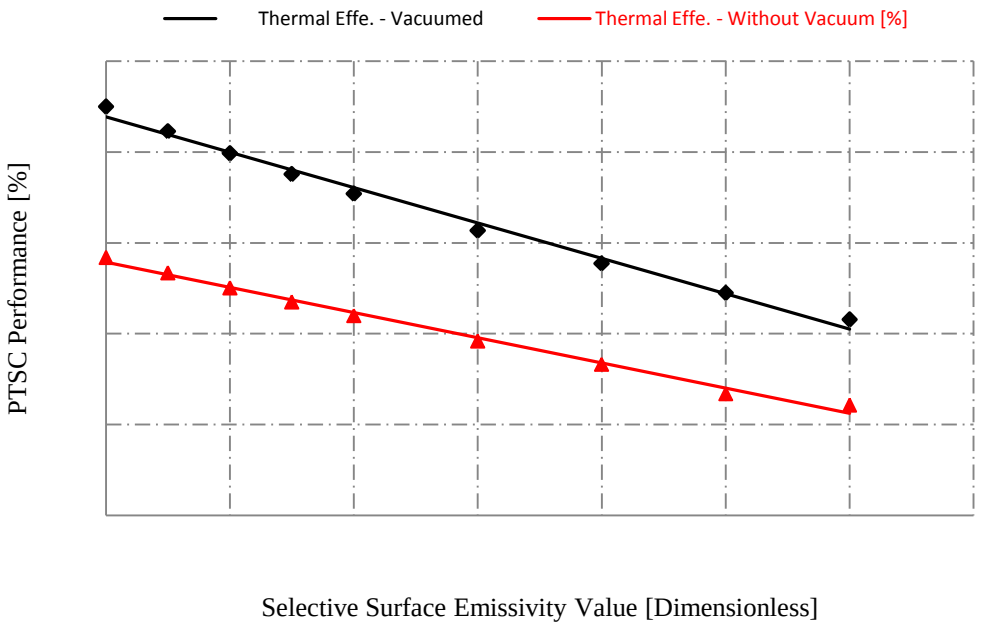

Figure 5.6 The variation of the PTSC performance with the selective surface absorber tube emittance.

5.1.7 The Effect of the Selective Surface Absorber Tube Absorptance on the PTSC Thermal Performance

As seen below the PTSC performance decreases linearly with decrease the absorptance of the selective surface absorber tube, whereas the net useful heat gain which transferred to the working fluid is reduced by reducing the gross heat energy which absorbed by the selective surface absorbed tube.

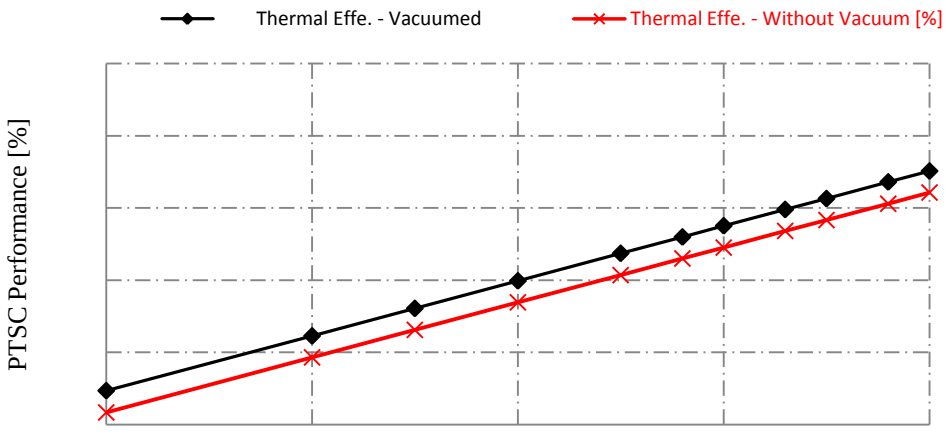

Figure 5.7 The variation of the PTSC performance with the selective surface absorber tube absorptance.

5.1.8 The Effect of the Reflectivity of the Reflector Surface on the PTSC Thermal Performance

The PTSC performance decreases linearly with decrease the reflectivity of the reflector surface, whereas the net useful heat gain which transferred to the working fluid is reduced by reducing the gross heat energy which absorbed by the selective surface absorbed tube.

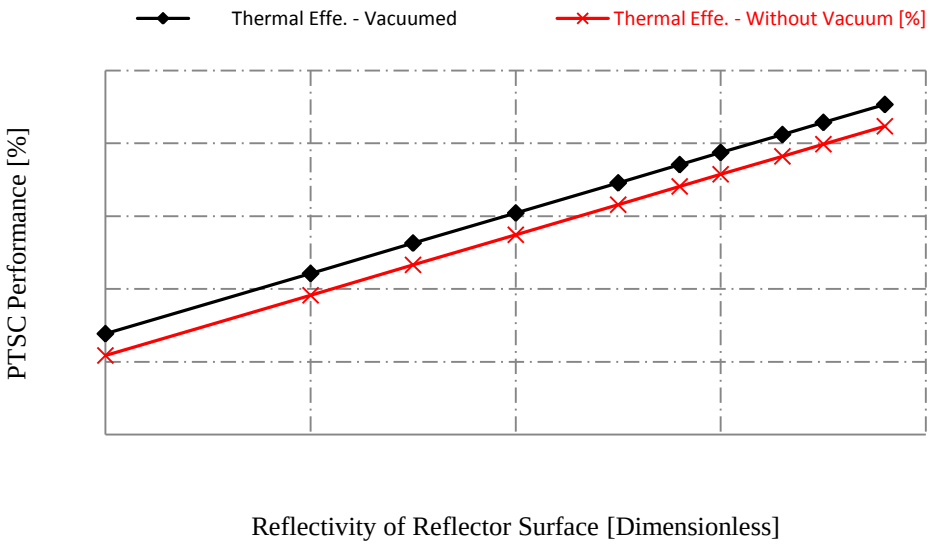

Figure 5.8 The variation of the PTSC performance with the reflectivity of the reflector surface

5.1.9 The Effect of the Collector Width on the PTSC Thermal Performance

According to the figure the variation of the collector performance with the collector width for the both cases can be divided into two regions; for vacuumed case, the collector performance decreased slowly with decreasing the collector width until collector width be equal to 1.75 m (when the concentration ratio equal to 7.96), while it starts to decrease rapidly under this dimension. But the non-vacuum case, the collector performance decreased slowly with decreasing the collector width until collector width be equal to 3 m (when the concentration ratio equal to 13.64), while it starts to decrease rapidly under this dimension. That's decreasing can be explained by the unshaded area reducing which directly affected the direct beams reflected into the absorber tube.

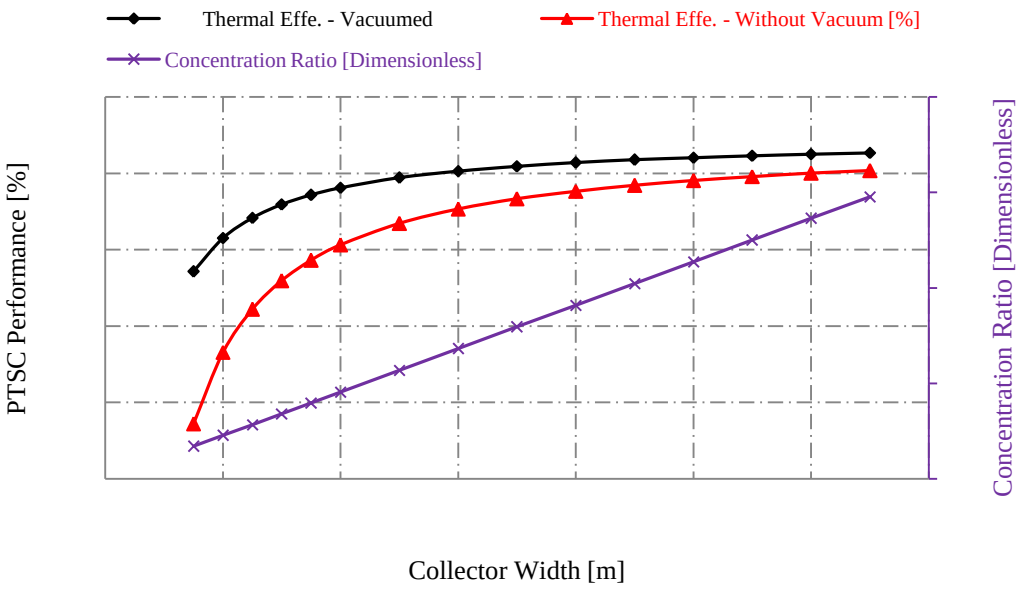

Figure 5.9 The variation of the PTSC performance with the collector width

5.1.10 The Effect of the Glass Cover Transmittance on the PTSC Thermal Performance

The PTSC performance decreased linearly with decreasing the transmittance value of the glass cover. That's decreasing can be explained by decreasing the gross heat gain which absorbed by the absorber tube.

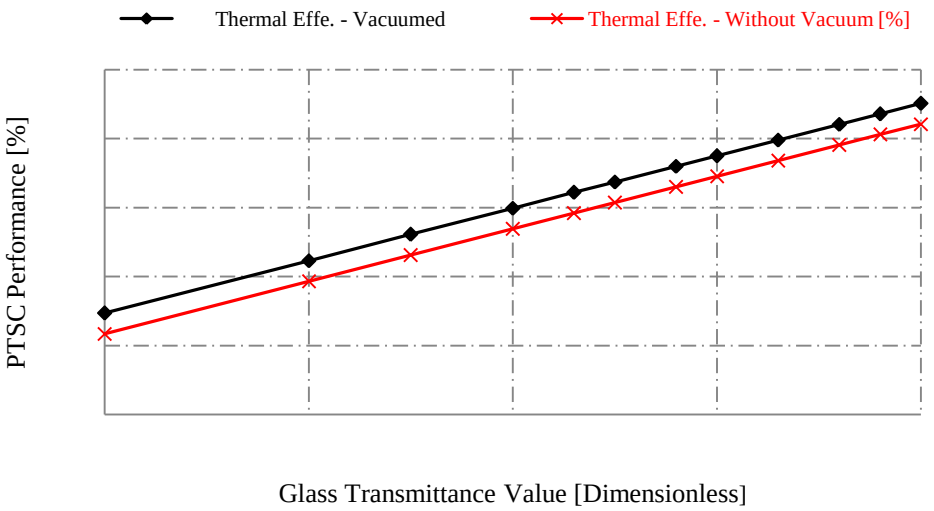

Figure 5.10 The variation of the PTSC performance with the glass cover transmittance value

5.1.11 The Effect of the Wind Speed on the PTSC Thermal Performance

The solar collector is exposed to the outside surrounding. Natural climate conditions are at impacts its performance. The PTSC efficiency reduces when the wind speed increases as indicated in figure 5.11.

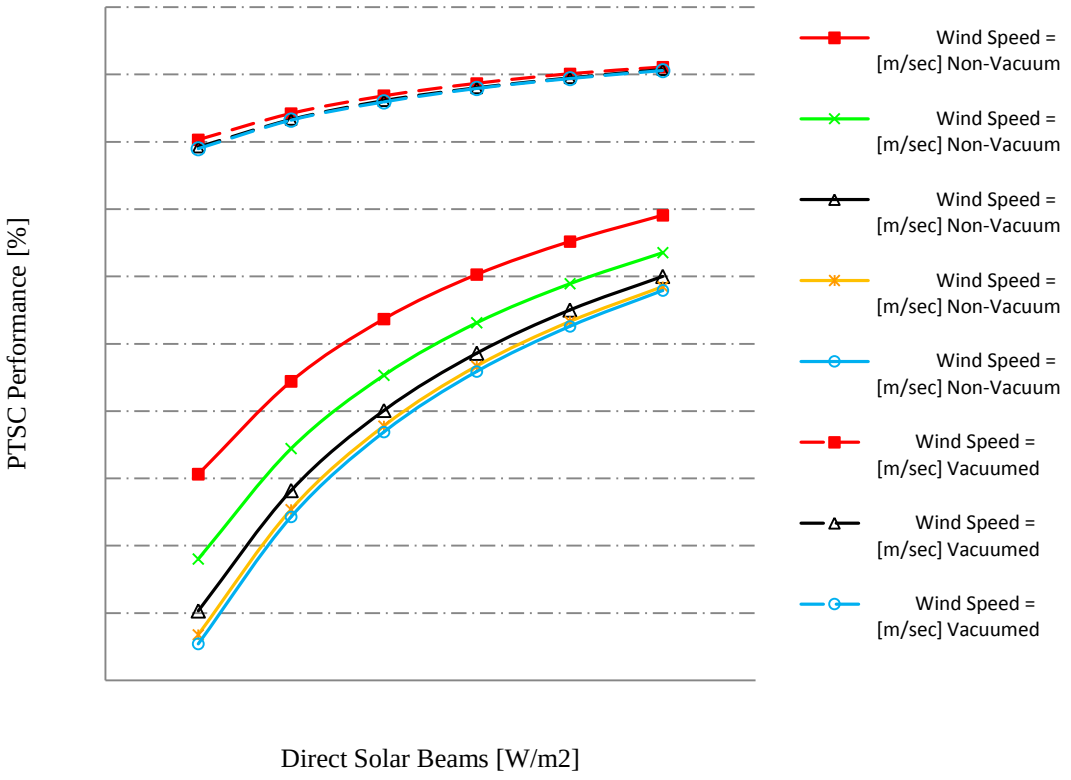

Figure 5.11 The variation of the PTSC performance with the wind speed

5.1.12 The Effect of Concentration Ratio on the PTSC Thermal Performance

The concentration ratio plays an important role in this variation (as shown below) this arises from the increasing the ratio of the heat losses to the gross heat gain. The parabolic form of the curve arises from the radiation heat losses which depend on the forth power of the temperature.

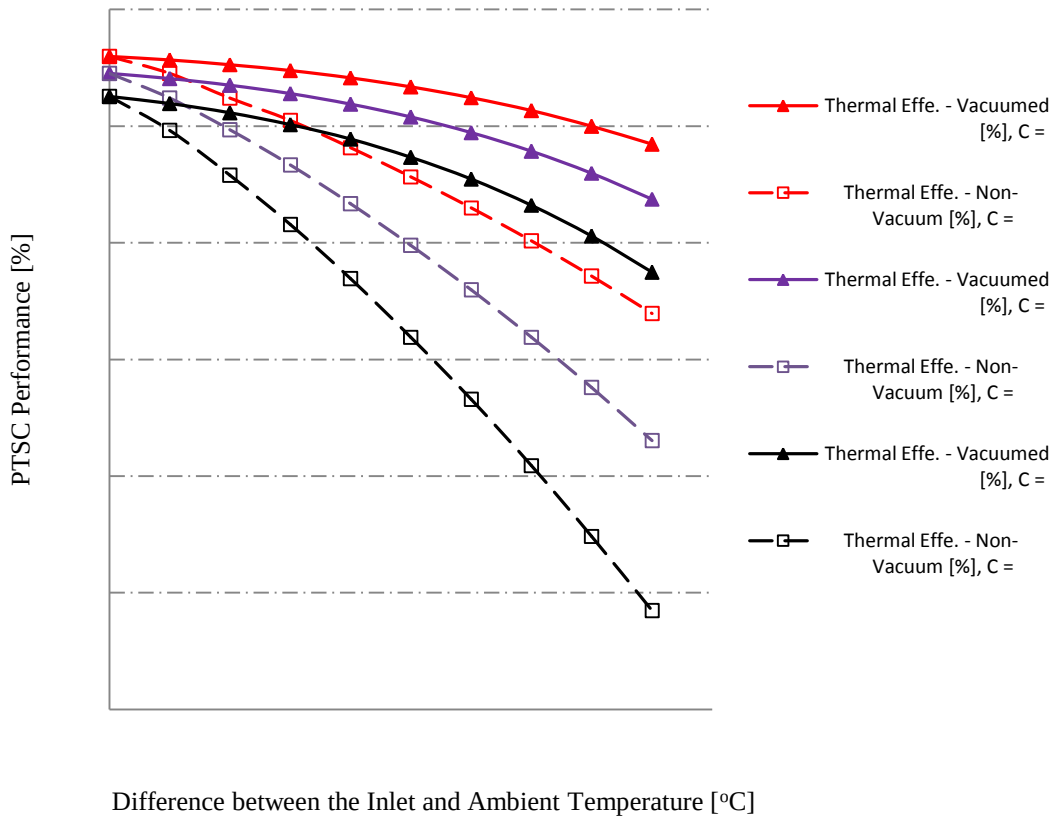

Figure 5.12 The variation of the PTSC performance with the concentration ratio and the difference between inlet and ambient temperature

5.1.13 The Effect of the Incident Angle on the PTSC Thermal Performance

The incident angle modifier factor K is a very important factor impacting on the solar efficiency. The efficiency of a PTSC decreases when the solar beam incident angle increases shown in figure 5.12.

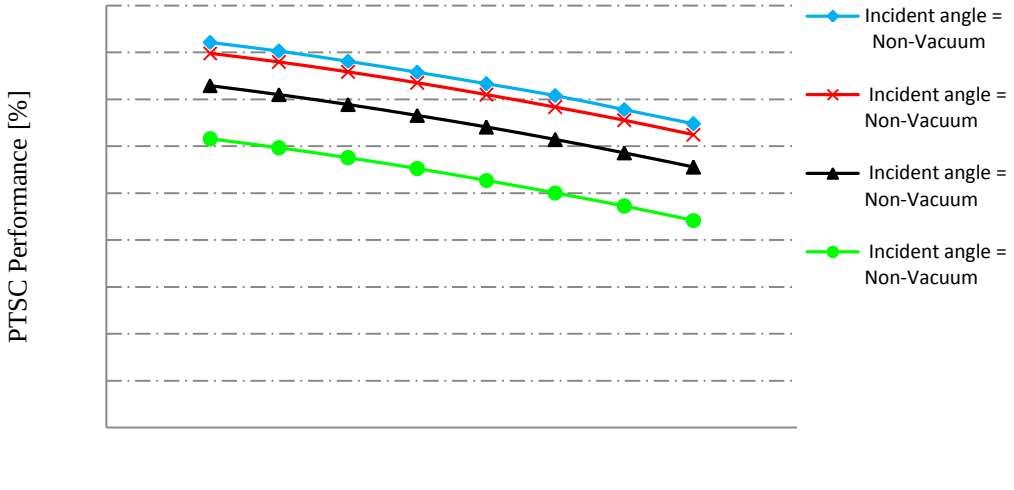

Figure 5.13 The variation of the PTSC performance with the incident angle

5.2 The Expected Mean Hourly, Daily, Monthly and Annually Output Power in İzmir City

Depending on the typical meteorological year data for Izmir city (Turkish State Meteorological Service, European Commission:Joint Research Center), The hourly output power of the PTSC which tracking the sun in north-south axis (from the east to the west) depending on the month of the year is determined as shown in next figure.

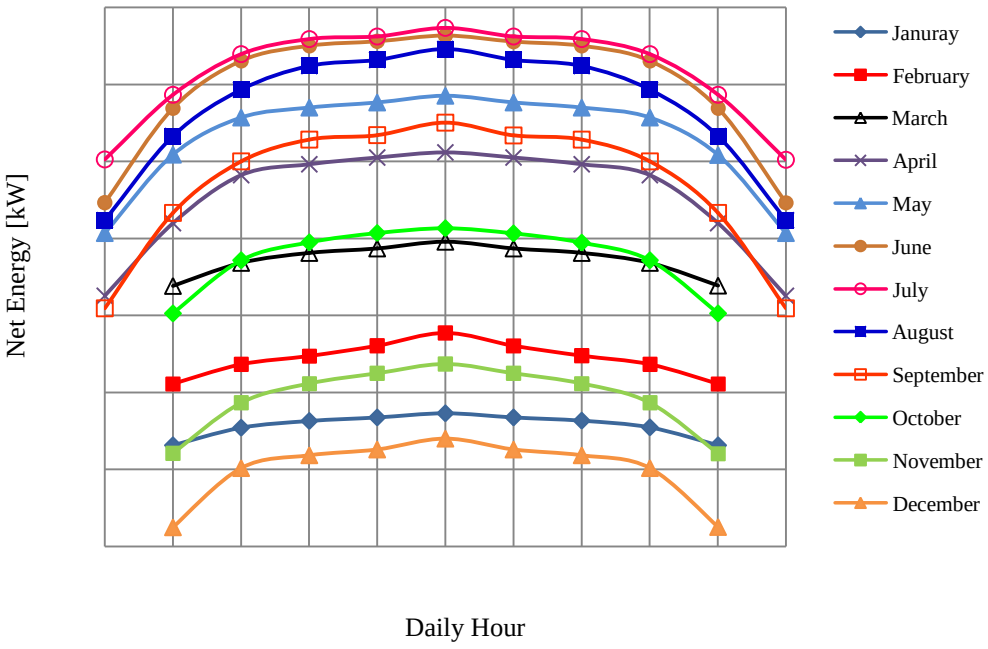

Figure 5.14 The mean hourly load of the PTSC based in Izmir city

As shown, the July month has the maximum hourly power capasity when the December month has a minimum and the long day time in the summer months make the mean daily and monthly power capasity higher than the winter months as shown in the figure 5.15 and 5.16 for three different state (sun tracking type and weather state), where the daily output power ranged between (53.6 – 179.4) kWh for single axis tracking real sky, (103.1 – 226.2) kWh for single axis tracking clear sky and (160.4 – 234.4) kWh for two axis tracking clear sky state.

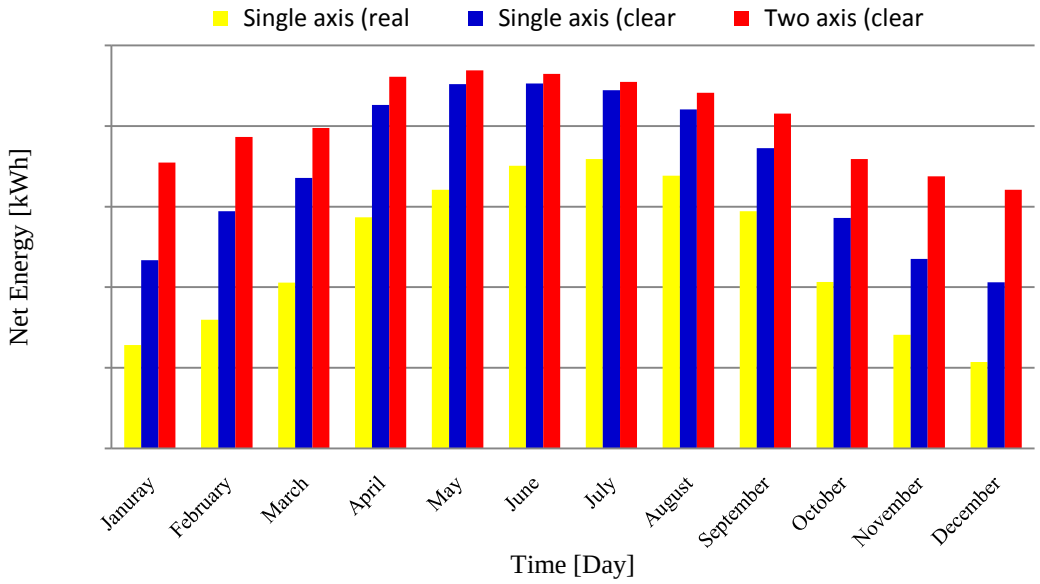

Figure 5.15 The mean daily load of the PTSC based in Izmir city

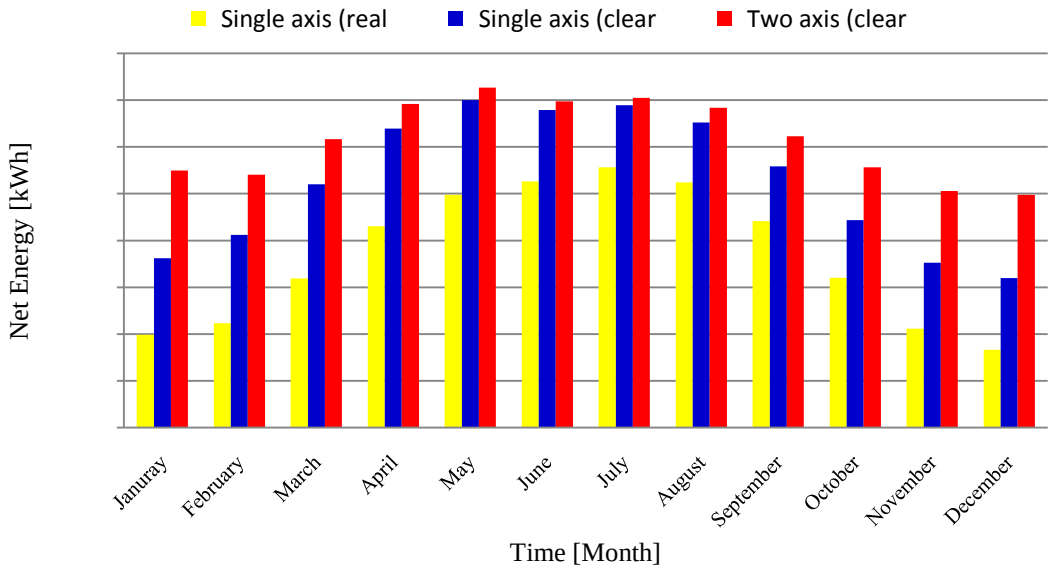

Figure 5.16 The mean monthly load of the PTSC based in Izmir city

The monthly output power ranged between (1662.7 – 5562) kWh for single axis tracking real sky, (3197.3 – 7002.2) kWh for single axis tracking clear sky and (4972.7 – 7268.6) kWh for two axis tracking clear sky state. Finally, the system which designed in this study can deliver a total output power of 44,143, 63,272 and 73,739 kWh per year for the three state respectively as shown in the next figure.

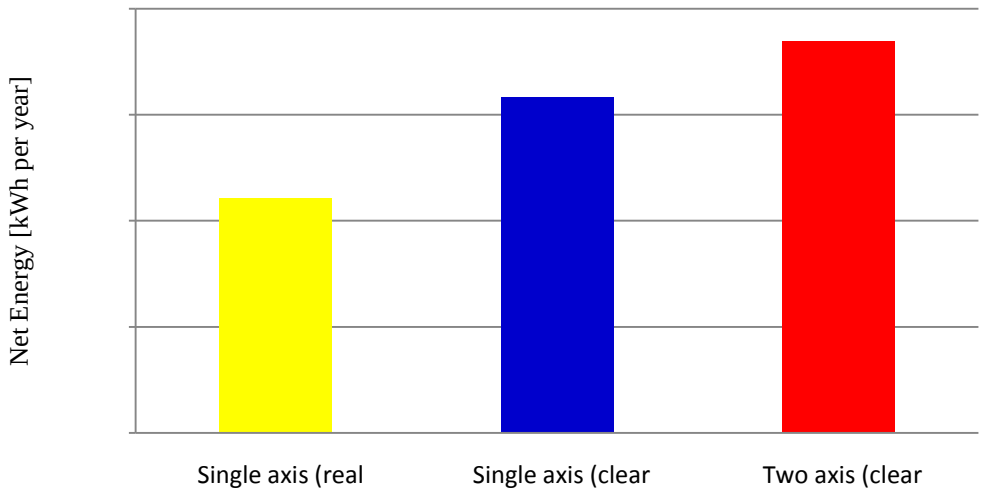

Figure 5.17 The annually load of the PTSC based in Izmir city

It's worth to mention here that the direct solar beams that fall on the plane surface of the PTSC which track the sun from the east to the west in a horizontal north-south axis for the three state (real and clear sky) are provided by multiply the global radiation data which taken from (European Commission:Joint Research Center) by 0.75 and 0.85 for real and clear sky states respectively, depending on the tilt of the plane surface from the horizontal [β] which have studied and explained in section 2.4. and from its equation [β] can be calculated as shown bellow in sample application,

Month	Hour	ϕ	δ	γ	ω	θ_z	ω_{ew}	γ_s'	γ_s	β
February	10:00	38	-13.29	-90	-30	58.5	107.5	-34.82	-34.82	43
May	09:00	38	18.8	-90	-45	43.5	64.16	-76.52	-76.52	42

CHAPTER SIX
DISCUSSION AND CONCLUSION

The thermal losses from the collector receiver are functions of operating temperature. The thermal losses through PTSC are changed in different ways depending on the receiver's configuration and operational conditions. The thermal losses are always existing (if there is a temperature difference between receiver and ambient) whenever solar radiation is available or not.

In order to understand the PTSC performance, several sets of calculations were carried out. These studies help us to make the sensitivity analysis for the design and operation parameters which affect the collector performance. The main design, environmental and operation parameters which affect the PTSC performance are obtained from the preliminary simulation studies (See Chapter 5).

The PTSC is the most and easiest applied collector type. The thermal losses of this type is low because of the receiver surface area is small, but the optical losses is high because it depends on the direct beams only. The performance can increase as the concentration ratio increases on condition that the heat losses decrease.

As a mathematical model, the developed heat transfer and energy balance PTSC model is very useful for solar heating and cooling system design. It not only helps to select the proper operating conditions and to detect the possible problems in the design of system, but also provides some basic figures for device's selection.

A rigorous mathematical model considering the geometrical, optical, environmental and thermal aspects has been carried out. The accuracy of the detailed simulation model is demonstrated in this study by comparison for thermal efficiency with steady state experimental data obtained by Sandia National Laboratories for PTSC with non-vacuum in the space between the receiver and glass cover working with single-phase thermal oil (Syltherm 800). Sixteen data points evaluated for thermal efficiency in both systems shown a maximum error of 6.21 % and the

minimum deviation is 0.12 % when the average deviation for the sixteen data is 0.1 % and the standard deviation is 2.17 %.

Typical performance calculations show that when hot-water at 150 ^{o}C flows through a 8 m by 5 m PTSC with 900 W/m^2 solar intensity, the estimated collector efficiency is about 71.89 % to give output power at about 25.88 kW.

Depending on the typical meteorological year data for Izmir city, the expected mean daily output power of the PTSC system which designed in this study can be determined to be ranges between (53.6 – 179.4) kWh. Also, it was found that the PTSC which designed in this study can produce a output power of up to 44,143 kWh per year under the same ambiance conditions.

The numerical model is based on the applications of governing equations and used general empirical correlations; for this reason, it is possible to make use of it with greater confidence to other fluids, mixtures and operating conditions (excluding two-phase flow); it allows using the model developed as an important tool to design and optimize these kinds of systems.

The overall optical efficiency η_{op} which is found in the consequence of the optical performance analyses for the parabolic solar collector can be the maximum collector performance $\eta_{max} = \eta_{op}$ ($\Delta T \rightarrow 0$) when it is accepted that there is no thermal losses. The thermal efficiency is reduced as increase the thermal losses which transfer from the selective absorber surface to the environment which depend directly on $\Delta T = T_{abs} - T_{gl}$.

The design of the selective surface absorber tube is limited by two opposite factors, where the diameter of the absorber tube should be large as much as possible in order to increase the optical performance by increasing the intercept factor, and on the other hand the diameter of the absorber tube should be small as much as possible in order to make the working fluid flow in turbulent state and reduce the thermal losses which depend on the outer surface area of the absorber tube.

It was easy to get high temperatures in parabolic trough collectors, because the controlling factor is a mass flow rate.

And finally, Solar Electricity Generating Systems are needed to meet the growing electricity demand and to be prepared to replace the fossil resources to reduce global emissions.

REFERENCES

Bakos, G.C. (2005). Design and construction of a two-axis Sun tracking system for parabolic trough collector (PTC) efficiency improvement, *Renewable energy*, 2006 (31), 2411–2421.

Bakos, G.C., Ioannidis, I., Tsagas, N.F. & Seftelis, I. (2000). Design, optimization and conversion efficiency determination of a line focus parabolic-trough solar collector (PTC), *Applied energy*, 2001 (68), 43–50.

Benford, F. & Bock, J.E., (1939). A time analysis of sunshine. *Trans. of American illumination engineering Soc.*, 1939 (34), 200.

Berdahl, P. & Martin, M., (1984). Emissivity of solar skies. *Solar energy*, 1984 (32), 5.

Bird, S.P., Drost, M.K., (1982). Assessment of generic solar thermal concept for large industrial process heat applications. *In: Proceedings of the ASME solar energy division*, Fourth annual conference, Albuquerque, NM.

Böer, K.W. & Duffie, J.A., (1985). *Advances in solar energy* (Vol. 2). New York: Plenum.

Braun, J.E. & Mitchell, J.C., (1983). Solar geometry for fixed and tracking surfaces. *Solar energy*, 1983 (31), 439.

Churchill, S.W., (1983). Free convection around immersed bodies. *Heat exchanger design handbook*, Hemisphere.

Churchill, S.W., (1975). Correlating equations for laminar and turbulent free convection from a horizontal cylinder. *Int. J. Heat mass transfer*, 1975 (18), 1049.

Cooper, P.I., (1969). The absorption of solar radiation in solar stills. *Solar energy*, 1969 (12), 3.

Çolak, L., (2003). Güneşi takip eden parabolik oluk tipi güneş kollektörlerinin matematiksel modellenmesi, tasarımı ve teknik optimizasyonu. *Graduate school of natural and applied sciences of Gazi university*, Doctoral thesis, Ankara: Gazi Uni. Library.

Dickinson, W.C. & Cheremisinoff, P.N., (1980). *Solar energy technology handbook* (Part A). New York: Marcel Dekker, Inc.

Dudley, V.E., Evans, L.R. & Matthews, W., (1995). Test results industrial solar technology parabolic trough solar collector. *Sandia Report*. New Mexico, Sandia National Laboratories.

Duffie, J.A. & Beckman, W.A., (1991). *Solar engineering of thermal processes* (2nd ed.). New York: John Wiley & Sons, Inc.

Eskin, N. (1998). Transient performance analysis of cylindrical parabolic concentrating collectors and comparison with experimental results. *Energy conversion & management*, 1999 (40), 175-191.

European Commission:Joint Research Center. *Solar irradiance data*. (n.d.). Retrieved August 29, 2010, from http://sunbird.jrc.it/pvgis/apps/radday.php

Gilett, W.B. & Moon, J.E., (1985). *Solar collectors test methods and design guidelines*. Holand: D. Reidel Publishing Co.

Goswami, D.Y., Kreith, F. & Kreider, J.F., (2000). *Principles of solar engineering* (2nd ed.). Philadelphia: Taylor & Francis.

Holman, J.P., (1976). *Heat transfer*. Tokyo: McGraw Hill Kogakusha Ltd.

Jesco, Z., (2008). Classification of solar collectors, *Engineering for rural development: Proceedings*. (22 – 27).

Karaduman, A., (1989), *Parabolic trough solar collector system design and construction*. *Graduate school of natural and applied sciences of METU university*, Master's thesis. Ankara: METU Library.

Kipp & Zonen, *Pyrheliometer*. (n.d.). Retrieved August 9, 2009, from http://www.kippzonen.com/?productgroup/881/Pyrheliometers.aspx&gclid=CNvx1-HusZsCFUgTzAodDnhERA

Kılıç, A. & Öztürk, A., (1983). *Güneş enerjisinin ilk uygulamaları*. Istanbul: Kipaş Dağıtımcılık.

Kreith, F. & Kreider, J.F., (1978). *Principles of solar engineering*. Washington, McGraw-Hill.

Kumar, K.R. & Reddy, K.S., (2008). Thermal analysis of solar parabolic trough with porous disc receiver. *Applied Energy*, 2009 (86), 1804–1812.

Li, M. & Wang, L.L. (2006). Investigation of evacuated tube heated by solar trough concentrating system. *Energy conversion and management*, 2006 (47), 3591–3601.

Mc Adams, W.H., (1954). *Heat transmission*. New York: Mc Graw Hill Book Co. Inc.

Meteoclima, *The black and white pyranometers*. (n.d.). Retrieved August 9, 2009, from http://www.fischer-barometer.de/english/index.htm?strahlung/messglobal.htm

Özturk, H.H. (2004). Experimental determination of energy and exergy efficiency of the solar parabolic-cooker, *Solar energy*, 2004 (77), 67–71.

Pfander, M., Lupfert, E. & Pistor, P. (2004). Infrared temperature measurements on solar trough absorber tubes. *Solar energy*, 2007 (81), 629–635.

Qu, M., Archer, D.H. & Masson, S.V. (2006). A linear parabolic trough solar collector

performance model. *Renewable energy resources and a greener future*, 2006 Vol.VIII-3-3.

Rabl, A., (1985). *Active solar collectors and their applications*. New York: Oxford Universiry Press.

Rapp, D., (1981). *Solar energy*. California: Prentice-Hall.

Riffelmann, K.J., Neumann, A. & Ulmer, S. (2004). Performance enhancement of parabolic trough collectorsby solar flux measurement in the focal region, *Solar energy*, 2006 (80), 1303–1313.

Rolim, M.M., Fraidenraich, N. & Tiba, C. (2007). Analytic modeling of a solar power plant with parabolic linear collectors, *Solar energy*, 2009 (83), 126–133.

Singh, P. & Cheema, L.S., (1976). Performance and optimization of a cylindrical parabola collector. *Solar energy*, 18, 135-141.

Spirkl, W., Ries, H, Muschawech, J. & Timinger, A. (1996). Optimized compact secondary reflectors for parabolic troughs with tubular absorbers. *Solar energy*, 1997 (61), 153-158.

Tyagi, S.K., Wang, S., Singhal, M.K., Kaushik, S.C. & Park, S.R. (2006). Exergy analysis and parametric study of concentrating type solar collectors. *International journal of thermal sciences*, 2007 (46), 1304–1310.

Turkish State Meteorological Service, (2008). *Meteorological year data* (Temperature & Wind Speed), İzmir.

Valan Arasu, A. & Sornakumar, T. (2006). Design, manufacture and testing of fiberglass reinforced parabola trough for parabolic trough solar collectors, *Solar energy*, 2007 (81), 1273–1279.

Valladares, O.G. & Velázquez, N., (2008). Numerical simulation of parabolic trough solar collector: improvement using counter flow concentric circular heat exchangers. *International journal of heat and mass transfer*, 2009 (52), 597-609.

APPENDIXES

Appendix-A

The Detailed Flow Chart of the Package Program

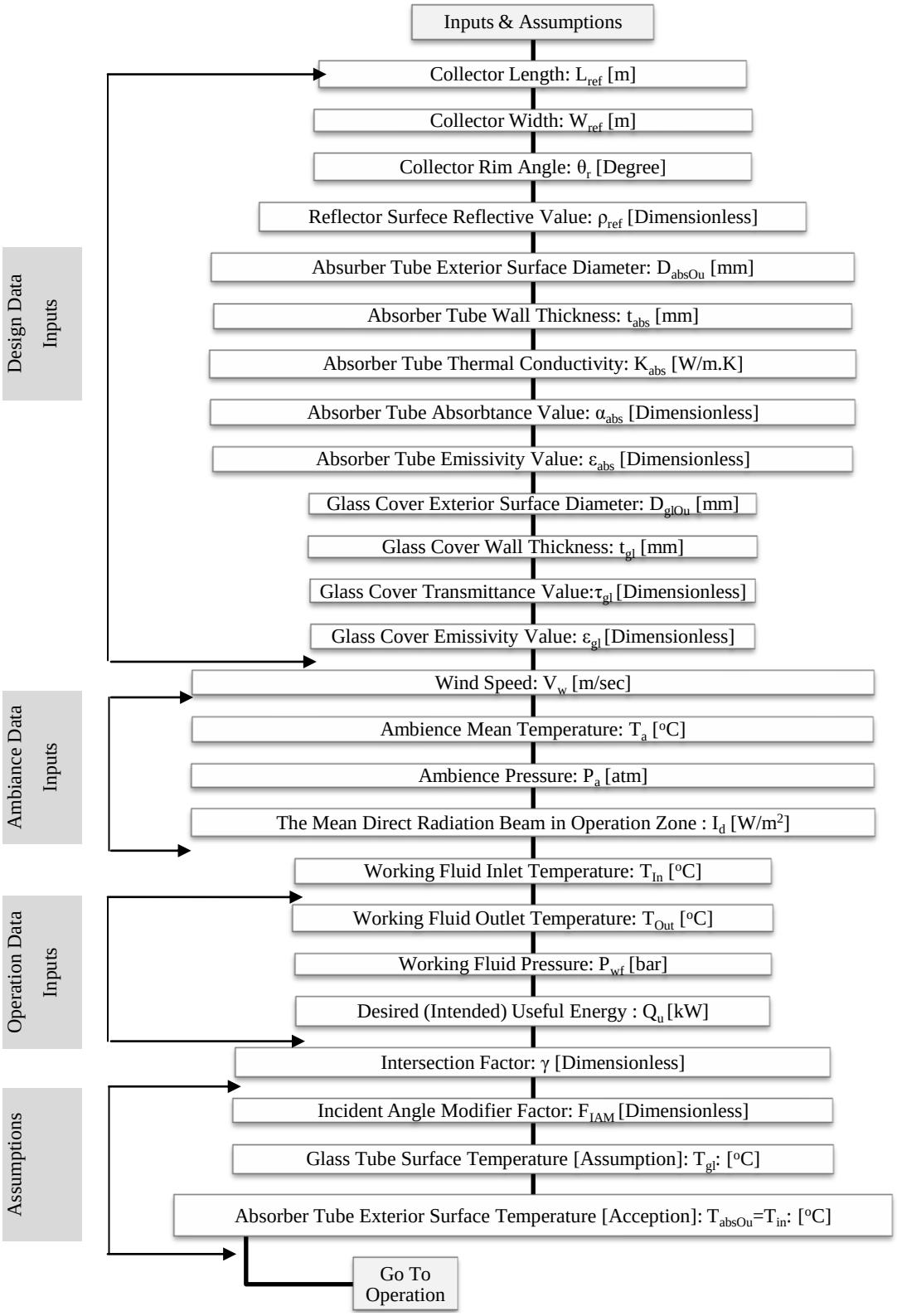

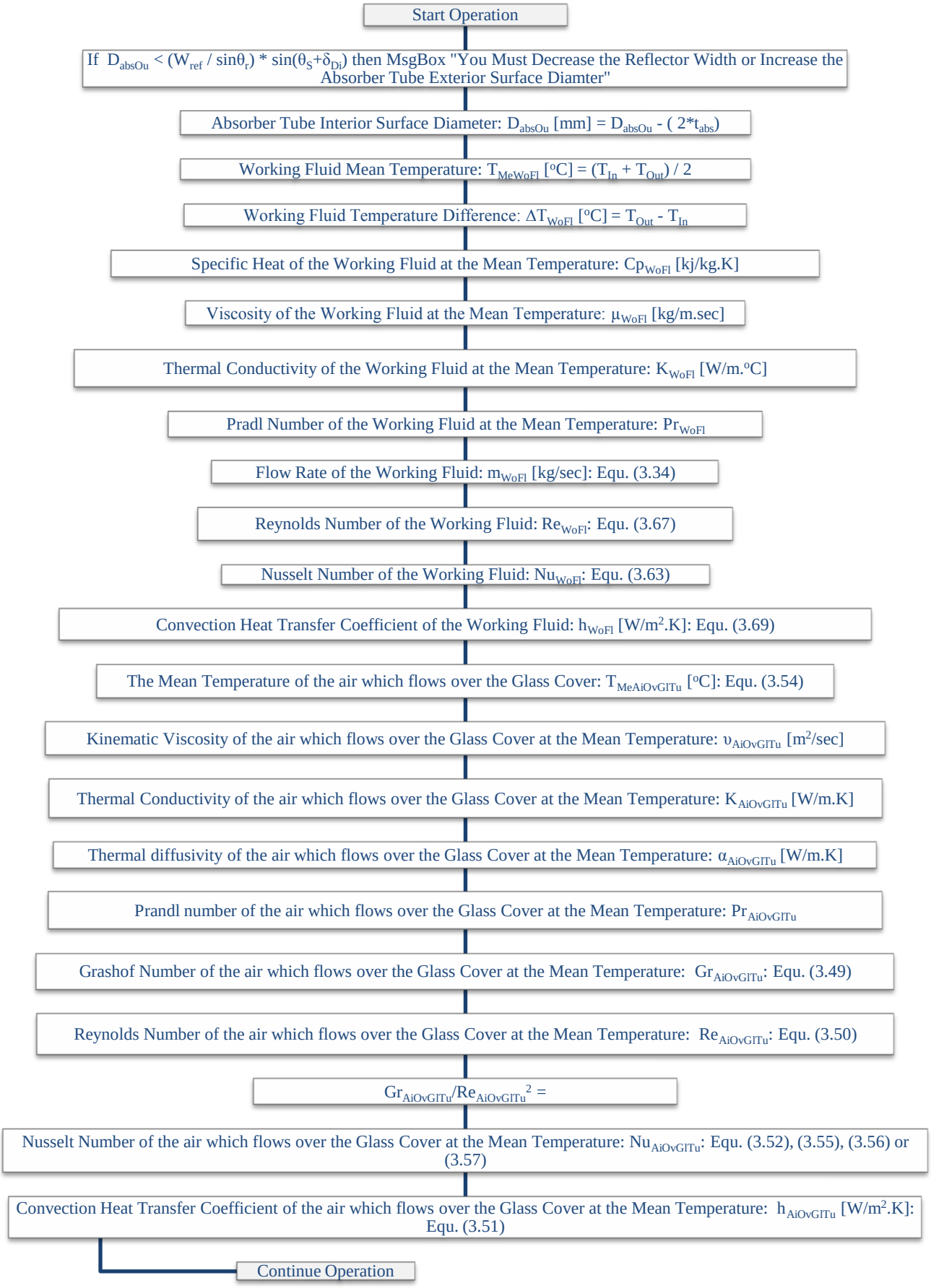
Start Operation
If $D_{absOu} < (W_{ref} / \sin\theta_r) * \sin(\theta_S+\delta_{Di})$ then MsgBox "You Must Decrease the Reflector Width or Increase the Absorber Tube Exterior Surface Diamter"
Absorber Tube Interior Surface Diameter: D_{absOu} [mm] = D_{absOu} - (2*t_{abs})
Working Fluid Mean Temperature: T_{MeWoFl} [°C] = (T_{In} + T_{Out}) / 2
Working Fluid Temperature Difference: ΔT_{WoFl} [°C] = T_{Out} - T_{In}
Specific Heat of the Working Fluid at the Mean Temperature: Cp_{WoFl} [kj/kg.K]
Viscosity of the Working Fluid at the Mean Temperature: μ_{WoFl} [kg/m.sec]
Thermal Conductivity of the Working Fluid at the Mean Temperature: K_{WoFl} [W/m.°C]
Pradl Number of the Working Fluid at the Mean Temperature: Pr_{WoFl}
Flow Rate of the Working Fluid: m_{WoFl} [kg/sec]: Equ. (3.34)
Reynolds Number of the Working Fluid: Re_{WoFl}: Equ. (3.67)
Nusselt Number of the Working Fluid: Nu_{WoFl}: Equ. (3.63)
Convection Heat Transfer Coefficient of the Working Fluid: h_{WoFl} [W/m^2.K]: Equ. (3.69)
The Mean Temperature of the air which flows over the Glass Cover: $T_{MeAiOvGlTu}$ [°C]: Equ. (3.54)
Kinematic Viscosity of the air which flows over the Glass Cover at the Mean Temperature: $\upsilon_{AiOvGlTu}$ [m^2/sec]
Thermal Conductivity of the air which flows over the Glass Cover at the Mean Temperature: $K_{AiOvGlTu}$ [W/m.K]
Thermal diffusivity of the air which flows over the Glass Cover at the Mean Temperature: $\alpha_{AiOvGlTu}$ [W/m.K]
Prandl number of the air which flows over the Glass Cover at the Mean Temperature: $Pr_{AiOvGlTu}$
Grashof Number of the air which flows over the Glass Cover at the Mean Temperature: $Gr_{AiOvGlTu}$: Equ. (3.49)
Reynolds Number of the air which flows over the Glass Cover at the Mean Temperature: $Re_{AiOvGlTu}$: Equ. (3.50)
$Gr_{AiOvGlTu}/Re_{AiOvGlTu}^2$ =
Nusselt Number of the air which flows over the Glass Cover at the Mean Temperature: $Nu_{AiOvGlTu}$: Equ. (3.52), (3.55), (3.56) or (3.57)
Convection Heat Transfer Coefficient of the air which flows over the Glass Cover at the Mean Temperature: $h_{AiOvGlTu}$ [W/m^2.K]: Equ. (3.51)
Continue Operation

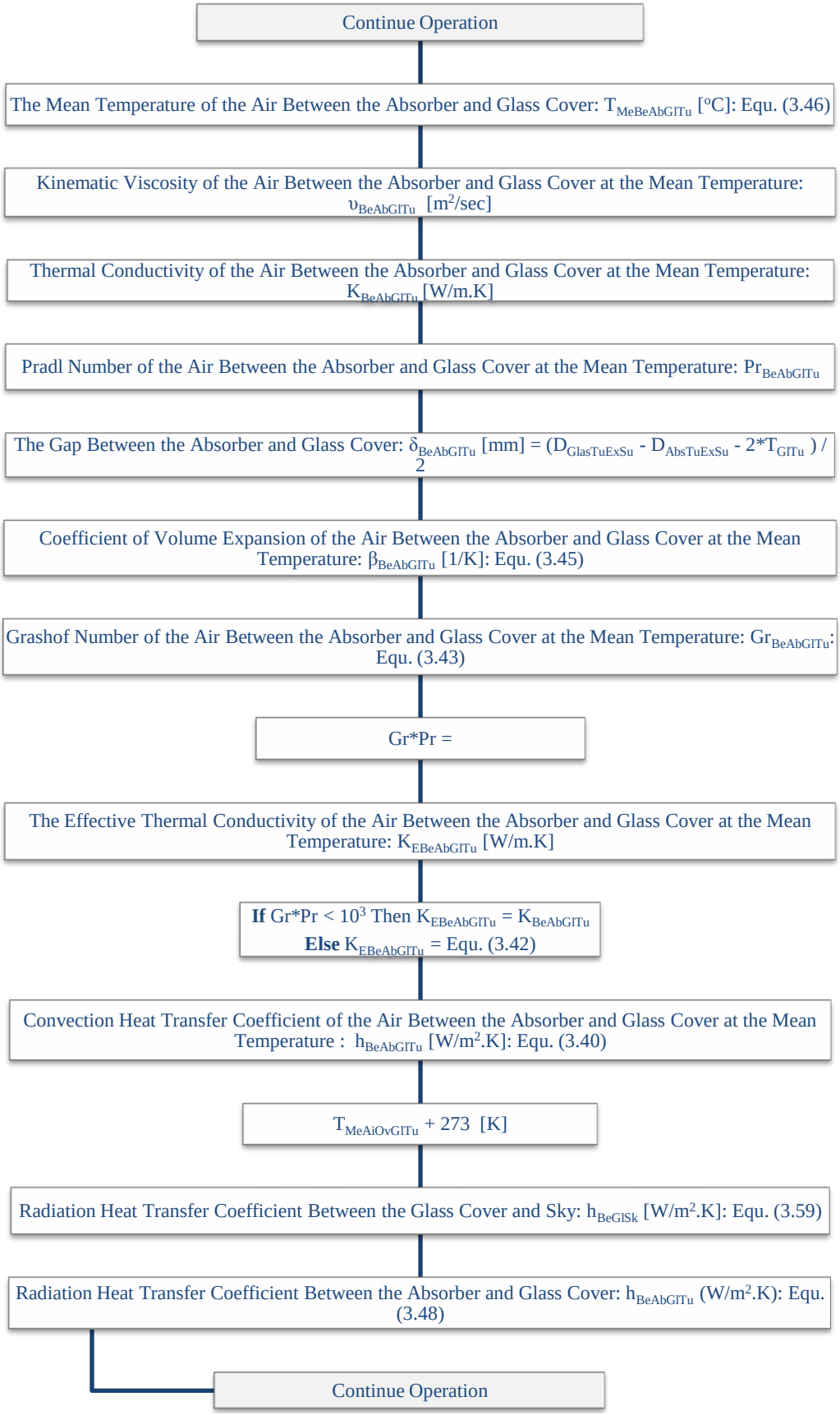
Continue Operation
The Mean Temperature of the Air Between the Absorber and Glass Cover: $T_{MeBeAbGlTu}$ [°C]: Equ. (3.46)
Kinematic Viscosity of the Air Between the Absorber and Glass Cover at the Mean Temperature: $\upsilon_{BeAbGlTu}$ [m^2/sec]
Thermal Conductivity of the Air Between the Absorber and Glass Cover at the Mean Temperature: $K_{BeAbGlTu}$ [W/m.K]
Pradl Number of the Air Between the Absorber and Glass Cover at the Mean Temperature: $Pr_{BeAbGlTu}$
The Gap Between the Absorber and Glass Cover: $\delta_{BeAbGlTu}$ [mm] = ($D_{GlasTuExSu}$ - $D_{AbsTuExSu}$ - 2*T_{GlTu}) / 2
Coefficient of Volume Expansion of the Air Between the Absorber and Glass Cover at the Mean Temperature: $\beta_{BeAbGlTu}$ [1/K]: Equ. (3.45)
Grashof Number of the Air Between the Absorber and Glass Cover at the Mean Temperature: $Gr_{BeAbGlTu}$: Equ. (3.43)
Gr*Pr =
The Effective Thermal Conductivity of the Air Between the Absorber and Glass Cover at the Mean Temperature: $K_{EBeAbGlTu}$ [W/m.K]
If Gr*Pr < 10^3 Then $K_{EBeAbGlTu} = K_{BeAbGlTu}$
Else $K_{EBeAbGlTu}$ = Equ. (3.42)
Convection Heat Transfer Coefficient of the Air Between the Absorber and Glass Cover at the Mean Temperature : $h_{BeAbGlTu}$ [W/m^2.K]: Equ. (3.40)
$T_{MeAiOvGlTu}$ + 273 [K]
Radiation Heat Transfer Coefficient Between the Glass Cover and Sky: h_{BeGlSk} [W/m^2.K]: Equ. (3.59)
Radiation Heat Transfer Coefficient Between the Absorber and Glass Cover: $h_{BeAbGlTu}$ (W/m^2.K): Equ. (3.48)
Continue Operation

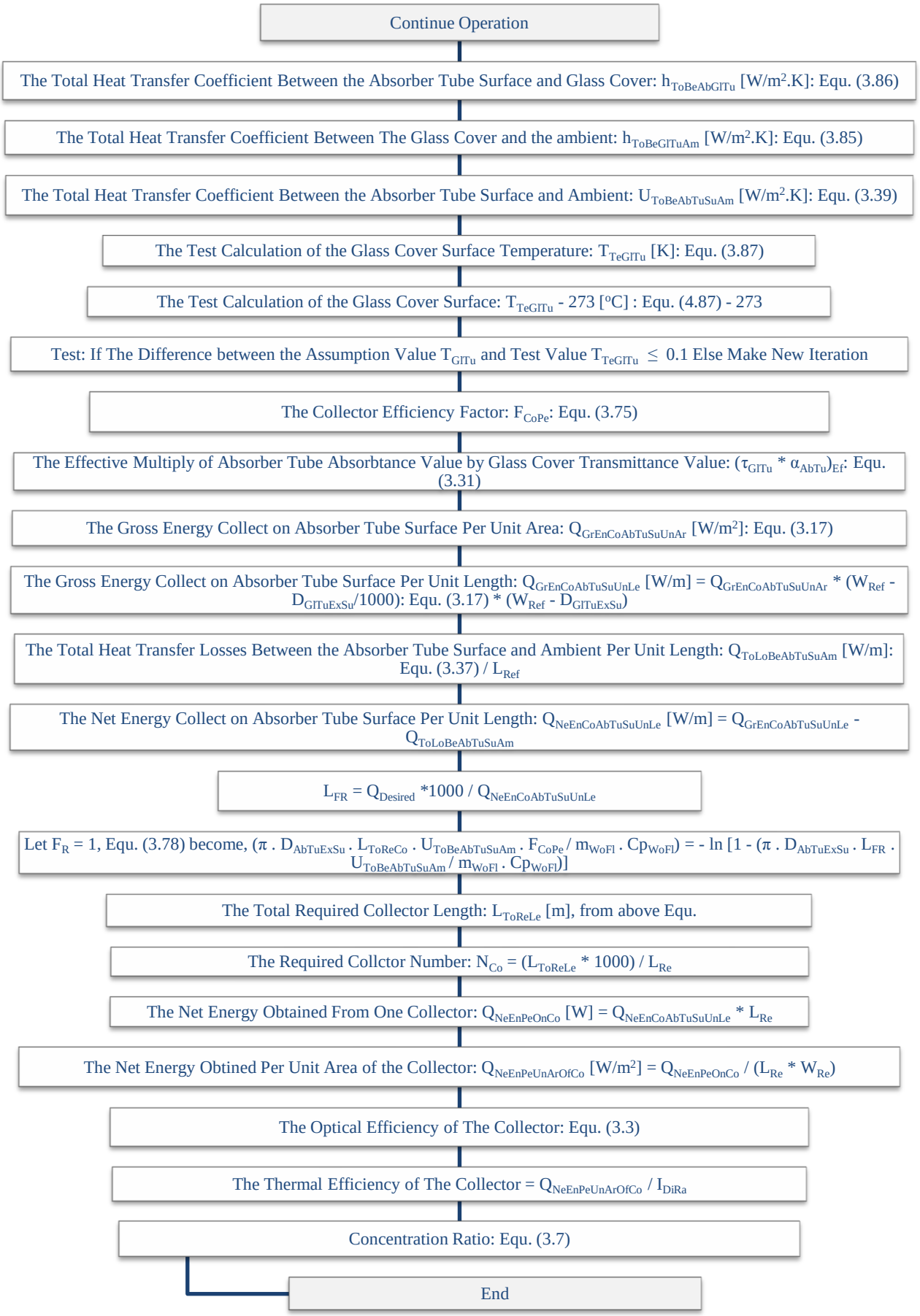
Continue Operation
The Total Heat Transfer Coefficient Between the Absorber Tube Surface and Glass Cover: $h_{ToBeAbGlTu}$ [W/m^2.K]: Equ. (3.86)
The Total Heat Transfer Coefficient Between The Glass Cover and the ambient: $h_{ToBeGlTuAm}$ [W/m^2.K]: Equ. (3.85)
The Total Heat Transfer Coefficient Between the Absorber Tube Surface and Ambient: $U_{ToBeAbTuSuAm}$ [W/m^2.K]: Equ. (3.39)
The Test Calculation of the Glass Cover Surface Temperature: T_{TeGlTu} [K]: Equ. (3.87)
The Test Calculation of the Glass Cover Surface: T_{TeGlTu} - 273 [^{o}C] : Equ. (4.87) - 273
Test: If The Difference between the Assumption Value T_{GlTu} and Test Value T_{TeGlTu} $\leq$ 0.1 Else Make New Iteration
The Collector Efficiency Factor: F_{CoPe}: Equ. (3.75)
The Effective Multiply of Absorber Tube Absorbtance Value by Glass Cover Transmittance Value: $(\tau_{GlTu} * \alpha_{AbTu})_{Ef}$: Equ. (3.31)
The Gross Energy Collect on Absorber Tube Surface Per Unit Area: $Q_{GrEnCoAbTuSuUnAr}$ [W/m^2]: Equ. (3.17)
The Gross Energy Collect on Absorber Tube Surface Per Unit Length: $Q_{GrEnCoAbTuSuUnLe}$ [W/m] = $Q_{GrEnCoAbTuSuUnAr}$ * (W_{Ref} - $D_{GlTuExSu}$/1000): Equ. (3.17) * (W_{Ref} - $D_{GlTuExSu}$)
The Total Heat Transfer Losses Between the Absorber Tube Surface and Ambient Per Unit Length: $Q_{ToLoBeAbTuSuAm}$ [W/m]: Equ. (3.37) / L_{Ref}
The Net Energy Collect on Absorber Tube Surface Per Unit Length: $Q_{NeEnCoAbTuSuUnLe}$ [W/m] = $Q_{GrEnCoAbTuSuUnLe}$ - $Q_{ToLoBeAbTuSuAm}$
$L_{FR} = Q_{Desired} * 1000 / Q_{NeEnCoAbTuSuUnLe}$
Let F_R = 1, Equ. (3.78) become, (π . $D_{AbTuExSu}$. L_{ToReCo} . $U_{ToBeAbTuSuAm}$. F_{CoPe} / m_{WoFl} . Cp_{WoFl}) = - ln [1 - (π . $D_{AbTuExSu}$. L_{FR} . $U_{ToBeAbTuSuAm}$ / m_{WoFl} . Cp_{WoFl})]
The Total Required Collector Length: L_{ToReLe} [m], from above Equ.
The Required Collctor Number: N_{Co} = (L_{ToReLe} * 1000) / L_{Re}
The Net Energy Obtained From One Collector: $Q_{NeEnPeOnCo}$ [W] = $Q_{NeEnCoAbTuSuUnLe}$ * L_{Re}
The Net Energy Obtined Per Unit Area of the Collector: $Q_{NeEnPeUnArOfCo}$ [W/m^2] = $Q_{NeEnPeOnCo}$ / (L_{Re} * W_{Re})
The Optical Efficiency of The Collector: Equ. (3.3)
The Thermal Efficiency of The Collector = $Q_{NeEnPeUnArOfCo}$ / I_{DiRa}
Concentration Ratio: Equ. (3.7)
End

Appendix-B

The Code of the Package Program

```
Form1 - 1

'Project:                       Parabolic Trough Solar Collector Designer and Performance Calculator
'By:                            Sabah Beyatlı
'Date:                          September 2010

Option Explicit

    'Dimension in Module-Level
        Const SoInAn As Currency = 0.53     'Solar Intercept Angle                                                  [Degree]
        Const DiAn As Currency = 0.9        'Dispersion Angle                                                       [Degree]
        Const Pi As Currency = 3.1415926    'Pi Value
        Const GravAc As Currency = 9.81     'gravitational acceleration                                             [m/s2]
        Const StBoCons As Currency = 5.669 'Stefan Boltzman Constant (Attention: without multiply with E-8 to avoid make its value equal zer
o)    [W/m2.K4]
        Const RefSil As Currency = 0.94     'Reflective Value Of The Silver
        Const RefGol As Currency = 0.76     'Reflective Value Of The Gold
        Const RefAlu As Currency = 0.82     'Reflective Value Of The Aluminum
        Const RefCop As Currency = 0.75     'Reflective Value Of The Copper
        Const RefAcr As Currency = 0.86     'Reflective Value Of The Acrylic Coated Aluminum
        Const RefMir As Currency = 0.88     'Reflective Value Of The Mirror
        Const RefCus As Currency = 0.88     'Reflective Value Of The Custom Polished Aluminum Thin Film (Alanod)
        Dim ColWi As Currency               'Collector Width                                                        [m]
        Dim ColRiAn As Currency             'Collector Rim Angle                                                    [m]
        Dim AbsExDi As Currency             'Absurber Tube Exterior Surface Diameter                                [mm]
        Dim AbsInDi As Currency             'Absurber Tube Interior Surface Diameter                                [mm]
        Dim AbsWaTh As Currency             'Absorber Tube Wall Thickness                                           [mm]
        Dim AbsExTe As Currency             'Absurber Tube Exterior Surface Temperature                             [C]
        Dim WoFlInTe As Currency            'Working Fluid Inlet Temperature                                        [C]
        Dim WoFlOuTe As Currency            'Working Fluid Outlet Temperature                                       [C]
        Dim WoFlMeTe As Currency            'Working Fluid Mean Temperature                                         [C]
        Dim WoFlSpHe As Currency            'Specific Heat Of The Working Fluid At The Mean Temperature             [kj/kg.K]
        Dim WoFlVis As Currency             'Viscosity Of The Working Fluid At The Mean Temperature                 [kg/m.sec]
        Dim WoFlThCo As Currency            'Thermal Conductivity Of The Working Fluid At The Mean Temperature      [W/m.C]
        Dim WoFlPrNu As Currency            'Pradl Number Of The Working Fluid At The Mean Temperature
        Dim WoFlMaFlRa As Currency          'Flow Rate of the Working Fluid                                         [kg/sec]
        Dim DeUsEn As Currency              'Desired (Intended) Useful Energy                                       [kw]
        Dim WoFlReNu As Currency            'Renolds Number Of The Working Fluid
        Dim WoFlNusNu As Currency           'Nusselt Number Of The Working Fluid
        Dim ConHeTrCoeInAbs As Currency     'Convection Heat Transfer Coefficient of the Working Fluid              [W/m2.K]
        Dim MeTeAiOvGl As Currency          'Mean Temperature Of The Air Flows Over The Glass Tube                  [C]
        Dim TeAmb As Currency               'Ambience Mean Temperature                                              [C]
        Dim GlTe As Currency                'Glass Tube Surface Temperature                                         [C]
        Dim GlTeTest As Currency            'Glass Tube Surface Temperature Test
        Dim KiVisAiOvGl As Currency         'Kinematic Viscosity of the air which flows over the Glass Tube at the Mean Temperature  [m2/sec]
        Dim ThCoAiOvGl As Currency          'Thermal Conductivity of the air which flows over the Glass Tube at the Mean Temperature [W/m.K]
        Dim ReNuAiOvGl As Currency          'Reynolds Number Of  The Air Which Flows Over  The Glass Tube At TheMean Temperature
        Dim GlExDi As Currency              'Glass Tube Exterior Surface Diameter                                   [mm]
        Dim GlWaTh As Currency              'Glass Tube Wall Thickness                                              [mm]
        Dim WinSp As Currency               'Wind Speed                                                             [m/sec]
        Dim NusNuAiOvGl As Currency         'Nusselt Number Of  The Air Which Flows Over  The Glass Tube At TheMean Temperature
        Dim ConHeTrCoeAiOvGl As Currency    'Convection Heat Transfer Coefficient of the air which flows over the Glass Tube at the Mean Temp
erature         [W/m2.K]
        Dim MeTeAiBetAbsGl As Currency      'The Mean Temperature Of The Air Between The Absorber And Glass Tubes        [C]
        Dim KiVisAiBetAbsGl                 'Kinematic Viscosity Of The Air Between The Absorber And Glass Tubes At The Mean Temperature  [m2
```

```
/sec]
        Dim ThCoAiBetAbsGl                  'Thermal Conductivity of the air Between The Absorber And Glass Tubes At The Mean Temperature [W/
m.K]
        Dim PrNuAiBetAbsGl As Currency      'Pradl Number of the air Between The Absorber And Glass Tubes At The Mean Temperature
        Dim GapBetAbsGl As Currency         'The Gap Between the Absorber and Glass Tubes                              [mm]
        Dim VoExpCoAiBetAbsGl As Currency   'Volume Expansion Coefficient Of The Air Between The Absorber And Glass Tubes At The Mean Tempera
ture            [1/K]
        Dim GrNuAiBetAbsGl As Currency      'Grashof Number Of The Air Between The Absorber And Glass Tubes At The Mean Temperature
        Dim EfThCoAiBetAbsGl As Currency     'Effective Thermal Conductivity Of The Air Between The Absorber And Glass Tubes At The Mean Tem
perature       [W/m.K]
        Dim ConHeTrCoeAiBetAbsGl As Currency 'Convection Heat Transfer Coefficient of the Air Between the Absorber and Glass Tubes at the Me
an Temperature [W/m2.K]
        Dim RadHeTrCoeBetGlSk As Currency    'Radiation Heat Transfer Coefficient Between the Glass Tube and Sky                    [W/m2.K]
        Dim GlEmVa As Currency               'Glass Tube Emissivity Value
        Dim RadHeTrCoeBetAbsGl As Currency   'Radiation Heat Transfer Coefficient Between the Absorber and Glass Tubes             [W/m2.K]
        Dim AbsEmVa As Currency              'Absorber Tube Emissivity Value
        Dim TotHeTrCoeBetAbsGl As Currency   'The Total Heat Transfer Coefficient Between the Absorber Tube Surface and Glass Tube [W/m2.K]
        Dim TotHeTrCoeBetGlAmb As Currency   'The Total Heat Transfer Coefficient Between The Glass Tube and the ambient           [W/m2.K]
        Dim TotHeTrCoeBetAbsAmb As Currency  'The Total Heat Transfer Coefficient Between the Absorber Tube Surface and Ambient    [W/m2.K]
        Dim ColPerFac As Currency            'Collector Performance Factor
        Dim AbsThCo As Currency              'Absorber Tube Thermal Conductivity                                  [W/m.K]
        Dim TotHeTrCoeBetWoFlAmb As Currency 'The Total Heat Transfer Coefficient Between the Working Fluid and Ambient           [W/m2.K]
        Dim EfMulAbsAbsorVaGlTransVa As Currency  'The Effective Multiply of Absorber Tube Absorbtance Value by Glass Tube Transmittance Val
ue
        Dim AbsAbsorVa As Currency           'Absorber Tube Absorbtance Value
        Dim GlTransVa As Currency            'Glass Tube Transmittance Value
        Dim RefReflVa As Currency            'Reflective Value Of The Reflector
        Dim GroEnOnAbsPerUnAr As Currency    'The Gross Energy Collect on Absorber Tube Surface per Unit Area  [W/m2]
        Dim DirRadBeam As Currency           'The Mean Direct Radiation Beam In Operation Zone                  [W/m2]
        Dim IntFac As Currency               'Intercept Factor
        Dim IncAnMoFac As Currency           'Incident Angle Modifier Factor
        Dim GroEnOnAbsPerUnLe As Currency    'The Gross Energy Collect on Absorber Tube Surface Per Unit Length
    [W/m]
        Dim TotHeLoBetAbsAmbPerUnLe As Currency  'The Total Heat Transfer Losses Between the Absorber Tube Surface and Ambient Per Unit Leng
th   [W/m]
        Dim NetEnOnAbsUnLe As Currency           'The Net Energy Collect on Absorber Tube Surface Unit Length
    [W/m]
        Dim TotLeWiReToNetEnOnAbs As Currency    'The total length with respect to The Net Energy Collect on Absorber Tube Surface
    [m]
        Dim ReqColLe As Currency                 'The Total Required Collector Length                    [m]
        Dim ReqColNu As Currency                 'The Required Collctor Number
        Dim ColLe As Currency                    'Collector Length                                       [m]
        Dim NetEnPerOneCol As Currency           'The Net Energy Obtained From One Collector             [W]
        Dim NetEnPerUnAr As Currency             'The Net Energy Obtined Per Unit Area of the Collector  [W/m2]
        Dim OptEff As Currency                   'The Optical Efficiency of The Collector
        Dim TherEff As Currency                  'The Thermal Efficiency of The Collector
        Dim ConcRat As Currency                  'Concentration Ratio
        Dim Ho As Currency                       'Distance between the focal point and rim base          [mm]
        Dim RaRi As Currency                     'Radius of the parabola at the rim angle                [mm]
        Dim FoLe As Currency                     'Focal Length                                           [mm]
        Dim PaEqCo As Currency                   'Parabola Equation Constant                             [mm]
        Dim Href As Currency                     'Parabola Depth                                         [mm]
        Dim PaArLe As Currency                   'Parabola Arc Length                                    [mm]
```

```
Form1 - 3

        Dim CriDirRadBeam As Currency            'Critical Direct Solar Beam Intensity                    [W/m2]
        Dim GrNuAiOvGl As Currency               'Grashof Number Of The Air over glass cover
        Dim VoExpCoAiOvGl As Currency            'Volume Expansion Coefficient Of The Air over glass cover [1/K]
        Dim CoTrTyTe As Currency                 'Convection heat transfer type test
        Dim ThDiAiOvGl As Currency               'Thermal diffusivity Of The Air over glass cover        [m2/sec]
        Dim PrNuAiOvGl As Currency               'Prandtl Number of the air over glass
        Dim RayNuAiOvGl As Currency              'Rayleigh number of the air over glass
        Dim PerAbsExDi As Currency               'Perfect Absorber Tube Exterior Diameter if the Dispersion Angle taken zero

Private Sub chkNewReflectorType_Click()
    If chkNewReflectorType = 1 Then
        cboSelectReflectorType.Enabled = False
        Label7.Enabled = True
        txtTheReflectiveValueOfNewReflectorType.Enabled = True
    Else
        cboSelectReflectorType.Enabled = True
        Label7.Enabled = False
        txtTheReflectiveValueOfNewReflectorType.Enabled = False
    End If
End Sub

Private Sub chkNewWorkingFluid_Click()
    If chkNewWorkingFluid.Value = 1 Then
        cboSelectWorkingFluid.Enabled = False
        Label22.Enabled = True
        txtSpecificHeatAtTheMeanTemperature.Enabled = True
        Label26.Enabled = True
        Label23.Enabled = True
        txtViscosityAtTheMeanTemperature.Enabled = True
        Label27.Enabled = True
        Label24.Enabled = True
        txtThermalConductivityAtTheMeanTemperature.Enabled = True
        Label28.Enabled = True
        Label25.Enabled = True
        txtPradlNumberAtTheMeanTemperature.Enabled = True

    Else
        cboSelectWorkingFluid.Enabled = True
        Label22.Enabled = False
        txtSpecificHeatAtTheMeanTemperature.Enabled = False
        Label26.Enabled = False
        Label23.Enabled = False
        txtViscosityAtTheMeanTemperature.Enabled = False
        Label27.Enabled = False
        Label24.Enabled = False
        txtThermalConductivityAtTheMeanTemperature.Enabled = False
        Label28.Enabled = False
        Label25.Enabled = False
        txtPradlNumberAtTheMeanTemperature.Enabled = False
    End If
End Sub

Private Sub cmdCalculate_Click()
```

Form1 - 4

```
    'dimension in Local_level

        Dim blnIterationFix As Boolean

If txtCollectorLength.Text = "" Or txtCollectorWidth.Text = "" Or txtCollectorRimAngle.Text = "" Or _
        txtAbsorberTubeExteriorSurfaceDiameter.Text = "" Or txtAbsorberTubeWallThickness.Text = "" Or _
        txtAbsorberTubeThermalConductivity.Text = "" Or txtAbsorberTubeAbsorbtanceValue.Text = "" Or _
        txtAbsorberTubeEmissivityValue.Text = "" Or (cboSelectReflectorType.Text = "Select Reflector Type" And chkNewReflectorType.Value = 0
) Or _
        (optVacuumPacked.Value = False And optWithoutVacuum.Value = False) Or (optGreenGlass.Value = False And optWhiteGlass.Value = False)
Or _
        txtGlassTubeExteriorSurfaceDiameter.Text = "" Or _
        txtGlassTubeWallThickness.Text = "" Or txtGlassTubeTransmittanceValue.Text = "" Or _
        txtGlassTubeEmissivityValue.Text = "" Or (cboSelectWorkingFluid.Text = "Select Working Fluid" And _
        chkNewWorkingFluid.Value = 0) Or txtWindSpeed.Text = "" Or txtAmbienceMeanTemperature.Text = "" Or _
        txtTheMeanDirectRadiationBeamInOperationZone.Text = "" Or txtWorkingFluidInletTemperature.Text = "" Or _
        txtWorkingFluidOutletTemperature.Text = "" Or txtDesiredIntendedUsefulEnergy.Text = "" Or _
        txtInterceptFactor.Text = "" Or txtIncidentAngleModifierFactor.Text = "" Or _
        txtGlassTubeSurfaceTemperature.Text = "" Then

        MsgBox "You need to fill all the texts to make calculation for your design.", vbInformation, "Request"

Else
        'convert the text values to numeric value
        ColWi = Val(txtCollectorWidth)                                  'm
        ColRiAn = Val(txtCollectorRimAngle) * (3.141592 / 180)
        AbsExDi = Val(txtAbsorberTubeExteriorSurfaceDiameter) / 1000    'm
        AbsWaTh = Val(txtAbsorberTubeWallThickness) / 1000              'm
        WoFlInTe = Val(txtWorkingFluidInletTemperature)                 'C
        WoFlOuTe = Val(txtWorkingFluidOutletTemperature)                'C
        DeUsEn = Val(txtDesiredIntendedUsefulEnergy) * 1000             'W
        TeAmb = Val(txtAmbienceMeanTemperature)                         'C
        GlTe = Val(txtGlassTubeSurfaceTemperature)                      'C
        GlExDi = Val(txtGlassTubeExteriorSurfaceDiameter) / 1000        'm
        WinSp = Val(txtWindSpeed)                                       'm/sec
        GlWaTh = Val(txtGlassTubeWallThickness) / 1000                  'm
        GlEmVa = Val(txtGlassTubeEmissivityValue)
        AbsEmVa = Val(txtAbsorberTubeEmissivityValue)
        AbsThCo = Val(txtAbsorberTubeThermalConductivity)               '[w/m.K]
        AbsAbsorVa = Val(txtAbsorberTubeAbsorbtanceValue)
        GlTransVa = Val(txtGlassTubeTransmittanceValue)
        IntFac = Val(txtInterceptFactor)
        IncAnMoFac = Val(txtIncidentAngleModifierFactor)
        ColLe = Val(txtCollectorLength)                                 'm
        DirRadBeam = Val(txtTheMeanDirectRadiationBeamInOperationZone) 'W

        'calculate the Absurber Tube Interior Surface Diameter
        AbsInDi = AbsExDi - (2 * AbsWaTh)

        'calculate Working Fluid Mean Temperature
        WoFlMeTe = (WoFlInTe + WoFlOuTe) / 2
```

```
        'Acception
        AbsExTe = WoFlMeTe

        'calculate the Thermophysical Properties for the working fluid at the mean temperature
        '(Attention, the viscosity values of the working fluid multiply by 1000 to avoid
        'the diveded by zero when the Renolds Number calculates at next steps)
        If chkNewWorkingFluid.Value = 1 Then                    'Thermophysical Properties for New Working Fluid
            WoFlSpHe = Val(txtSpecificHeatAtTheMeanTemperature) * 1000
            WoFlVis = Val(txtViscosityAtTheMeanTemperature) * 1000
            WoFlThCo = Val(txtThermalConductivityAtTheMeanTemperature)
            WoFlPrNu = Val(txtPradlNumberAtTheMeanTemperature)
        Else
            If cboSelectWorkingFluid.ListIndex = 0 Then         'Thermophysical Properties for Water
                WoFlSpHe = (((WoFlMeTe ^ 4) / (10 ^ 9)) - 6 * ((WoFlMeTe ^ 3) / (10 ^ 7)) + 0.000105 * (WoFlMeTe ^ 2) - 0.005 * WoFlMeTe + 4
.25) * 1000
                WoFlVis = 1000 * 0.037 * (WoFlMeTe ^ (-1.06))
                WoFlThCo = -3 * ((WoFlMeTe ^ 4) / (10 ^ 11)) + 2 * ((WoFlMeTe ^ 3) / (10 ^ 8)) - ((WoFlMeTe ^ 2) / (10 ^ 5)) + 0.002 * WoFlM
eTe + 0.567
                WoFlPrNu = -5 * ((WoFlMeTe ^ 3) / (10 ^ 8)) + 8 * ((WoFlMeTe ^ 2) / (10 ^ 5)) - 0.029 * WoFlMeTe + 3.873

            ElseIf cboSelectWorkingFluid.ListIndex = 1 Then     'Thermophysical Properties for Syltherm 800
                WoFlSpHe = ((WoFlMeTe ^ 2) / (10 ^ 6)) + 1.707 * WoFlMeTe + 1575
                WoFlVis = 1000 * 0.008 * Exp(-(0.01 * WoFlMeTe))
                WoFlThCo = -((WoFlMeTe ^ 2) / (10 ^ 9)) - 0.00018 * WoFlMeTe + 0.138
                WoFlPrNu = 7150 * (WoFlMeTe ^ (-1.11))
            End If
            txtSpecificHeatAtTheMeanTemperature = Val(WoFlSpHe) / 1000
            txtViscosityAtTheMeanTemperature = Val(WoFlVis) / 1000
            txtThermalConductivityAtTheMeanTemperature = Val(WoFlThCo)
            txtPradlNumberAtTheMeanTemperature = Val(WoFlPrNu)
        End If

        'Calculate the geometry parameters of the PTSC
        Ho = ((ColWi / 2) / Tan(ColRiAn)) * 1000
        RaRi = ((ColWi / 2) / Sin(ColRiAn)) * 1000
        FoLe = (RaRi * (1 + Cos(ColRiAn))) / 2
        PaEqCo = 4 * FoLe
        Href = FoLe - Ho
        PaArLe = 2 * (((ColWi * 1000) / 4) * Sqr(1 + ((4 * Href) / (ColWi * 1000)) ^ 2) + ((ColWi * 1000) ^ 2 / (16 * Href)) * Log(Sqr(1 + (
(4 * Href) / (ColWi * 1000)) ^ 2) + ((4 * Href) / (ColWi * 1000))))

        'calculate Flow Rate of the working fluid
        WoFlMaFlRa = DeUsEn / (WoFlSpHe * (WoFlOuTe - WoFlInTe))

        'calculate Renolds Number Of The Working Fluid
        '(Attention the Renolds Number Multyply with 1000 to compensate the (Viscosity*1000) above)
        WoFlReNu = 1000 * (4 * WoFlMaFlRa) / (WoFlVis * Pi * AbsInDi)

        'calculate Nusselt Number Of The Working Fluid
        WoFlNusNu = 0.023 * (WoFlReNu ^ 0.8) * (WoFlPrNu ^ 0.4)

        'calculate Convection Heat Transfer Coefficient of the Working Fluid
        ConHeTrCoeInAbs = (WoFlNusNu * WoFlThCo) / AbsInDi
```

```
        'Loop to find the correct value for the glass tube temperature
Do Until blnIterationFix = True Or GlTe > 120    'test
    If Abs(GlTe - GlTeTest) > 0.05 Then   'test
        GlTe = GlTe + 0.1     'test

        'calculate Mean Temperature Of The Air Flows Over The Glass Tube
        MeTeAiOvGl = (TeAmb + GlTe) / 2

        'calculate the Thermophysical Properties for the Air Which Flows Over  The Glass Tube at the mean temperature
        KiVisAiOvGl = (-(1 / (10 ^ 10)) * (MeTeAiOvGl ^ 3) + (9 / (10 ^ 7)) * (MeTeAiOvGl ^ 2) + 0.00087 * MeTeAiOvGl + 0.137)
        ThCoAiOvGl = (8 / (10 ^ 5)) * MeTeAiOvGl + 0.024
        ThDiAiOvGl = ((9 / (10 ^ 7)) * (MeTeAiOvGl ^ 2) + 0.00137 * MeTeAiOvGl + 0.202)
        PrNuAiOvGl = KiVisAiOvGl / ThDiAiOvGl

        'calculate Reynolds Number Of The Air Which Flows Over The Glass Tube At TheMean Temperature
        ReNuAiOvGl = 10000 * (WinSp * GlExDi) / KiVisAiOvGl

        'calculate Volume Expansion Coefficient Of The Air over glass cover
        VoExpCoAiOvGl = 1 / (MeTeAiOvGl + 273)

        'calculate Grashof number of the air flows over the glass cover
        GrNuAiOvGl = (GravAc * VoExpCoAiOvGl * (GlTe - TeAmb) * (GlExDi ^ 3)) / ((KiVisAiOvGl / 10000) ^ 2)

        'To avoid the divided by zero (when Reynolds Number Of The Air Which Flows Over The Glass equal to zero)
        If ReNuAiOvGl = 0 Then
            If GrNuAiOvGl < 0 Then
            GrNuAiOvGl = GrNuAiOvGl * (-1)
            NusNuAiOvGl = (0.6 + (((PrNuAiOvGl * GrNuAiOvGl) / 300) / (1 + (0.5 / PrNuAiOvGl) ^ (9 / 16)) ^ (16 / 9))) ^ (2 / 6)
            Else
            NusNuAiOvGl = (0.6 + (((PrNuAiOvGl * GrNuAiOvGl) / 300) / (1 + (0.5 / PrNuAiOvGl) ^ (9 / 16)) ^ (16 / 9))) ^ (2 / 6)
            End If
        Else

        'Find the convection transfer type (Natural, Forced or Mixed) Of The Air Which Flows Over The Glass Tube
        CoTrTyTe = GrNuAiOvGl / (ReNuAiOvGl ^ 2)

        'calculate Nusselt Number Of The Air Which Flows Over  The Glass Tube At The Mean Temperature
        If CoTrTyTe < 0.95 Then
            If ReNuAiOvGl < 1000 Then
            NusNuAiOvGl = 0.4 + (0.54 * (ReNuAiOvGl ^ 0.52))
            Else
            NusNuAiOvGl = 0.3 * (ReNuAiOvGl ^ 0.6)
            End If
        ElseIf CoTrTyTe > 1.05 Then
            NusNuAiOvGl = (0.6 + (((PrNuAiOvGl * GrNuAiOvGl) / 300) / (1 + (0.5 / PrNuAiOvGl) ^ (9 / 16)) ^ (16 / 9))) ^ (2 / 6)
        ElseIf CoTrTyTe <= 1.05 Or CoTrTyTe >= 0.95 Then

            'find the Rayleigh number of the air over glass cover
            RayNuAiOvGl = (GravAc * VoExpCoAiOvGl * (GlTe - TeAmb) * (GlExDi ^ 3)) / (((KiVisAiOvGl * ThDiAiOvGl) / 10000) ^ 2)
            NusNuAiOvGl = (0.6 + ((0.387 * (RayNuAiOvGl) ^ (1 / 6)) / (1 + (0.559 / PrNuAiOvGl) ^ (9 / 16)) ^ (8 / 27))) ^ 2
        End If
        End If
```

```
        'calculate Convection Heat Transfer Coefficient of the air which flows over the Glass Tube at the Mean Temperature
        ConHeTrCoeAiOvGl = (ThCoAiOvGl * NusNuAiOvGl) / (GlExDi)

        If optVacuumPacked.Value = True Then
            ConHeTrCoeAiBetAbsGl = 0
        Else
            'calculate The Mean Temperature Of The Air Between The Absorber And Glass Tubes
            MeTeAiBetAbsGl = (AbsExTe + GlTe) / 2

            'calculate the Thermophysical Properties of the Air Between The Absorber And Glass Tubes at the mean temperature
            KiVisAiBetAbsGl = 1000 * 5 * ((MeTeAiBetAbsGl + 273) ^ 1.808) * (10 ^ (-10))
            ThCoAiBetAbsGl = 0.00016 * ((MeTeAiBetAbsGl + 273) ^ 0.893)
            PrNuAiBetAbsGl = 6 * ((MeTeAiBetAbsGl + 273) ^ 2) * (10 ^ (-7)) - 0.0006 * (MeTeAiBetAbsGl + 273) + 0.835

            'calculate The Gap Between the Absorber and Glass Tubes
            GapBetAbsGl = (GlExDi - AbsExDi - (2 * GlWaTh)) / 2

            'calculate Volume Expansion Coefficient Of The Air Between The Absorber And Glass Tubes At The Mean Temperature
            VoExpCoAiBetAbsGl = 1 / (MeTeAiBetAbsGl + 273)

            'calculate Grashof Number Of The Air Between The Absorber And Glass Tubes At The Mean Temperature
            GrNuAiBetAbsGl = (GravAc * VoExpCoAiBetAbsGl * (AbsExTe - GlTe) * (GapBetAbsGl ^ 3)) / ((KiVisAiBetAbsGl / 1000) ^ 2)

            'calculate Effective Thermal Conductivity Of The Air Between The Absorber And Glass Tubes At The Mean Temperature
            If (GrNuAiBetAbsGl * PrNuAiBetAbsGl) < 1000 Then
                EfThCoAiBetAbsGl = ThCoAiBetAbsGl
            Else
                EfThCoAiBetAbsGl = 0.11 * ThCoAiBetAbsGl * ((GrNuAiBetAbsGl * PrNuAiBetAbsGl) ^ 0.29)
            End If

            'calculate Convection Heat Transfer Coefficient of the Air Between the Absorber and Glass Tubes at the Mean Temperature
            ConHeTrCoeAiBetAbsGl = 2 * EfThCoAiBetAbsGl / (AbsExDi * (Log(GlExDi / AbsExDi)))
        End If

        'calculate Radiation Heat Transfer Coefficient Between the Glass Tube and Sky
        RadHeTrCoeBetGlSk = 4 * (StBoCons * (10 ^ (-8))) * GlEmVa * ((MeTeAiOvGl + 273) ^ 3)

        'calculate Radiation Heat Transfer Coefficient Between the Absorber and Glass Tubes
        RadHeTrCoeBetAbsGl = ((StBoCons * (10 ^ (-8))) * (((GlTe + 273) ^ 2) + ((AbsExTe + 273) ^ 2)) * ((GlTe + 273) + (AbsExTe + 273))) /
((1 / AbsEmVa) + ((AbsExDi / GlExDi) * ((1 / GlEmVa) - 1)))

        'calculate The Total Heat Transfer Coefficient Between the Absorber Tube Surface and Glass Tube
        TotHeTrCoeBetAbsGl = RadHeTrCoeBetAbsGl + ConHeTrCoeAiBetAbsGl

        'calculate The Total Heat Transfer Coefficient Between The Glass Tube and the ambient
        TotHeTrCoeBetGlAmb = RadHeTrCoeBetGlSk + ConHeTrCoeAiOvGl

        'calculate The Total Heat Transfer Coefficient Between the Absorber Tube Surface and Ambient
        TotHeTrCoeBetAbsAmb = 1 / ((1 / TotHeTrCoeBetGlAmb) + ((AbsExDi / GlExDi) * (1 / TotHeTrCoeBetAbsGl)))

        'The Test Calculation of the Glass Tube Surface
        GlTeTest = ((AbsExDi * TotHeTrCoeBetAbsGl * AbsExTe + GlExDi * TotHeTrCoeBetGlAmb * TeAmb) / (AbsExDi * TotHeTrCoeBetAbsGl + GlExDi
```

```
* TotHeTrCoeBetGlAmb))
    Else    'test
        blnIterationFix = True     'test
    End If                   'test
Loop                       'test

    If blnIterationFix = False Then 'test
        Dim strLessThanEarlyEntered As String
        strLessThanEarlyEntered = "Please, Enter Glass Tube Surface Temperature Less Than " & FormatNumber(GlTeTest, 0)
        MsgBox strLessThanEarlyEntered, vbQuestion, "Warning"  'test
    Else 'test

        'The Collector Performance Factor
        ColPerFac = 1 / (TotHeTrCoeBetAbsAmb * ((1 / TotHeTrCoeBetAbsAmb) + (AbsExDi / (ConHeTrCoeInAbs * (AbsInDi))) + ((AbsExDi / (2 * Abs
ThCo)) * (Log(AbsExDi / (AbsInDi))))))

        'The Total Heat Transfer Coefficient Between the Working Fluid and Ambient
        TotHeTrCoeBetWoFlAmb = ColPerFac * TotHeTrCoeBetAbsAmb

        'The Effective Multiply of Absorber Tube Absorbtance Value by Glass Tube Transmittance Value
        If optGreenGlass = True Then
            EfMulAbsAbsorVaGlTransVa = 1.02 * (AbsAbsorVa * GlTransVa)
        Else
            EfMulAbsAbsorVaGlTransVa = 1.01 * (AbsAbsorVa * GlTransVa)
        End If

        'Select the Reflective Value
        If chkNewReflectorType.Value = 0 Then
            If cboSelectReflectorType.ListIndex = 0 Then
                RefReflVa = RefAcr
            ElseIf cboSelectReflectorType.ListIndex = 1 Then
                RefReflVa = RefAlu
            ElseIf cboSelectReflectorType.ListIndex = 2 Then
                RefReflVa = RefCop
            ElseIf cboSelectReflectorType.ListIndex = 3 Then
                RefReflVa = RefCus
            ElseIf cboSelectReflectorType.ListIndex = 4 Then
                RefReflVa = RefGol
            ElseIf cboSelectReflectorType.ListIndex = 5 Then
                RefReflVa = RefMir
            ElseIf cboSelectReflectorType.ListIndex = 6 Then
                RefReflVa = RefSil
            End If
            txtTheReflectiveValueOfNewReflectorType.Text = Val(RefReflVa)
        Else
            RefReflVa = Val(txtTheReflectiveValueOfNewReflectorType)
        End If

        'The Gross Energy Collect on Absorber Tube Surface by Unit Area
        GroEnOnAbsPerUnAr = DirRadBeam * RefReflVa * IntFac * EfMulAbsAbsorVaGlTransVa * IncAnMoFac

        'The Gross Energy Collect on Absorber Tube Surface Per Unit Length
        GroEnOnAbsPerUnLe = GroEnOnAbsPerUnAr * (ColWi - GlExDi)
```

```
        'The Total Heat Transfer Losses Between the Working Fluid Tube Surface and Ambient per unit length
        TotHeLoBetAbsAmbPerUnLe = TotHeTrCoeBetWoFlAmb * Pi * AbsExDi * (AbsExTe - TeAmb)

        'The Net Energy Collect on Absorber Tube Surface Unit Length
        NetEnOnAbsUnLe = GroEnOnAbsPerUnLe - TotHeLoBetAbsAmbPerUnLe

        'the total length with respect to The Net Energy Collect on Absorber Tube Surface
        TotLeWiReToNetEnOnAbs = DeUsEn / NetEnOnAbsUnLe

        'The Total Required Collector Length
        ReqColLe = ((WoFlSpHe * WoFlMaFlRa) / (TotHeTrCoeBetAbsAmb * Pi * AbsExDi * ColPerFac)) * ((-1) * Log(1 - ((TotHeTrCoeBetAbsAmb * Pi
 * AbsExDi * TotLeWiReToNetEnOnAbs) / (WoFlSpHe * WoFlMaFlRa))))

        'The Required Collctors Number
        ReqColNu = ReqColLe / ColLe

        'The Net Energy Obtained From One Collector
        NetEnPerOneCol = NetEnOnAbsUnLe * ColLe

        'The Net Energy Obtined Per Unit Area of the Collector
        NetEnPerUnAr = NetEnPerOneCol / (ColLe * ColWi)

        'The Optical Efficiency of The Collector
        OptEff = 100 * GroEnOnAbsPerUnAr / DirRadBeam

        'The Thermal Efficiency of The Collector
        TherEff = 100 * NetEnPerUnAr / DirRadBeam

        'The Critical Direct Solar Beam
        CriDirRadBeam = (TotHeTrCoeBetAbsAmb * Pi * AbsExDi * (WoFlInTe - TeAmb)) / ((ColWi - GlExDi) * (OptEff / 100))

        'Concentration Ratio
        ConcRat = ColWi / (Pi * AbsExDi)

        'Format Outputs and show in labels
        lblTheExactGlassTubeSurfaceTemperature.Caption = FormatNumber(GlTe)
        lblConcentrationRatio.Caption = FormatNumber(ConcRat)
        lblWorkingFluidMassFlowRate.Caption = FormatNumber(WoFlMaFlRa, 3)
        lblOpticalEfficiencyOfTheCollector.Caption = FormatNumber(OptEff)
        lblThermalEfficiencyOfTheCollector.Caption = FormatNumber(TherEff)
        lblTheTotalRequiredCollectorLength.Caption = FormatNumber(ReqColLe)
        lblTheRequiredCollctorsNumber.Caption = FormatNumber(ReqColNu, 1)
        lblTheNetEnergyObtainedFromOneCollector.Caption = FormatNumber(NetEnPerOneCol) / 1000

        cmdCalculate.Enabled = False
        mnuCalculateCalculate.Enabled = False
        cmdCheckDesignAvailability.Enabled = False
        mnuCalculateCheckDesignAvailability.Enabled = False
        cmdClearOutputs.Enabled = True
        mnuEditClearOutputs.Enabled = True
        cmdPrintForm.Enabled = True
        mnuFilePrint.Enabled = True
```

```
        'Determine the Perfect Absorber Tube Exterior Diameter if the Dispersion Angle taken zero
        PerAbsExDi = (ColWi * 1000 / Sin(ColRiAn)) * Sin((SoInAn * (3.141592 / 180)) / 2)

    End If    'test
End If
End Sub

Private Sub cmdCheckDesignAvailability_Click()

        'Dimension in Local-Level
        Dim InfoDesAv As String

        'convert the text values to numeric value
        ColWi = Val(txtCollectorWidth)
        ColRiAn = Val(txtCollectorRimAngle) * (3.141592 / 180)
        AbsExDi = Val(txtAbsorberTubeExteriorSurfaceDiameter) / 1000

        'make sure that the design is Availability
    If IsNumeric(txtCollectorWidth.Text) = False Or IsNumeric(txtCollectorRimAngle) = False Or IsNumeric(txtAbsorberTubeExteriorSurfaceDiame
ter) = False Then
        MsgBox "To Check Your Design Availability, Please Fill the Collector Width, Collector Rim Angle and Absorber Tube Exterior Surface D
iameter Texts.", vbInformation, "Request"
    Else
        If AbsExDi < ((ColWi / Sin(ColRiAn)) * Sin(((SoInAn * (3.141592 / 180)) / 2) + ((DiAn * (3.141592 / 180)) / 2))) Then
            InfoDesAv = "You Need to Do one of Follow State to Avoid the Losses in Direct Beams:" & vbCrLf & "1. Decrease The Collector Widt
h." & vbCrLf & "2. Increase the Absorber Tube Exterior Surface Diamter." & vbCrLf & "3. Increase The Rim Angle To Possible Limit, For More I
nformation Go To Help Menu."
            MsgBox InfoDesAv, vbOKOnly, "Request"
            txtCollectorWidth.SetFocus
        Else
            MsgBox "There is No Problem with Your Design Availibility, You Can Continue Calculate!", vbOKOnly, "Confirm Message"
            cmdCalculate.Enabled = True
            cmdCalculate.Default = True
            mnuCalculateCalculate.Enabled = True
            cmdClearAll.Enabled = True
            mnuEditClearAll.Enabled = True
        End If
    End If
End Sub

Private Sub cmdClearAll_Click()

        'clear all
        txtCollectorLength.Text = ""
        txtCollectorWidth.Text = ""
        txtCollectorRimAngle.Text = ""
        txtAbsorberTubeExteriorSurfaceDiameter.Text = ""
        txtAbsorberTubeWallThickness.Text = ""
        txtAbsorberTubeThermalConductivity.Text = ""
        txtAbsorberTubeAbsorbtanceValue.Text = ""
        txtAbsorberTubeEmissivityValue.Text = ""
        cboSelectReflectorType.Text = "Select Reflector Type"
```

```
        chkNewReflectorType.Value = 0
        txtTheReflectiveValueOfNewReflectorType.Text = ""
        optGreenGlass.Value = False
        optWhiteGlass.Value = False
        optVacuumPacked.Value = False
        optWithoutVacuum.Value = False
        txtGlassTubeExteriorSurfaceDiameter.Text = ""
        txtGlassTubeWallThickness.Text = ""
        txtGlassTubeTransmittanceValue.Text = ""
        txtGlassTubeEmissivityValue.Text = ""
        cboSelectWorkingFluid.Text = "Select Working Fluid"
        chkNewWorkingFluid.Value = 0
        txtSpecificHeatAtTheMeanTemperature.Text = ""
        txtViscosityAtTheMeanTemperature.Text = ""
        txtThermalConductivityAtTheMeanTemperature.Text = ""
        txtPradlNumberAtTheMeanTemperature.Text = ""
        txtWindSpeed.Text = ""
        txtAmbienceMeanTemperature.Text = ""
        txtTheMeanDirectRadiationBeamInOperationZone.Text = ""
        txtWorkingFluidInletTemperature.Text = ""
        txtWorkingFluidOutletTemperature.Text = ""
        txtDesiredIntendedUsefulEnergy.Text = ""
        txtInterceptFactor.Text = ""
        txtIncidentAngleModifierFactor.Text = ""
        txtGlassTubeSurfaceTemperature.Text = ""
        lblTheExactGlassTubeSurfaceTemperature.Caption = ""
        lblConcentrationRatio.Caption = ""
        lblWorkingFluidMassFlowRate.Caption = ""
        lblOpticalEfficiencyOfTheCollector.Caption = ""
        lblThermalEfficiencyOfTheCollector.Caption = ""
        lblTheTotalRequiredCollectorLength.Caption = ""
        lblTheRequiredCollctorsNumber.Caption = ""
        lblTheNetEnergyObtainedFromOneCollector.Caption = ""
        cmdCalculate.Enabled = False
        cmdCheckDesignAvailability.Enabled = True
        cmdPrintForm.Enabled = False
        mnuFilePrint.Enabled = False
        txtCollectorLength.SetFocus
        GlTeTest = 0
End Sub

Private Sub cmdClearOutputs_Click()

        'clear Outputs
    If lblTheNetEnergyObtainedFromOneCollector.Caption = "" Then
        MsgBox "Sorry, There Are No Outputs To Clear.", vbInformation, "Request"
    Else
        lblTheExactGlassTubeSurfaceTemperature.Caption = ""
        lblConcentrationRatio.Caption = ""
        lblWorkingFluidMassFlowRate.Caption = ""
        lblOpticalEfficiencyOfTheCollector.Caption = ""
        lblThermalEfficiencyOfTheCollector.Caption = ""
        lblTheTotalRequiredCollectorLength.Caption = ""
```

```
        lblTheRequiredCollctorsNumber.Caption = ""
        lblTheNetEnergyObtainedFromOneCollector.Caption = ""
        cmdCalculate.Enabled = True
        cmdCalculate.Default = True
        cmdCheckDesignAvailability.Enabled = True
        cmdPrintForm.Enabled = False
        mnuFilePrint.Enabled = False
        GlTeTest = 0
    End If
End Sub

Private Sub cmdExit_Click()

    'terminate the program
    End
End Sub

Private Sub cmdPrintForm_Click()

    'print
    Printer.Print ""
    Printer.FontItalic = False
    Printer.ForeColor = vbRed
    Printer.FontSize = 12
    Printer.FontBold = True
    Printer.FontUnderline = True
    Printer.Print Tab(5); "Inputs"
    Printer.FontSize = 10
    Printer.FontBold = False
    Printer.FontUnderline = False
    Printer.ForeColor = vbRed
    Printer.Print ""
    Printer.Print Tab(10); "Design Data Inputs"
    Printer.ForeColor = vbBlue
    Printer.Print Tab(15); "Collector Inputs"
    Printer.ForeColor = vbBlack
    Printer.Print Tab(20); "Collector Length"; Tab(50); "[m]:"; Tab(60); ColLe
    Printer.Print Tab(20); "Collector Width"; Tab(50); "[m]:"; Tab(60); ColWi
    Printer.Print Tab(20); "Collector Rim Angle"; Tab(50); "[Degree]:"; Tab(61); FormatNumber((ColRiAn / (3.141592 / 180)), 0)
    Printer.ForeColor = vbBlue
    Printer.Print Tab(15); "Absorber Tube Inputs"
    Printer.ForeColor = vbBlack
    Printer.Print Tab(20); "Exterior Diameter"; Tab(50); "[mm]:"; Tab(60); (AbsExDi * 1000)
    Printer.Print Tab(20); "Wall Thickness"; Tab(50); "[mm]:"; Tab(60); (AbsWaTh * 1000)
    Printer.Print Tab(20); "Thermal Conductivity"; Tab(50); "[W/m.K]:"; Tab(60); AbsThCo
    Printer.Print Tab(20); "Absorbtance Value:"; Tab(60); AbsAbsorVa
    Printer.Print Tab(20); "Emissivity Value:"; Tab(60); AbsEmVa
    Printer.ForeColor = vbBlue
    Printer.Print Tab(15); "Working Fluid Inputs"
    Printer.ForeColor = vbBlack
If chkNewWorkingFluid.Value = 1 Then
    Printer.Print Tab(20); "Selected Working Fluid"; Tab(61); "New Working Fluid"
Else
```

```
Form1 - 13

    If cboSelectWorkingFluid.ListIndex = 0 Then
        Printer.Print Tab(20); "Selected Working Fluid"; Tab(61); "Water"
    Else
        Printer.Print Tab(20); "Selected Working Fluid"; Tab(61); "Syltherm 800"
    End If
End If
    Printer.Print Tab(20); "Specific Heat"; Tab(50); "[kj/kg.K]:"; Tab(61); FormatNumber((WoFlSpHe / 1000), 3)
    Printer.Print Tab(20); "Viscosity"; Tab(50); "[kg/m.sec]:"; Tab(61); (WoFlVis / 1000)
    Printer.Print Tab(20); "Thermal Conductivity"; Tab(50); "[W/m.C]:"; Tab(60); WoFlThCo
    Printer.Print Tab(20); "Prandl Number:"; Tab(60); WoFlPrNu
    Printer.ForeColor = vbBlue
    Printer.Print Tab(15); "Reflector Inputs"
    Printer.ForeColor = vbBlack
If chkNewReflectorType.Value = 1 Then
    Printer.Print Tab(20); "Selected Reflector"; Tab(61); "New Reflector"
Else
    Printer.Print Tab(20); "Selected Reflector"; Tab(61); cboSelectReflectorType.Text
End If
    Printer.Print Tab(20); "Reflective Value:"; Tab(60); RefReflVa
    Printer.ForeColor = vbBlue
    Printer.Print Tab(15); "Glass Cover Inputs"
    Printer.ForeColor = vbBlack
If optGreenGlass.Value = True Then
    Printer.Print Tab(20); "Glass Type:"; Tab(61); "Green Glass"
Else
    Printer.Print Tab(20); "Glass Type:"; Tab(61); "White Glass"
End If
If optVacuumPacked.Value = True Then
    Printer.Print Tab(20); "Vacuum State:"; Tab(61); "Vacuum-Packed"
Else
    Printer.Print Tab(20); "Vacuum State:"; Tab(61); "Without Vacuum"
End If
    Printer.Print Tab(20); "Exterior Diameter"; Tab(50); "[mm]:"; Tab(60); (GlExDi * 1000)
    Printer.Print Tab(20); "Wall Thickness"; Tab(50); "[mm]:"; Tab(60); (GlWaTh * 1000)
    Printer.Print Tab(20); "Transmittance Value:"; Tab(60); GlTransVa
    Printer.Print Tab(20); "Emissivity Value:"; Tab(60); GlEmVa
    Printer.ForeColor = vbRed
    Printer.Print Tab(10); "Ambiance Data Inputs"
    Printer.ForeColor = vbBlack
    Printer.Print Tab(20); "Wind Speed"; Tab(50); "[m/sec]:"; Tab(60); WinSp
    Printer.Print Tab(20); "Ambiance Temperature"; Tab(50); "[C]:"; Tab(60); TeAmb
    Printer.Print Tab(20); "Direct Radiation"; Tab(50); "[W/m2]:"; Tab(60); DirRadBeam
    Printer.ForeColor = vbRed
    Printer.Print Tab(10); "Operation Data Inputs"
    Printer.ForeColor = vbBlack
    Printer.Print Tab(20); "Inlet Temperature"; Tab(50); "[C]:"; Tab(60); WoFlInTe
    Printer.Print Tab(20); "Outlet Temperature"; Tab(50); "[C]:"; Tab(60); WoFlOuTe
    Printer.Print Tab(20); "Desired Useful Energy"; Tab(50); "[kW]:"; Tab(60); (DeUsEn / 1000)
    Printer.ForeColor = vbRed
    Printer.Print Tab(10); "Accepted Data Inputs"
    Printer.ForeColor = vbBlack
    Printer.Print Tab(20); "Intercept Factor"; Tab(60); IntFac
    Printer.Print Tab(20); "IAMF"; Tab(60); IncAnMoFac
```

```
    Printer.Print Tab(10); "-------------------------------------------------------------------------------------------------------------------
------------"
    Printer.ForeColor = vbRed
    Printer.FontSize = 12
    Printer.FontBold = True
    Printer.FontUnderline = True
    Printer.Print Tab(5); "Outputs"
    'Printer.Print ""
    Printer.FontSize = 10
    Printer.FontBold = False
    Printer.FontUnderline = False
    Printer.ForeColor = vbRed
    Printer.Print Tab(10); "PTSC Geometry Parameters"
    Printer.ForeColor = vbBlack
    Printer.Print Tab(20); "Radius of The Parabola at The Rim Angle"; Tab(100); "[mm]:"; Tab(110); FormatNumber(RaRi, 0)
    Printer.Print Tab(20); "Focal Length"; Tab(100); "[mm]:"; Tab(110); FormatNumber(FoLe, 0)
    Printer.Print Tab(20); "Parabola Depth"; Tab(100); "[mm]:"; Tab(110); FormatNumber(Href, 0)
    Printer.Print Tab(20); "Parabola Arc Length"; Tab(100); "[mm]:"; Tab(110); FormatNumber(PaArLe, 0)
    Printer.Print Tab(20); "Parabola Equation"; Tab(100); "[mm]:"; Tab(110); "y2 = "; FormatNumber(PaEqCo, 0); ".x"
    Printer.Print Tab(20); "Perfect Absorber Tube Exterior Diameter if the Dispersion Angle taken zero"; Tab(100); "[mm]:"; Tab(110); Format
Number(PerAbsExDi, 1)
    Printer.ForeColor = vbRed
    Printer.Print Tab(10); "Heat Transfer Coefficients"
    Printer.ForeColor = vbBlack
    Printer.Print Tab(20); "Convection Heat Transfer Coeff. Inside The Absorber Tube"; Tab(100); "[W/m2.K]:"; Tab(110); FormatNumber(ConHeTr
CoeInAbs, 1)
    Printer.Print Tab(20); "Convection Heat Transfer Coeff. Between The Absorber Tube And Glass Cover"; Tab(100); "[W/m2.K]:"; Tab(110); For
matNumber(ConHeTrCoeAiBetAbsGl, 1)
    Printer.Print Tab(20); "Convection Heat Transfer Coeff. Over The Glass Cover"; Tab(100); "[W/m2.K]:"; Tab(110); FormatNumber(ConHeTrCoeA
iOvGl, 1)
    Printer.Print Tab(20); "Radiation Heat Transfer Coeff. Between The Glass Cover And Sky"; Tab(100); "[W/m2.K]:"; Tab(110); FormatNumber(R
adHeTrCoeBetGlSk, 1)
    Printer.Print Tab(20); "Radiation Heat Transfer Coeff. Between The Absorber Tube And Glass Cover"; Tab(100); "[W/m2.K]:"; Tab(110); Form
atNumber(RadHeTrCoeBetAbsGl, 1)
    Printer.Print Tab(20); "Glass Temperature"; Tab(100); "[C]:"; Tab(110); FormatNumber(GlTe, 1)
    Printer.Print Tab(20); "Critical Direct Solar Beams Intensity"; Tab(100); "[W/m2]:"; Tab(110); FormatNumber(CriDirRadBeam, 1)
    Printer.ForeColor = vbRed
    Printer.Print Tab(10); "PTSC Performance Outputs"
    Printer.ForeColor = vbBlue
    Printer.Print Tab(20); "Concentration Ratio"; Tab(110); FormatNumber(ConcRat, 1)
    Printer.Print Tab(20); "Working Fluid Mass Flowrate"; Tab(100); "[kg/sec]:"; Tab(110); FormatNumber(WoFlMaFlRa, 4)
    Printer.Print Tab(20); "Optical Efficiency"; Tab(110); FormatNumber(OptEff, 2)
    Printer.Print Tab(20); "Thermal Efficiency"; Tab(110); FormatNumber(TherEff, 2)
    Printer.Print Tab(20); "Required Collector Length"; Tab(100); "[m]:"; Tab(110); FormatNumber(ReqColLe, 1)
    Printer.Print Tab(20); "Required Collector Numbers"; Tab(110); FormatNumber(ReqColNu, 1)
    Printer.Print Tab(20); "Net Energy Obtained From One Collector"; Tab(100); "[kW]:"; Tab(110); FormatNumber((NetEnPerOneCol / 1000), 2)
    Printer.Print Tab(20); "Heat Losses Per Unit Length"; Tab(100); "[kW/m]:"; Tab(110); FormatNumber((TotHeLoBetAbsAmbPerUnLe / 1000), 3)
    Printer.Print ""
    Printer.ForeColor = vbRed
    Printer.FontItalic = True
    Printer.FontUnderline = True
    Printer.FontBold = True
    Printer.FontSize = 8
```

```
    Printer.Print Tab(130); " By: Sabah Beyatlı"
    Printer.EndDoc
    cmdPrintForm.Enabled = False
    mnuFilePrint.Enabled = False
End Sub

Private Sub mnuCalculateCalculate_Click()

    Call cmdCalculate_Click
End Sub


Private Sub mnuCalculateCheckDesignAvailability_Click()

    Call cmdCheckDesignAvailability_Click
End Sub

Private Sub mnuEditClearAll_Click()

    Call cmdClearAll_Click
End Sub

Private Sub mnuEditClearOutputs_Click()

    Call cmdClearOutputs_Click
End Sub

Private Sub mnuFileExit_Click()

    Call cmdExit_Click
End Sub

Private Sub mnuFilePrint_Click()
    Call cmdPrintForm_Click
End Sub

Private Sub mnuHelpAbout_Click()

    frmAbout.Show
End Sub

Private Sub mnuHelpDesignAvailability_Click()

    frmDesignAvailability.Show
End Sub

Private Sub mnuHelpIAMF_Click()

    frmIAMF.Show
End Sub

Private Sub mnuHelpInterceptFactor_Click()
```

```
    frmInterceptFactor.Show
End Sub

Private Sub mnuHelpPTSC_Click()

    frmPTSC.Show
End Sub

Private Sub mnuHelpPTSCGeometryParameters_Click()

frmPTSCGeometryParameters.Show
End Sub
```

Appendix-C

The Form of the Package Program

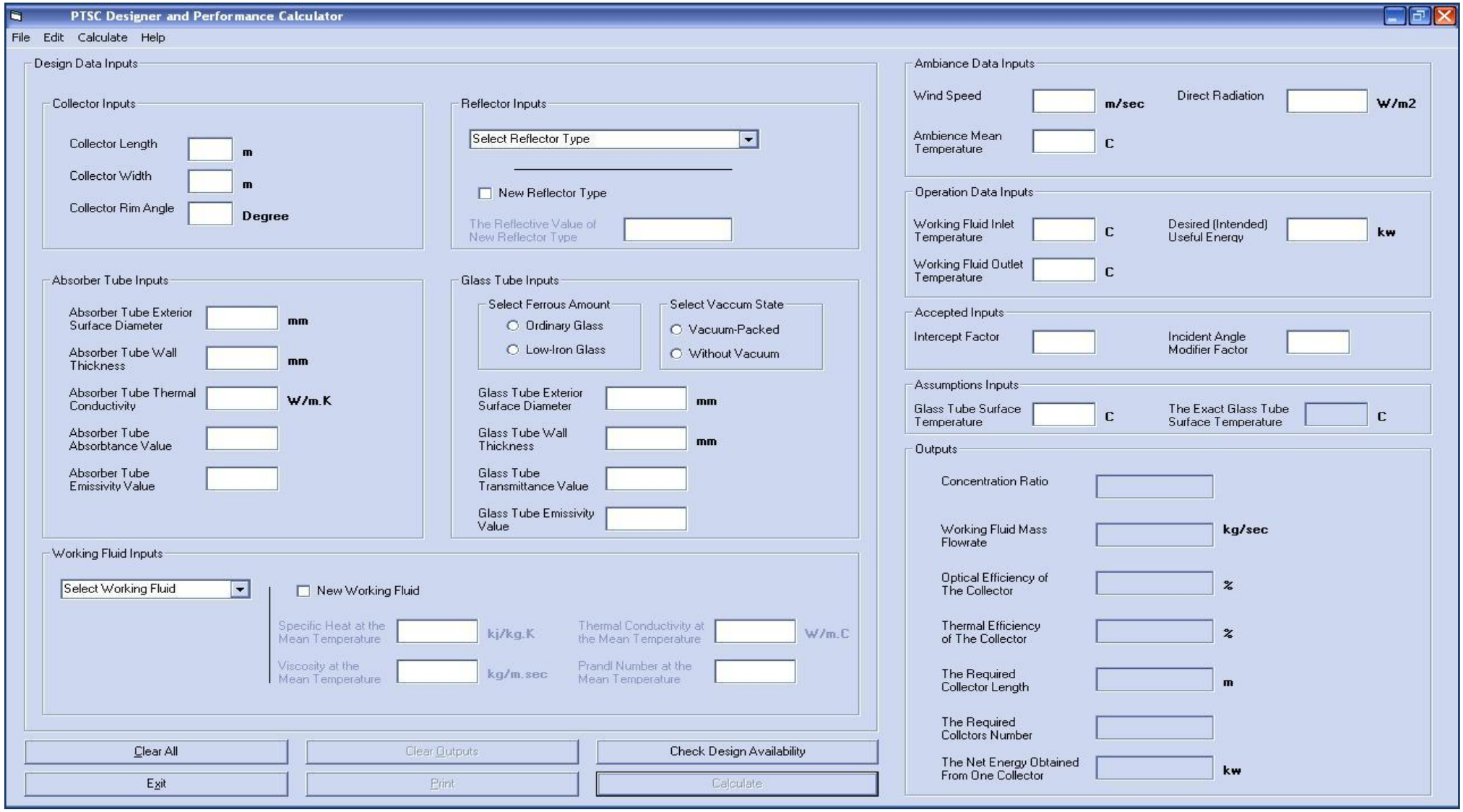

Appendix-D

The Print Outputs of the Sample Thermal Performance Calculation of the PTSC

Inputs

Design Data Inputs

Collector Inputs

Collector Length	[m]:	8
Collector Width	[m]:	5
Collector Rim Angle	[Degree]:	70

Absorber Tube Inputs

Exterior Diameter	[mm]:	70
Wall Thickness	[mm]:	1.2
Thermal Conductivity	[w/m.K]:	27
Absorbtance Value:		0.96
Emissivity Value:		0.09

Working Fluid Inputs

Selected Working Fluid		Syltherm 800
Specific Heat	[kj/kg.K]:	1.857
Viscosity	[kg/m.sec]:	0.0015364
Thermal Conductivity	[w/m.C]:	0.1083
Prandl Number:		24.7115

Reflector Inputs

Selected Reflector		Custom polished aluminum thin film (Alanod)
Reflective Value:		0.88

Glass Cover Inputs

Glass Type:		White Glass
Vacuum State:		Vacuum-Packed
Exterior Diameter	[mm]:	115
Wall Thickness	[mm]:	2
Transmittance Value:		0.96
Emissivity Value:		0.88

Ambiance Data Inputs

Wind Speed	[m/sec]:	4
Ambiance Temperature	[C]:	30
Direct Radiation	[w/m2]:	900

Operation Data Inputs

Inlet Temperature	[C]:	150
Outlet Temperature	[C]:	180
Desired Useful Energy	[kw]:	25

Accepted Data Inputs

Intercept Factor		0.96
IAMF		0.95

Outputs

PTSC Geometry Parameters

Radius of The Parabola at The Rim Angle	[mm]:	2,660
Focal Length	[mm]:	1,785
Parabola Depth	[mm]:	875
Parabola Arc Length	[mm]:	5,383
Parabola Equation	[mm]:	y2 = 7,141.x

Heat Transfer Coefficients

Convection Heat Transfer Coeff. Inside The Absorber Tube	[w/m2.K]:	130.6
Convection Heat Transfer Coeff. Between The Absorber Tube And Glass Cover	[w/m2.K]:	0.0
Convection Heat Transfer Coeff. Over The Glass Cover	[w/m2.K]:	33.4
Radiation Heat Transfer Coeff. Between The Glass Cover And Sky	[w/m2.K]:	5.6
Radiation Heat Transfer Coeff. Between The Absorber Tube And Glass Cover	[w/m2.K]:	1.1
Glass Temperature	[C]:	32.2
Critical Direct Solar Beams Intensity	[W/m2]:	12.2

PTSC Performance Outputs

Concentration Ratio		22.7
Working Fluid Mass Flowrate	[kg/sec]:	0.4488
Optical Efficiency		74.70
Thermal Efficiency		71.89
Required Collector Length	[m]:	7.8
Required Collector Numbers		1.0
Net Energy Obtained From One Collector	[kw]:	25.88
Heat Losses Per Unit Length	[kw/m]:	0.049

By: Sabah Beyatlı

Appendix-E

The Thermophysical Properties of the Thermal Oil (SYLTHERM 800)

Temperature [^oC]	Density [kg/m^3]	Specific Heat [J/kg.K]	Dynamic Viscosity 0.001*[kg/m.sec]	Kinematic Viscosity [mm^2/sec]	Thermal Conductivity [W/m.K]	Prandtl Number
-40	992	1507	50.63	51.04	0.146	522.6
-30	982	1524	35.38	36.03	0.144	374.4
-20	973	1541	25.81	26.53	0.142	280.1
-10	963	1558	19.57	20.32	0.141	216.2
0	954	1575	15.30	16.04	0.139	173.4
10	945	1592	12.26	12.97	0.137	142.5
20	936	1609	10.01	10.69	0.135	119.3
30	927	1626	8.31	8.96	0.133	101.6
40	918	1643	7.00	7.63	0.131	87.8
50	909	1660	5.95	6.55	0.129	76.6
60	900	1677	5.11	5.68	0.127	67.5
70	891	1695	4.43	4.97	0.126	59.6
80	882	1712	3.86	4.38	0.124	53.3
90	874	1729	3.39	3.88	0.122	48.0
100	865	1746	2.99	3.46	0.120	43.5
110	856	1763	2.65	3.10	0.118	39.6
120	847	1780	2.36	2.79	0.116	36.2
130	838	1797	2.11	2.52	0.114	33.3
140	829	1814	1.89	2.28	0.112	30.6
150	820	1831	1.70	2.07	0.111	28.0
160	811	1848	1.54	1.90	0.109	26.1
170	802	1865	1.39	1.73	0.107	24.6
180	793	1882	1.26	1.59	1.105	22.6
190	783	1900	1.15	1.47	1.103	21.2
200	774	1917	1.05	1.36	1.101	19.9
210	764	1934	0.96	1.26	0.099	18.8
220	755	1951	0.88	1.17	0.097	17.7
230	745	1968	0.81	1.09	0.095	16.8
240	735	1985	0.74	1.01	0.094	15.6
250	725	2002	0.69	0.95	0.092	15.0
260	714	2019	0.63	0.88	0.090	14.1
270	704	2036	0.59	0.84	0.088	13.7
280	693	2053	0.54	0.78	0.086	12.9
290	682	2070	0.50	0.73	0.084	12.3
300	671	2087	0.47	0.70	0.082	12.0
310	660	2104	0.44	0.67	0.080	11.6
320	649	2122	0.41	0.63	0.079	11.0
330	637	2139	0.38	0.60	0.077	10.6
340	625	2156	0.36	0.58	0.075	10.3
350	613	2173	0.33	0.54	0.073	9.8
360	600	2190	0.31	0.52	0.071	9.6
370	587	2207	0.29	0.49	0.069	9.3
380	574	2224	0.28	0.49	0.067	9.3
390	561	2241	0.26	0.46	0.065	9.0
400	547	2258	0.25	0.46	0.064	8.8

Appendix-F

The Typical Meteorological Year Data of Izmir City (Temperature & Wind Speed)

	Daily Time [Hour] / Month	7	8	9	10	11	12	13	14	15	16	17
TEMPERATURE [°C]	**Januray**		8.16	9.11	10.1	10.82	11.23	11.37	10.89	9.76	8.46	
	February		9.83	11.08	12.02	12.55	12.85	13.21	13.11	12.23	10.98	
	March		15.5	16.79	17.62	18.16	18.21	18.5	18.28	17.8	16.8	
	April	18	18.8	19.67	20.21	20.96	21.2	21.6	21.4	20.99	20	18.8
	May	21.5	23	24	24.7	25.2	25.6	25.5	25.2	24.5	23.5	22.3
	June	26.9	28.5	29.59	30.1	30.9	29.9	31.3	31	30.7	29.8	28.9
	July	28.1	29.4	30.7	31.5	32.2	32.6	32.7	32.6	32	31.3	30.2
	August	28.2	29.7	31.2	32.1	32.6	32.9	33	32.9	32.4	31.9	31
	September	23.5	25.1	26.25	26.8	27.3	27.4	27.6	27.3	26.79	25.8	24.7
	October		20.8	21.7	22.6	23.2	23.6	23.6	23.1	22.2	21.2	
	November		16.5	17.3	17.9	18.6	18.8	19	18.5	17.6	16.9	
	December		11.8	12.7	13.4	13.8	13.8	13.8	13.5	12.6	11.9	
WIND SPEED [m/sec]	**Januray**		1.76	2.19	2.09	2.02	2.08	1.97	1.7	1.64	1.76	
	February		2.17	2.35	2.31	2.51	2.37	2.34	2.48	2.45	2.1	
	March		2.89	2.6	2.8	2.86	2.97	2.87	3.12	2.56	2.58	
	April	2.56	2.82	2.75	2.94	2.55	2.49	2.89	2.59	2.57	2.12	1.98
	May	1.88	1.97	2.44	2.51	3.05	3.59	3.57	3.73	3.5	3.45	2.76
	June	2.62	2.2	3.05	3.31	3.52	3.92	4.33	4.47	4.67	4.57	3.28
	July	2.81	3.29	3.28	4.11	4.65	4.83	5.1	4.88	4.96	4.66	3.83
	August	2.3	3.02	3.3	3.99	4.42	5.33	5.14	4.8	5.22	4.6	3.7
	September	2.69	2.92	2.89	3.51	3.85	4.05	4.3	4.37	3.79	3.57	3.18
	October		2.57	2.73	3.05	3.13	3.4	3.9	3.65	3.36	2.81	
	November		2.24	2.13	2.57	2.89	2.77	2.74	2.83	2.63	2.65	
	December		3.32	3.49	3.3	3.17	3.27	3.13	2.85	2.8	2.61	

The Solar Irradiance Data of Izmir City

(http://sunbird.jrc.it/pvgis/apps/radday.php)

	Daily Time [Hour] / Month	7	8	9	10	11	12	13	14	15	16	17
Global Radiation [W/m^2] Single axis (real)	**Januray**		317	338	346	350	355	350	346	338	317	
	February		390	413	423	435	450	435	423	413	390	
	March		506	533	545	550	558	550	545	533	506	
	April	494	580	637	650	658	664	658	650	637	580	494
	May	568	661	705	717	723	731	723	717	705	661	568
	June	604	716	772	790	795	802	795	790	772	716	604
	July	655	732	780	798	801	811	801	798	780	732	655
	August	583	683	738	766	773	786	773	766	738	683	583
	September	479	592	653	679	684	699	684	679	653	592	479
	October		473	536	557	568	574	568	557	536	473	
	November		307	367	390	402	413	402	390	367	307	
	December		220	290	305	312	325	312	305	290	220	
Global Radiation [W/m^2] Single axis (clear)	**Januray**		483	535	550	562	574	562	550	535	483	
	February		625	673	689	695	700	695	689	673	625	
	March		686	777	788	793	799	793	788	777	686	
	April	550	758	862	875	881	887	881	875	862	758	550
	May	640	800	909	915	920	925	920	915	890	800	640
	June	648	799	893	922	927	931	927	922	893	799	648
	July	634	780	873	903	908	911	908	903	873	780	634
	August	552	750	837	866	870	874	870	866	837	750	552
	September	435	661	760	785	789	797	789	785	760	661	435
	October		555	665	682	691	703	691	682	665	555	
	November		427	558	573	581	588	581	573	558	427	
	December		346	497	513	521	533	521	513	497	346	
Global Radiation [W/m^2] Two axis (clear)	**Januray**		684	727	852	911	925	911	852	727	684	
	February		671	856	948	983	1001	983	948	856	671	
	March		773	873	947	984	988	984	947	873	773	
	April	586	785	930	957	976	982	976	957	930	785	586
	May	663	820	950	960	971	978	970	952	908	820	663
	June	671	816	897	938	956	960	956	938	897	816	671
	July	637	792	881	926	945	949	945	926	881	792	637
	August	569	755	862	918	942	948	942	918	862	755	569
	September	445	687	826	899	933	941	933	899	826	687	445
	October		611	789	883	927	937	927	883	789	611	
	November		506	735	853	908	922	908	853	735	506	
	December		428	696	829	891	907	891	829	696	428	

Appendix-G

List of Symbols

Nomenclature

A	Area	$[m^2]$
a	Collector width	[m]
C	Concentration ratio	
c	Specific heat	$[J/kg.^oC]$
D	Diameter	[m]
F	Shape factor	
F_E	Collector efficiency factor	
F_F	Collector flow factor	
F_R	Collector removal factor	
f	Focus distance	[m]
Gr	Grashof number	
g	Gravitational acceleration	$[m/sec^2]$
H	Height	[m]
h	Heat transfer coefficient	$[W/m^2.K]$
I_{cd}	Critical direct solar beams intensity	$[W/m^2]$
I_d	Direct solar beams intensity	$[W/m^2]$
L	Length	[m]
K	Incident angle modifier factor	
K_{gl}	Glass cover transmission τ_{gl} coefficient	$[m^{-1}]$
k	Thermal conductivity	[W/m.K]
m	Mass flow rate	[kg/sec]
Nu	Nusselt Number	
Pr	Prandl number	
Q	Heat	[W]
Re	Reynolds Number	
r	Radius	[m]
r_r	Maximum reflector radius	[m]

S	Constant direct solar beams at the entrance of the atmosphere	[1367 W/m^2]
T	Temperature	[^oC, K]
t	Thickness	[m]
t	Time	[Hour]
U	Heat transfer coefficient	[$W/m^2.K$]
V	Velocity	[m/sec]
W	Width	[m]
W_p	Parabola length	[m]
wf	Working fluid	

Greek symbols

α	Absorbance	
β	Volumetric expansion coefficient	[K^{-1}]
γ	Intersection factor	
δ	Distance	[m]
δ	Dispersion angle	[Degree]
ε	Emissivity	
η	Efficiency	
θ	Incident Angle	[Degree]
$\boldsymbol{\theta_s}$	Constant sun beams incidence angle	[0.267^o or $16^{'}$]
μ	Viscosity	[kg/m.sec]
ν	Kinematic viscosity	[m^2/sec]
ρ	Density	[kg/m^3]
ρ	Reflectivity	
σ	Stefan-Boltzman constant	[5.669×10^{-8} W/m^2K^4]
τ	Transmittance	
φ_r	Rim angle	[Degree]

Subscripts

a	Ambient

abs	Selective surface absorber tube
apr	Aperture
C	Convection
dp	Dew Point
e	effective
G	Gross
gl	Glass
In	Inner, Inlet
L	Loss
m	mean
max	Maximum
o	Overall
op	Optical
Ou	Outer, Outlet
R	Radiation
ref	Reflector
s	Sky
Sh	Shaded
th	Thermal
U	Useful
UnSh	Unshaded
W	Wind
wf	Working fluid

Abbreviations

CPC	Compound Parabolic Collectors
IST	Industrial Solar Technology
PTSC	Parabolic Trough Solar Collectors